Evolutionary Dynamics of Pine Squirrels (*Tamiasciurus*) in Western North America

Andreas Shintaro Chavez

A dissertation

submitted in partial fulfillment of the

requirements for the degree of

Doctor of Philosophy

University of Washington

2013

Reading Committee:

George James Kenagy, Chair

Adam Leaché

Joseph Felsenstein

Program Authorized to Offer Degree:

Biology

University of Washington

Abstract

Evolutionary Dynamics of Pine Squirrels (*Tamiasciurus*) in Western North America

Andreas Shintaro Chavez

Chair of the Supervisory Committee:

Professor Emeritus, George James Kenagy

Department of Biology

The evolution of new phenotypes and species is a population genetic process that is governed by four fundamental forces: natural selection, drift, mutation, and gene flow. Ecological genetics is the reciprocal interaction between population genetic theory and empirical observations from nature and the laboratory. Here I present a study in which I synthesize ecological information with population genetic studies in order to better understand how and why organisms diversify at the genetic, phenotypic, and species level. Pine squirrels (Genus: *Tamiasciurus*) are an important study organism for investigating the early stages of adaptation and speciation in nature because they are comprised of only recently divergent lineages, form narrow hybrid zones, show sharp goegraphic variation in several phenotypic traits of ecological interest, such as fur coloration and cranial morphology associated with bite force, and are a model organism

for behavioral and ecological research. Pine squirrels (also known as tree squirrels) are ubiquitous across coniferous forests of North America and are comprised of only two recognized species: the Douglas squirrel (*T. douglasii)* and the North American red squirrel (*T. hudsonicus*). In my first chapter, I show with molecular divergence analyses using multilocus genetic data that these two species split less than a half million years ago. I also use phylogenetic inference and isolation with migration models to resolve the biogeographic puzzle of red squirrels occurring on Vancouver Island despite the closest mainland regions being occupied by Douglas squirrels. A species tree analysis using 15 nuclear loci indicates that the origin of squirrels on the island was likely from *T. hudsonicus* populations that occurred in interior montane regions that apparently persisted south of continental ice during the LGM. Surprisingly, phylogenetic analysis with mtDNA shows that all island squirrels carry the mtDNA of the sister species *T. douglasii*. We found historical migration between *T. douglasii* and island *T. hudsonicus*, but no historical migration between *T. douglasii* and mainland *T. hudsonicus* using IM models. These findings show a complex colonization and migration history between both mainland species and the island population. In my second chapter, I examined hybrid zone dynamics between the two squirrel species along an environmental gradient in the North Cascade Mountains of southern British Columbia and northern Washington. I found that genetic and phenotypic variation had steeper clines than a neutral genetic marker, which suggests that divergent selection is overriding gene flow in maintaining distinction between these species. Furthermore, all phenotypic clines were centered in a forest ecotone, thereby implicating environmental factors as being responsible for the location of the species boundary. Furthermore, I detected hybridization occurring to at

least the F_2 generation, which supports the notion that hybrid inviability is not as strong as environmental forces in maintaining distinction between species at this hybrid zone. In my third chapter, I show differential patterns of clinal variation in several ecologically important traits within Douglas squirrels (*T. douglasii*) along a forest gradient in Oregon. Ventral fur color shows a relatively sharp clinal transition from deep orange in the coastal region to a whitish-yellow, which coincides with a gradient in tree canopy openness. In contrast, cranial morphology varies continuously and gradually and does not show any sharp transitions, which is surprising given the abrupt changes in size and hardness of their primary food source, the cones from which they extract seeds. Collectively, my dissertation research provides an integrative examination of the contemporary processes of selection and gene flow that have shaped phenotypic variation and the genetic structure of pine squirrels in western North America.

CONTENTS

LIST OF TABLES

LIST OF FIGURES

ACKNOWLEDGMENTS

I am truly grateful to my advisor, Jim Kenagy, for allowing me the opportunity to carry out this research, for his patience, endless generosity, and moral support throughout my time in graduate school. Jim has been a great mentor, colleague, and inspiration. In addition, I am indebted to my supervisory graduate committee, Joe Felsenstein, Toby Bradshaw, Adam Leaché, and Kerry Naish for their insight, guidance, and insistence on setting rigorous standards for myself. Adam deserves special recognition for allowing me to be an affiliate of his lab and serving as a "secondary" mentor. I am also very grateful to Jeff Bradley, Burke Museum Mammals collection manager, for providing me resources, logistical support, and friendship.

I also extend my gratitude to Sharlene Santana, Lorenz Hauser, Josh Tewksbury, Ray Huey, Sievert Rowher, Billie Swalla, Barbara Wakamoto, and many other UW faculty for their guidance and support. Many graduate students and postdocs (current and former) are also deserving of my gratitude for helping me develop my ideas and for providing friendship, including a special thanks to Dou Yang, Stevan Springer, Jaquan Horton, Robin Elahi, Matt McElroy, Sylvia Yang, Max Maliska, Chris Himes, Corey Welch, Josh Whorley, Jared Grummer, Rebecca Harris, Charles Linkem, David Haak, Meade Krosby, Brooks Miner, Katrina Claw, Eligio Martinez, and Tracy Larson. I also thank Carl Saltzberg, Mike Bianchi, Jack DeLap, Jeff Corneil, Sean Maher, and Brian Arbogast for their field assistance and scientific collaboration. I also thankful to the folks of UW GOMAP, UW SACNAS chapter, UW Biology Diversity Committee, UW Biology BGOODD for providing me an arena to share and grow my interests in improving diversity issues in the sciences.

I owe a special thanks to the Burke Museum of Natural History and Culture, Beaty Biodiversity Museum at the University of British Columbia, Humboldt State University Vertebrate Museum, Monte L. Bean Life Science Museum at Brigham Young University, Museum of Natural History at the University of Puget Sound, Museum of Southwest Biology, Museum of Vertebrate Zoology (University of California), Royal BC Museum, New Mexico Museum of Natural History, University of Alaska Museum of the North, University of Michigan Museum of Zoology, and University of Kansas Natural History Museum for providing tissue loans. The American Society of Mammalogists, American Museum of Natural History, University of Washington Graduate Opportunities & Minority Achievement Program, NIH/NHGRI Genome Training Grant provided financial support.

Finally, I am indebted to my family and friends. Chris Knaus, Paul Fine, and Christian Flores provided me encouragement and confidence during my pursuit of a PhD. My parents, Kazue and Javier Chavez, were invaluable in supporting my decision to go back to school following a brief career as a federal wildlife biologist. Their reassurance in my decision to follow my dreams has meant the world to me. My sister, Yoko Komatzusaki, and her family and my mother and father-in-law, Sally and Michael Johnson, also were instrumental in helping me persevere by providing me with unwavering support. Finally, I would like to thank my dear wife Laura Johnson Chavez. She has shown me the meaning of love and unconditional support and I am very grateful to share my life with her.

Andreas S. Chavez

CHAPTER 1

Diversification and Gene Flow in Nascent Lineages of Island and Mainland North American Pine Squirrels (*Tamiasciurus*)

Abstract

Insular populations provide an opportunity to study geographic processes and timing of lineage diversification that lead to speciation. Pleistocene climate fluctuations and associated glacial coverage in temperate latitudes have created incipient divergence in many boreal forest mammals. We use phylogenetic and population genetic analyses with multilocus genetic data on North American pine squirrels (*Tamiasciurus*) to test several hypotheses for the refugial origin and colonization of squirrels on Vancouver Island, Canada, which holds a biogeographically peculiar population. The nuclear DNA of island squirrels (*T. hudsonicus*) indicates that they colonized the island around the last glacial maximum (LGM) from interior montane lineages that apparently persisted south of continental ice during the LGM. Surprisingly, phylogenetic analysis with mitochondrial DNA shows that all samples on Vancouver Island carry mitochondrial DNA of the sister species *T. douglasii*. Based on bioclimatic modeling, we suggest that nonclimatic factors favored colonization of Vancouver Island by *T. hudsonicus* instead of *T. douglasii*. We propose that the founding *T. hudsonicus* population carried introgressed mtDNA from nearby mainland *T. douglasii*, as also reflected by contemporary hybridization of the two species on the mainland. Study of geologically and climatologically dynamic systems offers important opportunities to understand biogeographic processes driving evolutionary diversification.

Introduction

Islands have served as important models for understanding the evolutionary and ecological processes underlying population divergence. In theoretical evolutionary genetics, island models have been used as mathematical metaphors to explain evolutionary forces involved in population subdivision and speciation (Wright 1931; Mayr 1982; Slatkin 1985; Barton 1996; Gavrilets and Hastings 1996). Gene flow is one of the important evolutionary forces promoting divergence of populations in island systems. On one hand gene flow can initiate divergence through the founding of new populations that later become isolated (Slatkin 1985). On the other hand, extensive gene flow between nearly isolated populations may homogenize their genetic divergence. Wright (1931) proposed a set of island models to examine population differentiation under the assumption that counteracting forces of gene flow, drift, and mutation are at equilibrium. More recent advances in population genetic theory, such as the Isolation-with-Migration (IM) model (Nielsen and Wakeley 2001; Hey and Nielsen 2007), differ from Wright's island models because they do not assume equilibrium and they can jointly estimate multiple parameters such as population size, divergence time, and migration rates. This nonequilibrium scenario is an important advancement for empirical studies investigating populations that have recently separated.

In nature, island systems have provided important arenas for understanding the biogeographic factors important in the process of speciation (Losos and Ricklefs 2009). Continental islands provide an important opportunity to study the early stages of lineage diversification, because their divergence from source populations and magnitude of isolation are often tightly associated with known geographic events, such as island emergence in response to changes in sea level or coverage of land masses by glaciation (Conroy et al. 1999; Thornton

2007). Such events combine with other biogeographically relevant factors, such as proximity to source populations, in order to influence measurable population genetic parameters such as timing of divergence, rates of gene flow, and changes in population size.

Pleistocene glacial cycles played a major role in the isolation of populations in North America (Shafer et al. 2010). The Pacific Northwest has a series of near-shore continental islands (Fig. 1) that harbor genetically divergent populations (Cook et al. 2006). Persistence of insular populations was strongly affected, in combination, by fluctuations in historic sea level, expansion and contraction of continental ice sheets, and major topographical variation. The last major advance of the Cordilleran Ice Sheet westward out of the mountains of British Columbia reached the edge of the continent and nearby islands 20,000 years ago (Booth et al. 2003). Many insular mammal species were extirpated by this last glacial advance and were subsequently unable to recolonize coastal islands from the mainland during deglaciation (Heaton and Grady 2003). On the contrary, fossil and molecular evidence shows that a few modern insular populations of mammals were able to persist through the last glacial maximum (LGM) in a coastal refugium on the margins of the continental ice sheet (Demboski et al. 1999; Cook et al. 2006; Carrara et al. 2007). Furthermore, some of these insular populations along the extreme north Pacific Coast also served as a source for recolonization of mainland regions during deglaciation (Weckworth et al. 2011). The more southerly portion of the Northwest coast has not been as well studied as the far north for its role as a coastal refugium and potential source for recolonization of the mainland.

Vancouver Island has played a puzzling and poorly understood role as a glacial refugium throughout the Pleistocene. It is the largest (460 km long) and most southern of a series of islands along the northern Pacific Coast (Fig. 1) and is separated from the mainland by as little as 3 km.

Despite its proximity to the continent and similarity of habitats with the nearby mainland region, Vancouver Island's small-mammal fauna is surprisingly depauperate, with only eight of the mainland's 23 species represented (Nagorsen 2005). This extremely low mammal diversity may be due to the coverage of most of the island's terrestrial exposure by the Cordilleran Ice Sheet during the LGM (Clague and James 2002; Booth et al. 2003), followed by limited recolonization during deglaciation. However, Vancouver Island may have supported ice-free regions during this period, particularly on exposed mountain peaks (Haggarty and Hebda 1997) or along the continental shelf, as proposed for the Alexander Archipelago and Haida Gwaii further to the north (Byun et al. 1997; Carrara et al. 2007). Geological and paleontological support for a coastal refugium has been limited due to the submergence of these areas owing to higher sea levels following deglaciation (Fedje and Josenhans 2000). Explorations of coastal refugium hypotheses associated with Vancouver Island mammals using molecular techniques are few (Steppan et al. 2011) in comparison to more extensive studies of the more northern islands (Cook et al. 2006; Topp and Winker 2008).

Pine squirrels of the genus *Tamiasciurus* present an unusual opportunity to examine the role of near-shore islands in lineage divergence because of their enigmatic biogeographic configuration along the northern Pacific Coastal region. Red squirrels (*T. hudsonicus*) on Vancouver Island are separated from inland, trans-montane populations of red squirrels on the mainland by a coastal area of over 150 km width that contains an intervening population of the congeneric Douglas squirrel, *T. douglasii* (Fig. 1). Several testable hypotheses could explain the timing of island colonization and factors that led to this odd biogeographic arrangement. First, recent molecular evidence from coniferous tree species that are ecologically important for pine squirrels suggests that forests might have persisted on the island through the LGM (Godbout et

al. 2008). Therefore it is possible that red squirrels were also able to persist on the island and potentially recolonize mainland regions during deglaciation (Fig 2A). Alternatively, red squirrels may have recolonized the island following deglaciation from ice-free refugia located north or south of the continental ice (Fig. 2B & C). Finally, the taxonomic description of red squirrels on Vancouver Island may be wrong, such that the island squirrels are actually Douglas squirrels that recolonized from the mainland during deglaciation (Fig 2D). Red squirrels on Vancouver Island are visually recognized by their white ventral coloration, in contrast to orange ventral color of Douglas squirrels on the mainland (Nagorsen 2005). White ventral coloration may be ancestral in pine squirrels, with orange being subsequently derived on the mainland in Douglas squirrels following their divergence and isolation from the Vancouver Island population.

The rich documentation of the Pacific Northwest Pleistocene paleoenvironment (Ritchie 1987; Menounos et al. 2009) provides a basis for testing hypotheses of colonization and lineage diversification in northwestern North America. We integrate phylogenetic, population genetic, and ecological niche modeling to test several hypotheses regarding the origin and timing of colonization of *Tamiasciurus* on Vancouver Island. To provide a broad context for the origin of the Vancouver Island population, we examine phylogenetic patterns of diversification within the genus *Tamiasciurus* as a whole using multi-locus nuclear sequence data with species-tree methods. We also infer phylogenetic relationships using mitochondrial DNA (mtDNA) and examine factors that may contribute to topological discordance between nuclear and mitochondrial phylogenies. Next, we explore gene flow patterns between Vancouver Island and various mainland populations by implementing analyses using an IM model. Finally, we use ecological niche modeling to measure climatic niche similarity between the two species at

different time intervals throughout the Pleistocene to show the significance of abiotic niche variables in shaping the current biogeographic arrangement of these squirrels.

Materials and Methods

Study Organism Taxonomy

Many of the analytical methods used in this study require the proper assignment of samples to species or populations. However, the low levels of genetic differentiation in pine squirrels (genus *Tamiasciurus*) make the assignment a challenge. The genus is currently recognized as containing three species: *T. hudsonicus* (the North American red squirrel), *T. douglasii* (the Douglas squirrel), and *T. mearnsi* (Mearns's squirrel) (Lindsay 1981; Thorington and Hoffmann 2005). However, previous molecular studies have shown very little genetic differentiation between *T. mearnsi* and *T. douglasii* (Arbogast et al. 2001), as well as maintenance of genetic distinction between *T. hudsonicus* and *T. douglasii* despite their hybridization in a secondary contact zone (Chavez et al. 2011). For purposes of this research, we recognize only two species of pine squirrels, *T. hudsonicus* and *T. douglasii*, and we have estimated the number of genetically isolated groups (major lineages) within each species by using genetic assignment tests to place samples into groupings.

Collection Of Samples And Molecular Data

We sampled 165 specimens of *Tamiasciurus hudsonicus* and *T. douglasii* from 59 localities in North America (Fig. 1; Table S1). We used 92 frozen tissue samples from internal organs of specimens collected between 1984 and 2010, which are accessioned at the Burke Museum, University of Washington (UWBM); the Museum of Vertebrate Zoology, University of

California (MVZ); the Humboldt State University Vertebrate Museum (HSUVM); the Museum of Southwest Biology (MSB); the New Mexico Museum of Natural History (NMMNH); the University of Alaska Museum of the North (UAM); the Monte L. Bean Life Science Museum at Brigham Young University (BYU); and the University of Michigan Museum of Zoology (UMMZ). The remaining 73 samples were obtained in 2010 from snippets of foot pads or lips of museum study specimens originally collected between 1937 and 1989 and accessioned at the UWBM; Slater Museum of Natural History at the University of Puget Sound (PSM); Beaty Biodiversity Museum at the University of British Columbia (UBC); the Royal BC Museum (RBCM); and the University of Kansas Natural History Museum (KU). Research was conducted in adherence with guidelines of the American Society of Mammalogists (Sikes et al. 2011). We extracted whole genomic DNA from frozen tissue using the prescribed protocol of DNeasy Tissue Kit (Qiagen, Valencia, California). For samples from museum study skins genomic DNA was extracted following a protocol developed by Mullen and Hoekstra (2008), which included an ethanol wash every 3 hours for 24 hours to remove salts and polymerase chain reaction (PCR) inhibitors that may have been used in preserving museum skins.

We selected 15 nuclear introns from a panel of 40 markers identified as useful for phylogenetic analyses of closely related mammal species (Igea et al. 2010). Novel primers for screened loci were designed in conserved flanking exon regions and were based on alignments of several rodent and lagomorph genomes from the ENSEMBL database (http://www.ensembl.org). Primers were designed using PRIMER3 (Rozen and Skaletsky 2000) in flanking exonic regions with degenerate bases at sites where reference genomes differed. To improve marker performance in capillary sequencing, we designed new internal primers that improved amplification of *Tamiasciurus* samples and also reduced the length of amplicons to less than 800

base pairs (bp). We also amplified a 312-328 bp sequence of the mitochondrial DNA (mtDNA) control region using PCR with primers OSU5020L and OSU5021H (Wilson et al. 2005). Primer sequences, product lengths, optimal annealing temperatures and magnesium chloride volumes for both nuclear and mitochondrial markers are listed in Supplemental Table 2. Polymerase chain reactions (PCRs) were carried out in 15 µl reaction volumes that included 1× PCR buffer, primer-specific amounts of $MgCl_2$, 0.2 mM of each dNTP, 0.5 µM of each primer, and 1 U of Taq DNA polymerase and ~30 ng of genomic DNA template. Thermocycling conditions were as follows: 5 minutes at 95°C; 35 cycles of 45 seconds at 95°C, 30 seconds at primer-specific annealing temperature, and 1 minute at 72°C; and a final extension of 10 minutes at 72°C. PCR conditions were modified for samples from museum study skins by including 0.667 mg/ml bovine serum albumin to the PCR reaction and by increasing the number of amplification cycles to 45. We treated all PCR products with ExoSapIT (USB Corp.) to remove unincorporated nucleotides and primers. Capillary sequencing was performed on an ABI 3730 genetic analyzer (Applied Biosystems Inc.) with manual editing and alignments performed using SEQUENCHER 4.6 (Gene Codes Corp.). Nuclear intron sequences with multiple heterozygous sites were probabilistically phased using the program PHASE (Stephens et al. 2001) in DnaSP v. 4.9 (Rozas et al. 2003). We also acquired sequence data for 8 rodent and lagomorph taxa for the same 15 introns from the Ensembl Genome Browser (http://www.ensembl.org/index.html).

Population Structure

To more clearly identify the number of populations (major lineages) in *Tamiasciurus* and the assignment of our samples to those populations, we performed population structure and assignment test analyses for each species in STRUCTURE v. 2.3.3 (Pritchard et al. 2000) with

the phased nuclear intron alleles for each individual. This Bayesian method is a model-based Markov chain Monte Carlo (MCMC) approach that clusters individuals to minimize Hardy-Weinberg disequilibrium and gametic phase disequilibrium between loci within groups. STRUCTURE requires a user-defined number of populations (K) to test for the true populations numbers. We set the model parameters in this analysis to admixture with correlated allele frequencies among populations and performed 4 replicate runs for each value of K with a burn-in of 1×10^4 followed by 1×10^5 repetitions. We performed these runs for values of K ranging between 1 and 15 for *T. hudsonicus* samples and from 1 to 5 for *T. douglasii* samples. We also defined sampling location for each specimen to assist with the clustering by implementing the LOCPRIOR model (Hubisz et al. 2009). To select the most appropriate number of K from our data we plotted the average 'log-likelihood of the STRUCTURE model' Ln P(D) for each value of K and chose the value of K associated with a peak in the Ln P(D) or if the Ln P(D) plateaued we chose the smallest value of K at the beginning of the plateau (Pritchard et al. 2007).

Species Tree Inference

We used *BEAST (Heled and Drummond 2010) as implemented in BEAST v. 1.7.3 (Drummond and Rambound 2007) to reconstruct a *Tamiasciurus* species trees from the 15 nuclear intron dataset. *BEAST is a Bayesian Markov chain Monte Carlo method that coestimates multiple gene trees embedded in a shared species tree along with the effective population size and divergence times of both extant and ancestral lineages. For this method, the term ''species'' is not necessarily the same as the taxonomic rank and instead designates a group of individuals that likely have no recent history of breeding with individuals outside of that group (Heled and Drummond, 2010). Furthermore, the method requires that the assignment of individuals to

species (major lineages) be given *a priori*. Therefore, we used the results from the STRUCTURE analysis to inform the *BEAST analysis that there were 9 major lineages within *Tamiasciurus* and to which lineage each specimen was assigned to. *BEAST also uses models that assume the process of incomplete lineage sorting is the main cause of phylogenetic discordance between the species tree and gene trees. However, introgression is another process that leads to topological incongruence between gene trees and the species tree (Maddison 1997). Even though these two processes generate similar patterns of shared polymorphisms among lineages, the topologies and branch lengths that generate these patterns in accordance with the species tree can be very different (Holder et al. 2001; Joly et al. 2009). We attempted to minimize the possible effects of introgression on our species-tree estimation by selecting exemplar samples that were located in the core of each lineage's geographic distribution. This reduced the number of samples used for the species-tree estimate to 64 specimens for a total of 128 sequences. Finally, *BEAST also assumes no recombination within loci. Therefore, we trimmed sequences to non-recombining sections after analyzing for recombination breakpoints using the difference of sums of squares (DSS) method with a sliding window of 100 bp and a 10 bp step size in TOPALi v2.5 (Milne et al. 2009).

We discovered through our preliminary species-tree analyses that *Tamiasciurus* is very distantly related to the closest outgroup taxa. This made discerning the evolutionary relationships and divergence times of all the *Tamiasciurus* lineages difficult because their estimated branch lengths were extremely short relative to the branch lengths between *Tamiasciurus* and the outgroup (Ho et al. 2008). As a consequence, we performed a two-step species-tree reconstruction process to estimate divergence within *Tamiasciurus* without including outgroup taxa. First, we estimated divergence times in a fossil-calibrated species tree that included both

Tamiasciurus species with several rodent and lagomorph taxa (rodent-lagomorph species tree) in order to estimate the age of the first split in *Tamiasciurus*. For this analysis, we used five fossil calibrations with hard minimum and soft maximum bounds (with gamma or exponential distributions) as priors (Table S3). We used soft maximum bounds to allow the molecular data to correct for conflicting fossil information (Yang and Rannala 2006). Next, we used the estimated 95% highest probability density (HPD) interval representing the split between *T. hudsonicus* and *T. douglasii* with a normal distribution (Ho 2007) as the secondary calibration prior for the root of the *Tamiasciurus*-only species tree (Table S3). Secondary calibrations can be useful when primary calibration points are not available (Blair Hedges and Kumar 2004).

The program BEAUTi (part of the BEAST software package) was used to create the input XML file for *BEAST. For all species-tree analyses, we compared strict versus relaxed molecular clock models using likelihood ratio tests in PAUP* (Swofford 2003) and found a significant departure from a strict clock model for the rodent-lagomorph dataset, but no significant departure for the *Tamiasciurus* dataset. A strict molecular clock is appropriate for datasets that are used to estimate intraspecific relationships and divergence times for a couple of reasons, including (1) the low levels of rate variation between branches (Brown and Yang 2011), and (2) the overparameterization of the species-tree model when using a relaxed clock due to the low levels of phylogenetically informative sties in intraspecific datasets. For all analyses, we used the Hasegawa-Kishino-Yano (HKY) sequence evolution model (Hasegawa et al. 1985) and estimated base frequencies from the data. We also provided a starting species-tree for all analyses, which was assumed to follow a Yule speciation process. Analyses were run for 2 billion steps for the rodent-lagomorph species-tree and 1.5 billion steps for the *Tamiasciurus* species-tree, were logged at every 100,000 steps, and had the first 10% of the run discarded as burn-in.

We assessed stationarity by examining trace plots and whether effective sample size (ESS) values exceeded >200 using TRACER 1.5 (Rambaut and Drummond 2007). Three independent runs were performed for each species-tree estimate to assure convergence in the MCMC. We also checked if the priors had undue influence on the posterior estimates by running the analysis for each species-tree with an empty alignment (generated by BEAUTi). Summary trees were generated with TreeAnnotator v1.6.1, part of the BEAST package.

Mitochondrial Phylogenetic Inference

Phylogenetic analysis of the mitochondrial control region data for 54 *Tamiasciurus* individuals was performed in in BEAST v. 1.7.3. The best-fitting model for our phylogenetic analyses using the AIC score in jModeltest 0.1.1 (Posada 2008) and that was available in BEAST was the HKY + Gamma model of nucleotide substitution. The phylogenetic inference was analyzed for 100×10^6 generations (with trees sampled every 10,000 generations). The first 25% of sampled trees were discarded as burn-in after visual inspection using TRACER 1.5 (Rambaut and Drummond 2007) revealed that these initial samples had reached stationarity. In addition, we used the same 95% highest probability density (HPD) interval from the fossil-calibrated species tree analysis representing the split between *T. hudsonicus* and *T. douglasii* as a secondary calibration prior for the root of the mtDNA gene tree (Table S3).

Investigating Causes Of Mitochondrial-Nuclear Phylogenetic Discordance

To distinguish whether hybridization or incomplete lineage sorting (ILS) explains discordant relationships between the mitochondrial gene tree and nuclear species tree, we used a posterior-predictive-checking method (Joly et al. 2009) implemented in JML 1.0.1 (Joly 2012). We

specifically examined the hypothesis that mitochondrial introgression explains the closer relationship between Vancouver Island mtDNA lineage with the Douglas squirrel mtDNA clade rather than the red squirrel clade. JML uses posterior predictive checking to test whether the observed minimum distance between sequences of two species is smaller than expected under a scenario that does not account for hybridization. Replicate datasets are simulated using the coalescent from the posterior distribution of species trees from *BEAST outputs with branch lengths and population sizes. JML samples the species trees in order to generate a gene tree from which DNA sequences are then simulated. A test quantity, the minimum distance between sequences of two species, is then calculated for all replicated datasets to generate a posterior predictive distribution. The observed distance from the empirical dataset is finally compared to the posterior predictive distribution to calculate the probability that the observed distance is caused by hybridization (Joly et al. 2009). If the observed distance is smaller than 95% of the simulated valued, then we can reject ILS and conclude that the hypothesis of hybridization explains the topological discordance.

We used the output file containing the posterior distribution of 10,000 nuclear species trees from our previous *BEAST analysis on *Tamiasciurus* as the input file for the analysis in JML. We also included the mtDNA alignment as our reference sequence file. We used the mean clock rate from our previous mtDNA gene tree reconstruction in BEAST as a relative mutation rate for the JML control file.

Estimating Migration

We tested for the occurrence of historical nuclear gene flow between the *T. hudsonicus* population on Vancouver Island and three different mainland populations using IMa2 (Hey

2010). IMa2 uses a coalescent-based model of isolation with migration under a Bayesian framework to co-estimate the multilocus effective population sizes (present and ancestral), divergence times, and migration rates (Nielsen and Wakeley 2001; Hey and Nielsen 2004). IMa2 was recently modified to infer demographic parameters for multiple populations, *i.e.* two or more at a time including ancestral populations, rather than just two populations at a time (Hey 2010). However, we discovered through preliminary analyses that our data were not suited for an analysis including all populations. We defined populations based on four geographically discrete regions: (1) Vancouver Island that included all *T. hudsonicus* samples found only on Vancouver Island, (2) Northern that included *T. hudsonicus* samples only found in northern British Columbia, Yukon Territory, and Alaska, (3) Interior Montane that included *T. hudsonicus* samples found from the Coast Mountains of British Columbia southward to the Southern Rockies, and (4) Pacific Coastal that included all samples within the contiguous range of *T. douglasii* from British Columbia to California. In order to reduce the completion time for a sufficient run using the IMa2 program, we reduced the dataset to 94 randomly selected sequences. We also used the infinite sites mutation model of nucleotide substitution (Kimura 1969) because this is a reasonable model for studies with many nuclear gene loci sampled from closely related species (Hey 2011).

We performed several exploratory runs in IMa2 using 'MCMC mode' to determine the values for most efficient swapping of MCMC chains, but that also allowed for appropriate prior settings for population parameters (i.e. t [divergence time], Θ [theta], and m [migration rate]). We then performed three independent runs with different starting seeds in 'MCMC mode' to sample genealogies and obtain parameter estimates. We determined that a sufficient burn-in period of sampled genealogies was achieved after burn-in trend plots had reached a plateau. Next, we used

sampled genealogies from the 'MCMC mode' in a new analysis 'Load Geneologies Mode' to statistically evaluate whether the fully parameterized migration model ranked as a better model than four simpler nested models with fewer parameters using Akaike Information Criterion (AIC) (Table 1: Carstens et al. 2009). We also calculated two related information theoretical statistics to provide objective measures of model support: Akaike weights (ω_i), which is the normalized relative likelihoods of the model, and the evidence ratio ($E_{\min/i} = \omega_{min}/\omega_i$), which compares each model to the best model.

Ecological Niche Modeling

We gathered locality information from museum collections by searching VertNet (vertnet.org) for "*Tamiascuirus*" and downloading available records. We removed records that 1) were not georeferenced, 2) had coordinate uncertainty greater than 10 km, and 3) were sampled prior to 1950. We removed records that were duplicates of location. To account for spatial autocorrelation in sampling, the occurrence dataset was reduced by identifying pairwise distances of 10 km or less, and removal of one of the points until all occurrences were at least 10 km apart.

Bioclim variables (Hijmans et al. 2005) were obtained through WorldClim (worldclim.org), representing current and past climate conditions. Current conditions were estimated as trends from 1950–2000 and were available at 2.5 arc-minute resolutions. Data for the last glacial maximum (LGM) were available for two scenarios, CCSM (The Community Climate System Model) and MIROC (The Model for Interdisciplinary Research on Climate) reconstructions, and available at 2.5 arc-minutes, while the last interglacial (LIG) reconstruction was a representation of the CCSM scenario at 10 arc-minutes. For each era, we used 7 climate variables (annual mean temperature, mean diurnal temperature range, maximum temperature of

warmest month, minimum temperature of coldest month, annual precipitation, precipitation of wettest month, and precipitation of driest month) that have been shown to be relatively uncorrelated at large spatial scales (Jimémenz-Valverde et al. 2009).

To estimate the potential distribution of pine squirrels, we used an ecological niche model (ENM) approach, where we essentially built correlative models of occurrence and climate and projected these into geographic space. We implemented Maxent 3.3.3k (Philips et al. 2006), which results in a probability distribution of occurrence from constraints, in this case the environmental values associated with collection localities. To test our ability to predict points in novel environments, we split the *T. hudsonicus* set into west and east sets, and the *T. douglasii* into Sierra Nevada and Cascade sets, respectively (Table S4, Table S5). To create a representative background for these sets (Barve et al. 2011, Peterson et al. 2011, Anderson and Raza 2010, Soberón 2007), we buffered 100 km around each of the points because we did not expect that squirrels would disperse much farther (Larsen and Boutin 1994; Sun 1997); environmental data from current climate scenarios were clipped by these buffers. We set aside 20 percent of data from each set for testing model performance, using the remainder as a training set. Because model complexity can inhibit predictions for novel environmental space (Warren and Seifert 2011), we used the model selection feature of ENM Tools (Warren et al. 2010) that determines β settings for Maxent. We generated models for each spatial unit using the β with the lowest Akaike Information Criterion (AICc) score (Burnham and Anderson 2002) and projected these models onto the requisite partner background while converting the logistic output (Philips and Dudik 2008) to a presence/absence map using a minimum training presence threshold (Pearson et al. 2007). If the models were able to correctly predict points outside the spatial range, we were more confident in the ability to predict areas of potential occurrence in different eras. As

such, we determined the positive predictive value, i.e., the proportion of correctly predicted points, in the novel space.

To compare potential distributions at the different eras, we first repeated the buffering of occurrence points, clipping of environmental data, splitting into training and testing sets, and model selection, but for each species. We then generated Maxent models under the requisite β value, but used 10-fold cross-validation of the training set, and determined the positive predictive value of the aggregated thresholded (by minimum training presence) maps. Again, if we expect to mimic the potential distribution of the species, the positive predictive value should be high. The models were projected onto the extent of North America to cover the geographic range of both species, both LGM reconstructions, and LIG reconstruction. Results were summarized as the sum of the cross-validation models and clipped based on the limiting novel climate (Elith et al. 2010) and estimates of the extent of the glacial extent at LGM (Aber et al. 1995, Manley and Kauffman 2002) using a script and the R package raster (R Development Core Team 2012, Hijmans and van Etten. 2012). Similarity measures (Warren et al. 2008) were calculated through ENM tools at 3 scales: current climate, LGM reconstructions (CCSM and MIROC), and LIG, at an extent focused on Vancouver Island and surrounding mainland region.

Results

Population Structure

Based on our analysis of 15 nuclear introns, the inferred number of ancestral populations of *Tamiasciurus* in North America is nine, consisting of seven geographically segregated populations within *Tamiasciurus hudsonicus* [Ln P(D) = -1812.65] and two populations representing *T. douglasii* and *T. mearnsi* [Ln P(D) = -4017.5] (Fig. 1, Table S1). We also found

that about 7% of the samples possess genetic contributions from two or three geographically proximate populations (Fig. 1 checkered circles, Table S1).

Timing Of Divergence

Our analysis of *Tamiasciurus* lineages shows that contemporary populations have diverged from one another within only about the past 300,000 years (Fig. 3), during the Pleistocene, whereas the genus *Tamiasciurus* itself diverged from the sister genus *Sciurus* in the middle Miocene, over 8 million years ago (Fig. S1). Specifically, the most recent common ancestor (MRCA) of *T. douglasii* and *T. hudsonicus* was estimated at only 220,000 years ago, with a 95% highest posterior density (HPD) interval of 125,000-340,000 years ago (Fig. 3). The genus *Tamiasciurus* last shared a MRCA with *Sciurus* at around 8.52 million years ago (Ma) (95% HPD interval 8.00-9.55 Ma) (Fig. S1).

Within our species tree for *Tamiasciurus* (Fig. 3), most of the structuring has occurred within the *T. hudsonicus* clade (seven lineages), in contrast to that of *T. douglasii* (only two lineages). The most recent divergence has occurred between the TH-Vancouver Island and the more northerly TH-Mainland BC Coast lineages, only 4,600-20,000 years ago (Fig. 3). These two lineages are nested within a clade that includes three other interior montane lineages.

Mitochondrial Gene-Tree Inference

Our mtDNA gene tree for 54 *Tamiasciurus* specimens revealed structure consisting of two major clades that generally correspond with the two species (Fig. 4): (1) a *T. douglasii* clade of 14 specimens representing the geographic range of that species and 8 samples from Vancouver Island that are described as *T. hudsonicus*; and (2) a large and geographically expansive

continental clade of *T. hudsonicus*, represented by 32 specimens that span from Alaska, throughout the Rocky Mountains, and across the continent to eastern North America. The Vancouver Island lineages of *T. hudsonicus* are nested within the *T. douglasii* clade (Fig. 4) and thus their topology is discordant with that of the nuclear species tree (Fig. 3).

Distinguishing Hybridization From Incomplete Lineage Sorting

Our use of JML resulted in demonstration that incomplete lineage sorting cannot explain the data, thus sustaining the interpretation that hybridization has occurred. The analysis specifically showed evidence of mitochondrial introgression of *T. douglasii* mtDNA haplotypes into the Vancouver Island population. The observed pairwise genetic distance between Vancouver Island mtDNA lineages and *T. douglasii* lineages was smaller than 99% of the simulated minimum distance values (p-value < 0.001).

Gene Flow To And From Vancouver Island

Our analysis of historical nuclear gene flow shows three different patterns of directional migration (Table 2). The best-supported model (lowest AIC score) between the Vancouver Island and Interior Montane populations of *T. hudsonicus* supported a strict divergence model (Model 5) that contained zero migration following the divergence between these populations. The best-supported model between the Vancouver Island and Northern populations of *T. hudsonicus* contained unequal migration rates (Model 1) between the populations. However, the evidence ratio was very similar to the next best model (Model 5). Finally, the best-supported model between the Vancouver Island and Pacific Coastal populations of *T. douglasii* contained equal

migration (Model 2) between these two populations even though their migration rates were very low, at 0.0628.

Ecological Niche Modeling For Tamiasciurus

Our application of bioclimatic envelope modeling estimated broad geographic overlap in the potentially suitable ecological spaces of *Tamiasciurus hudsonicus* and *T. douglasii* over the past 130,000 years, i.e., from the time of the last interglacial, through the last glacial maximum, and continuing through the present (Fig. 5, Fig. S2, Table S6). Both species were predicted to have found habitat in suitable climatic space across much of western North America. Remarkably, the environment of Vancouver Island and surrounding mainland appears to have been suitable for both species throughout this entire period.

Discussion

*Origin And Diversification Of Pine Squirrels (*Tamiasciurus*)*

Diversification has occurred surprisingly recently in the evolutionary history of the genus *Tamiasciurus*, given that it split from its sister genus *Sciurus* about 8 - 9 million years ago. Our computation, based on 15 nuclear introns, indicates that the contemporary species did not arise until the past half a million years. Thus *Tamiasciurus* has apparently existed as a monotypic genus for 95% of its history. This is surprising given the vast contemporary distribution of the two species across North America. One explanation for the lack of early diversification in pine squirrels may be their ecological specialization on temperate coniferous forests (Steele 1998, 1999), which contrasts with the broad predominance of grassland communities in North America during the Miocene. The drier and warmer Miocene climates forced most boreal forest taxa to the

margins of the continent (Axelrod et al. 1991; Thompson and Fleming 1996; Williams et al. 2008). The contemporary distribution of the two *Tamiasciurus* species, together with the associated bioclimatic evidence (Fig. 5), illustrates the apparent historical elaboration of conditions that match the ecological niches currently occupied by these two species of coniferous tree specialists.

The changing paleoenvironments of the Pleistocene set the stage for diversification of *Tamiasciurus* into its multiple lineages. Our findings are consistent with previous divergence estimates (Arbogast et al. 2001) in showing that the first split in this genus, between *T. hudsonicus* and *T. douglasii*, followed the major climatic transition in which low-amplitude 40,000-year climatic cycles were replaced by high-amplitude 100,000-year climatic cycles that increased the severity and duration of cold periods (Head and Gibbard 2005). The repeated expansion and retreat of huge continental ice sheets that covered vast areas of northern North America and the associated changes in vegetation communities (Booth et al. 2003) suggest that large fluctuations also occurred in the distribution of *Tamiasciurus*. For example, most of the contemporary distribution of *Tamiasciurus* at high latitudes is found within areas that were covered by continental ice sheets during the last glacial maximum. Moreover, records of extralimital *Tamiasciurus* fossils from the Pleistocene are located in areas of the southern United States that no longer harbor boreal forest (Graham et al. 1996; Steele 1998, 1999).

Our nuclear phylogeny demonstrates that diversification was more extensive within the more broadly distributed *T. hudsonicus* than in *T. douglasii*. Diversification of the most recent lineages of *T. hudsonicus* (our lineages 4-8, Fig. 3) occurred along the major north-south mountainous axes of western North America that span from Vancouver Island and the coastal mountains of British Columbia to the southern Rocky Mountains. In contrast, the only significant

divergence found within *T. douglasii* is between the single major clade associated with the Cascade and Sierra Nevada ranges along the Pacific Coast and the relict population of *T. douglasii mearnsi* in the mountains of northern Baja California, Mexico. One explanation for the disparity in the rate of diversification between the two species may be the finer-scale geological subdivision in the Rocky Mountain range versus the more uniform character of the Pacific Coastal montane axis. The Rocky Mountains are comprised of many subranges that are separated by intervening lowland xeric habitats, whereas the Pacific Coastal montane axis is less subdivided and possesses a milder and more humid maritime climate that has promoted a proliferation of more or less continuous lowland forest.

Colonization Of Vancouver Island

Based on the nuclear phylogeny, the pine squirrel population on Vancouver Island originated from an interior continental refugium that harbored an ancestral source population of *T. hudsonicus* (Fig. 2C). Divergence between the Vancouver Island and coastal British Columbia populations occurred between 4,600 and 20,000 years ago, which suggests that dispersal onto the island from the mainland likely occurred following the Last Glacial Maximum (LGM), in the late Pleistocene. The recentness of this divergence does not support the coastal refugium scenario of *Tamiasciurus* persisting along an ice-free part of the outer coast of Vancouver Island during the LGM. Geological evidence shows that this region was severely impacted by the full expansion of the Cordilleran Ice Sheet onto Vancouver Island around 20,000 years ago (Blaise et al. 1990; Porter and Swanson 1998; Dallimore et al. 2008). The ice sheet during this period expanded from the mainland and is believed to have reached most of the continental shelf outside the west coast of Vancouver Island, which would have obliterated all of the island's terrestrial vegetation

(Clague and James 2002; Ward et al. 2003). Proponents of the coastal refugium hypothesis suggest that unglaciated high-elevation sites (nunataks) and some parts of the continental shelf that are now submerged may have harbored some plants and animals (Haggarty and Hebda 1997). However, this scenarios does not appear to have applied to pine squirrels.

Several previous studies have demonstrated similar westward expansion of plants and animals from an interior montane refugium into deglaciated coastal regions following the LGM (Richardson et al. 2002; Carstens et al. 2005; Brunsfeld et al. 2007). Even though the Vancouver Island lineage of *T. hudsonicus* is closely related to Rocky Mountain lineages, paleoecological reconstructions of Pacific Coastal regions during the LGM suggest that the island lineage may have originated from a closer coastal refugium south of the continental ice sheet. Plant macro-fossils and pollen records show that periglacial regions near the coast harbored cold-environment coniferous tree species, including *Picea engelmannii* (Engelmann spruce), *Pinus contorta* (lodgepole pine), and *Abies lasiocarpa* (subalpine fir) during the LGM (Barnosky 1981; Hicock et al. 1982; Heusser et al. 1999). We suspect that *T. hudsonicus* rather than *T. douglasii* may have occurred in this region, because this paleo-community shares many characteristics with the modern subalpine parkland environment now found in the northern Rocky Mountains (Barnosky et al. 1987), which is also currently inhabited by *T. hudsonicus*.

The timing and route of postglacial dispersal by mainland *T. hudsonicus* and other terrestrial mammals (Nagorsen and Keddie 2000; Wilson et al. 2009) onto Vancouver Island have been difficult to identify and were likely influenced by several factors, including postglacial adjustments in the earth's surface, changes in local and global sea levels, and transitions in vegetation communities (Clague et al. 1982, 1983; Riddihough 1982; Fairbanks 1989; Fedje et al. 2005). The post-LGM decay rate of the Cordilleran ice sheet was rapid, and by 14,000 years ago

major portions of Vancouver Island were already ice free (Hebda 1983; Huntley et al. 2001; Ward et al. 2003). The immense mass of the retreating Cordilleran ice sheet produced isostatic uplifts of the earth's surface and subsequent changes in sea level along the north Pacific coastline, including areas surrounding Vancouver Island (Hetherington et al. 2004; Dallimore et al. 2008; James et al. 2008). The extreme northern part of Vancouver Island is the most plausible area for a land bridge, and it remains an area of virtual contact with the mainland. Paleogeographical studies have shown sea-floor emergence with coniferous forests in the northern parts of the island around 12,000 years ago (Luternauer et al. 1989; Lacourse et al. 2003; Hutchinson et al. 2004; James et al. 2008). *Tamiasciurus hudsonicus* that crossed onto Vancouver Island at this time thus would have experienced a familiar vegetation community containing cold-environment conifers (Haggarty and Hebda 1997; Lacourse et al. 2003; Dyke 2005). Interestingly, gene flow between the Vancouver Island and mainland populations of *T. hudsonicus* appears to have been brief, as our migration analysis revealed a lack of gene flow following their divergence.

The current enigmatic and exceptional biogeographic arrangement of *T. hudsonicus* on Vancouver Island and intervening *T. douglasii* on the nearby mainland coast (Fig. 1) seems to be consistent with their respective strong historical ecological associations with the different forest communities with which they are associated across the rest of their respective current geographic ranges. Our ecological niche models for *T. hudsonicus* and *T. douglasii* show support for broad overlap of their abiotic niches. This pattern suggests that spatial segregation between the two species was not due to differences in gross climatic niche parameters, but rather that it may have been due to factors such as differential competitive abilities in different forest types (Smith 1968; 1970; 1981). T*amiasciurus hudsonicus* typically inhabits drier forests with cold winters, and *T.*

douglasii inhabits mesic forests with milder winters (Steele 1989; 1999). Paleoecological records from Vancouver Island and nearby mainland areas show dramatic changes in forest composition during the Holocene that are attributed to regional climate changes (Whitlock 1992; Brown and Hebda 2003; Dyke 2005). The warmer climate since the LGM led to the development of a more mesic forest in this region, whereas cold-coniferous species shifted further north, east, or upslope. The two species of squirrels on the mainland apparently responded to these changes by matching the distribution of their preferred forests. The fossil record shows that *Tamiasciurus*, like many other boreal mammals, showed strong niche conservatism (Martínez-Meyer et al. 2004) and moved with major northward shifts of boreal forests following the LGM; they completely abandoned areas that no longer supported boreal forests in the southern United States (Paleobiology Database, http://www.paleodb.org). We suspect that unusual biogeographic arrangement of pine squirrels in this region was due to the inability of the *T. hudsonicus* population on Vancouver Island to track its preferred forests northward following their isolation on the island.

The currently close proximity of Vancouver Island to the mainland (<3 km at the north end of the island) provides potential opportunities for interbreeding between the two pine squirrel species. These two species are known from a nearby hybrid zone on the mainland to be able to produce reproductively viable offspring (Chavez et al. 2011). Our nuclear gene flow findings show a history of gene flow, albeit at low levels, between the island population and *T. douglasii*. These findings are supported by our mtDNA phylogeny that shows all Vancouver Island lineages to be more closely related to *T. douglasii* than *T. hudsonicus* (Fig. 2D). This relationship is striking because the nuclear phylogeny shows the Vancouver lineage is sister to the interior montane lineage of *T. hudsonicus* and is distant from the *T. douglasii* lineage. Discordance

between phylogenies can also be attributed to incomplete lineage sorting. However, we have shown that hybridization is a better explanation for this discordance than incomplete lineage sorting. Our findings indicate that introgression of mtDNA haplotypes from mainland *T. douglasii* occurred into the island population. The lack of similar hybridization patterns from our nuclear analyses is perplexing. Given that individuals with introgressed mtDNA are found at least 100 kilometers from the center of the nearby hybrid zone (Chavez et al. 2011), we hypothesize that the founding population of *T. hudsonicus* on Vancouver Island may have already been introgressed with mtDNA from *T. douglasii*.

Northern Refugium

Vancouver Island represents the most southerly in a series of continental islands in the northern Pacific Coast region (Fig. 1) that is recognized for harboring endemic island mammal populations (Cook and McDonald 2001). Both molecular and fossil data support the persistence of many species of plants and mammals in a North Pacific Coastal Refugium on the Alexander Archipelago and Haida Gwaii during the LGM (Byun et al. 1999; Burg et al. 2005; Cook at al. 2006). Natural populations of *Tamiasciurus* are notably absent from the outer islands of the Alexander Archipelago and Haida Gwaii (MacDonald and Cook 2007; Palmer et al. 2007), suggesting that these islands, like Vancouver Island, did not serve as a coastal refugium for *Tamiasciurus* through the LGM. In fact, fossil records show that many small mammal species, unlike some large mammals such as bears (*Ursus arctos* and *U. americanus*), were extirpated by continental ice sheets during the LGM and were unable to recolonize these islands once favorable habitats returned (Conroy et al. 1999; Heaton and Grady 2003). The close genetic similarity of all northern *T. hudsonicus* populations (Fig. 3, number 3 TH-North) suggests there was only one

refugium for pine squirrels, far in the north. We suggest that no *T. hudsonicus* were present in the North Pacific Coastal Refugium (Cook et al. 2006) during the LGM, but that colonization of coastal southeastern Alaska that was formerly glaciated occurred from the more northerly refugium of the Alaskan and Yukon interior. The persistence of this northern *T. hudsonicus* lineage in the subarctic region reinforces the idea that an entire ecosystem of boreal biota existed in this area throughout the LGM (Anderson et al. 2006, 2011; Zazula et al. 2006; Godbout et al. 2008).

The duration of speciation events in mammals typically amounts to about two million years (Avise et al. 1998). We have demonstrated, through molecular data and a synthesis of ecological information, a much more rapid and recent divergence within the genus *Tamiasciurus* into two species, within only the past half million years. The existence of a narrow hybrid zone (Chavez et al. 2011) between these species is also suggestive of recent speciation. The close association of each of the two species with a specific, different forest environment and the ease with which their conspicuous behavior and distribution can be observed should provide further opportunities to examine the degree of their contemporary reproductive isolation and its relation to lineage diversification.

Literature Cited

Aber, J. S., J. P. Bluemle, J. Brigham-Grette, L. A, Dredge, D. J. Sauchyn, and D. L. Ackerman. 1995. Glaciotectonic map of North America, scale 1:6,500,000. Geological Society of America, Maps and Charts Series, MCH079.

Anderson, L. L., F. S. Hu, D. M. Nelson, R. J. Petit, and K. N. Paige. 2006. Ice-age endurance: DNA evidence of a white spruce refugium in Alaska. Proc. Nat. Acad. Sci. USA 103:12447-12450.

Anderson, P. M., and L. B. Brubaker. 1994. Vegetation history of northcentral Alaska: a mapped summary of late-Quaternary pollen data. Quat. Sci. Rev. 13:71-92.

Anderson, R. P., and A. Raza. 2010. The effect of the extent of the study region on GIS models of species geographic distributions and estimates of niche evolution: preliminary tests with montane rodents (genus *Nephelomys*) in Venezuela. J. Biogeogr. 37:1378-1393.

Arbogast, B. S., R. A. Browne, and P. D. Weigl. 2001. Evolutionary genetics and Pleistocene biogeography of North American tree squirrels (*Tamiasciurus*). J. Mammal. 82:302-319.

Avise, J. C., D. Walker, and G. C. Johns. 1998. Speciation durations and Pleistocene effects on vertebrate phylogeography. Proc. R. Soc. Lond B 265:1707-1712.

Axelrod, D. I., M. T. K. Arroyo, and P. H. Raven. 1991. Historical development of the temperate vegetation in the Americas. Rev. Chil. Hist. Nat. 64:413-446.

Barnosky, C. W. 1981. A record of late Quaternary vegetation from Davis Lake, southern Puget lowland, Washington. Quatern. Res. 16:221-239.

Barnosky, C. W., P. M. Anderson, and P. J. Bartlein. 1987. The Northwestern U.S. during deglaciation; Vegetational history and paleoclimatic implications. In: North America and Adjacent Oceans During the Last Deglaciation (eds. W. F. Ruddiman and H. E. Wright Jr.),pp. 289–321. The Geology of North America, Vol. K-3. Geological Society of America, Boulder, CO.

Barton, N. H., and J. Mallet. 1996. Natural selection and random genetic drift as causes of evolution on islands [and discussion]. Philos. Trans. R. Soc. Lond., B, Biol. Sci. 351:785-795.

Barve, N., V. Barve, A. Jiménez-Valverde, A. Lira-Noriega, S. P. Maher, A. Peterson, J. Soberóna, and F. Villalobos. 2011. The crucial role of area accessibility in ecological niche modeling and species distribution modeling. Ecol. Modell. 222:1810-1819.

Blair Hedges, S., and S. Kumar. 2004. Precision of molecular time estimates. Trends Genet. 20:242-247.

Blaise, B., J. J. Clague, and R. W. Mathewes. 1990. Time of maximum Late Wisconsin glaciation, west coast of Canada. Quatern. Res. 34:282-295.

Booth, D. B., K. G. Troost, J. J. Clague, R. B.Waitt. 2003. The Cordilleran ice sheet. Devel. Quat. Sci. 1:17–43.

Brown, K. J., and R. J. Hebda. 2003. Coastal rainforest connections disclosed through a Late Quaternary vegetation, climate, and fire history investigation from the Mountain hemlock zone on southern Vancouver Island, British Columbia, Canada. Rev. Palaeobot. Palyno. 123:247-269.

Brown, R. P., and Z. Yang. 2011. Rate variation and estimation of divergence times using strict and relaxed clocks. BMC Evol. Biol. 2011 11:271.

Brunsfeld S. J., T. R. Miller, and B. C. Carstens. 2007. Insights into the biogeography of the Pacific Northwest of North America: evidence from the phylogeography of *Salix melanopsis*. Syst. Bot. 32:129-139.

Burg, T. M., A. J. Gaston, K. Winker, and V. L. Friesen. 2005. Rapid divergence and postglacial colonization in western North American Steller's jays (*Cyanocitta stelleri*). Mol. Ecol. 14:3745-3755.

Burnham, K. P., and D. R. Anderson. 2002. Model selection and multi-model inference: a

practical information-theoretic approach. Springer. New York

Byun, S. A., B. F. Koop, and T. E. Reimchen. 1997. North American black bear mtDNA phylogeography: implications for morphology and the Haida Gwaii glacial refugium controversy. Evolution 51:1647-1653.

Byun, S. A., B. F. Koop, and T. E. Reimchen. 1999. Coastal refugia and postglacial colonization routes: A reply to Demboski, Stone, and Cook. Evolution 53:2013-2015.

Carrara, P. E., T. A. Ager, and J. F. Baichtal. 2007. Possible refugia in the Alexander Archipelago of southeastern Alaska during the late Wisconsin glaciation. Can. J. Earth Sci. 44:229-244.

Carstens, B. C., S. J. Brunsfeld, J. R. Demboski, J. M. Good, and J. Sullivan. 2005. Investigating the evolutionary history of the Pacific Northwest mesic forest ecosystem: hypothesis testing within a comparative phylogeographic framework. Evolution 59:1639–1652.

Carstens, B. C., H. N. Stoute, and N. M. Reid. 2009. An information‐theoretical approach to phylogeography. Mol. Ecol. 18:4270-4282.

Chavez, A. S., C. J. Saltzberg, and G. J. Kenagy 2011. Genetic and phenotypic variation

across a hybrid zone between ecologically divergent tree squirrels (*Tamiasciurus*). Mol. Ecol. 20:3350-3366.

Clague, J. J., and T. S James. 2002. History and isostatic effects of the last ice sheet in southern British Columbia. Quat. Sci. Rev. 21:71–87

Clague, J. J., J. R. Harper, R. J. Hebda, and D. E. Howes. 1982. Late Quaternary sea levels and crustal movements, Coastal British Columbia. Can. J. Earth Sci. 19:597-618.

Clague, J. J., J. L. Luternauer, and R. J. Hebda. 1983. Sedimentary Environments and Postglacial History of the Fraser River Delta and Lower Fraser River Valley, British Columbia. Can. J. Earth Sci. 20:1314-1326.

Conroy, C. J., J. R. Demboski, and J. A. Cook. 1999. Mammalian biogeography of the Alexander Archipelago of Southeast Alaska: a north temperate nested fauna. J. Biogeog. 26:343-352.

Cook, J. A., and S. O. MacDonald. 2001. Should endemism be a focus of conservation efforts along the north Pacific coast of North America? Biol. Conserv. 97:207-213.

Cook, J. A., N. G. Dawson, and S. O. MacDonald. 2006. Conservation of highly fragmented systems: The north temperate Alexander Archipelago. Biol. Conserv. 133:1-15.

Dallimore, A., R. J. Enkin, R. Pienitz, J. R. Southon, J. Baker, C. A. Wright, T. F. Pedersen, S. E. Calvert, T. Ivanochko, and R. E. Thomson. 2008. Postglacial evolution of a Pacific coastal fjord in British Columbia, Canada: interactions of sea-level change, crustal response, and environmental fluctuations — results from MONA core MD02-2494. Can. J. Earth Sci. 45:1345-1362.

Drummond, A., and A. Rambaut. 2007. Beast: Bayesian evolutionary analysis by sampling trees. BMC Evol. Biol. 7:214.

Dyke, A. S. 2005. Late Quaternary vegetation history of northern North America based on pollen, macrofossil, and faunal remains. Géogr. Phys. Quatern. 59:211-262.

Elith, J., M. Kearney, and S. Phillips. 2010. The art of modelling range‐shifting species. Method Ecol. Evol. 1:330-342.

Fairbanks, R. G. 1989. A 17,000-year glacio-eustatic sea level record: influence of glacial melting rates on the Younger Dryas event and deep-ocean circulation. Nature 342:637-642.

Fedje, D. W., and H. Josenhans. 2000. Drowned forests and archaeology on the continental shelf of British Columbia, Canada. Geology 28: 99–102.

Fedje, D. W., H. Josenhans, J. J. Clague, J. V. Barrie, D. J. W. Archer, and J. R. Southon. 2005. Hecate Strait paleoshorelines. In Haida Gwaii: Human History and Environment from the Time of Loon to the Time of the Iron People (eds. D. W. Fedje and R. W. Mathewes), pp. 21–37. UBC Press, Vancouver.

Gavrilets, S., and A. Hastings. 1996. Founder effect speciation: a theoretical reassessment. Am. Nat. 147:466-491.

Godbout, J., A. Fazekas, C. H. Newton, F. C. Yeh, and J. Bousquet. 2008. Glacial vicariance in the Pacific Northwest: evidence from a lodgepole pine mitochondrial DNA minisatellite for multiple genetically distinct and widely separated refugia. Mol. Ecol. 17:2463-2475.

Graham R. W., E. L. Lundelius, Jr., M. A. Graham et al. 1996. Spatial response of mammals to Late Quaternary environmental fluctuations. Science 272:1601-1606.

Haggarty, J. C., and R. J. Hebda. 1997. Brooks Peninsula: an ice age refugium on Vancouver Island. British Columbia Ministry of Environment, Lands and Parks, Occasional Paper No. 5, Victoria, Canada.

Hall, E. R. 1981. The mammals of North America. John Wiley and Sons, New York.

Hasegawa, M., H. Kishino, and T. Yano. 1985. Dating of the human-ape splitting by a

molecular clock of mitchondrial DNA. J. Mol. Evol. 22:160-174.

Head M. J., and P. L. Gibbard. 2005. Early-middle Pleistocene transitions: an overview and recommendation for the defining boundary. In: Early–Middle Pleistocene Transitions: The Land-Ocean Evidence. Special Publications, Vol. 247 (eds. M. J. Head and P. L. Gibbard), pp. 1–18. Geological Society, London.

Heaton, T., and F. Grady. 2003. The Late Wisconsin vertebrate history of Prince of Wales Island, Southeast Alaska. In: Ice age cave faunas of North America. (eds. B. W. Schubert, J. I. Mead, and R. W. Graham), pp. 17–53, Indiana University Press.

Hebda, R. J. 1983. Late-Glacial and Postglacial Vegetation History at Bear Cove Bog, Northeast Vancouver Island, British Columbia. Can. J. Bot. 61:3172-3192.

Heled, J., and A. Drummond. 2010. Bayesian inference of species trees from multilocus data. Mol. Biol. Evol. 27:570-580.

Hetherington, R., J. V. Barrie, R. G. B. Reid, R. MacLeod, and D. J. Smith. 2004. Paleogeography, glacially induced crustal displacement, and Late Quaternary coastlines on the continental shelf of British Columbia, Canada. Quat. Sci. Rev. 23:295-318.

Heusser C. J., L. E. Heusser, and D. M. Peteet. 1999. Humptulips revisited: a revised

interpretation of Quaternary vegetation and climate of western Washington, USA. Palaeogeogr. Palaeoclimatol. Palaeoecol. 150:191-221.

Hey, J. 2010. Isolation with migration models for more than two populations. Mol. Biol. Evol. 27:905-920.

Hey, J. 2011. Documentation for IMa2, pp. 60.

Hey, J., and R. Nielsen. 2004. Multilocus methods for estimating population sizes, migration rates and divergence time, With applications to the divergence of *Drosophila pseudoobscura* and *D. persimilis*. Genetics 167:747–760.

Hey, J., and R. Nielsen. 2007. Integration within the Felsenstein equation for improved Markov chain Monte Carlo methods in population genetics. Proc. Natl. Acad. Sci. USA 104:2785-2790.

Hicock, S. R., R. J. Hebda, and J. E. Armstrong. 1982. Lag of the Fraser glacial maximum in the Pacific Northwest: pollen and macrofossil evidence from western Fraser Lowland, British Columbia. Can. J. Earth Sci. 19:2288-2296.

Hijmans, R. J., S. E. Cameron, J. L. Parra, P. G. Jones, and A. Jarvis. 2005. Very high resolution interpolated climate surfaces for global land areas. Int. J. Climatol. 25: 1965-1978.

Hijmans R. J., and J. van Etten. 2012. Raster: geographic analysis and modeling with raster data, R package version 1.9-58.

Ho, S. Y. 2007. Calibrating molecular estimates of substitution rates and divergence times in birds. J. Avian Biol. 38:409-414.

Ho, S. Y., U. Saarma, R. Barnett, J. Haile, and B. Shapiro. 2008. The effect of inappropriate calibration: three case studies in molecular ecology. PLoS ONE 3:e1615.

Holder, M. T., J. A. Anderson, and A. K. Holloway. 2001. Difficulties in detecting hybridization. Syst. Biol. 50:978–982.

Hubisz, M. J., D. Falush, M. Stephens, and J. K. Pritchard. 2009. Inferring weak population structure with the assistance of sample group information. Mol. Ecol. Resour. 9:1322-1332.

Huntley, D. H., P. T. Bobrowsky, and J. J. Clague. 2001. Ocean Drilling Program Leg 169S: surficial geology, stratigraphy and geomorphology of the Saanich Inlet area, southeastern Vancouver Island, British Columbia. Mar. Geol. 174:247-241.

Hutchinson, I., T. S. James, J. J. Clague, J. V. Barrie, and K. W. Conway. 2004.

Reconstruction of late Quaternary sea-level change in southwestern British Columbia from sediments in isolation basins. Boreas 33:183-194.

Igea, J., J. Juste, and J. Castresana. 2010. Novel intron markers to study the phylogeny of closely related mammalian species. BMC Evol. Biol. 10:369.

James, T. S., E. J. Gowan, I. Hutchinson, J. J. Clague, J. V. Barrie, and K. W. Conway. 2009. Sea-level change and paleogeographic reconstructions, southern Vancouver Island, British Columbia, Canada. Quat. Sci. Rev. 28:1200-1216.

Jimémenz-Valverde, A., Y. Nakazawa, A. Lira-Noriega, and A. T. Peterson. 2009. Environmental correlation structure and ecological niche model projections. Biodiv. Informat. 6:28-35.

Joly, S. 2011. JML: testing hybridization from species trees. Mol. Ecol. Resour. 12:179-184.

Joly S., P. A. McLenachan,and P. J. Lockhart. 2009. A statistical approach for distinguishing hybridization and incomplete lineage sorting. Am. Nat. 174:E54–E70.

Kimura, M. 1969. The number of heterozygous nucleotide sites maintained in a finite population due to steady flux of mutations. Genetics 61:893-903.

Lacourse, T., R. W. Mathewes, and D. W. Fedje. 2003. Paleoecology of late-glacial

terrestrial deposits with in situ conifers from the submerged continental shelf of western Canada. Quatern. Res. 60:180-188.

Larsen, K. W., and S. Boutin. 1994. Movements, survival, and settlement of red squirrel (*Tamiasciurus hudsonicus*) offspring. Ecology 75:214-223.

Lindsay, S. L. 1981. Taxonomic and biogeographic relationships of Baja California chickarees (*Tamiasciurus*). J. Mammal. 62:673-682.

Losos, J. B., and R. E. Ricklefs. 2009. Adaptation and diversification on islands. Nature 457:830-836.

Luternauer, J. L., J. J. Clague, K. W. Conway, J. V. Barrie, B. Blaise, and R. W. Mathewes. 1989. Late Pleistocene terrestrial deposits on the continental shelf of western Canada: evidence for rapid sea-level change at the end of the last glaciation. Geology 17:357-360.

MacDonald, S. O., and J. A. Cook. 2007. The mammals and amphibians of Southeast Alaska. Museum of Southwestern Biology, Special Publication 8:1-191.

Maddison, W. P. 1997. Gene trees in species trees. Syst. Biol. 46:523–536.

Manley, W. F., and D. S. Kaufman. 2002. Alaska paleoglacier atlas. Institute of Arctic

and Alpine Research (INSTAAR), University of Colorado, Boulder, CO.

Martínez-Meyer, E., A. T. Peterson, and W. W. Hargrove. 2004. Ecological niches as stable distributional constraints on mammal species, with implications for Pleistocene extinctions and climate change projections for biodiversity. Global Ecol. Biogeogr. 13:305–314.

Mayr, E. 1982. The growth of biological thought: diversity, evolution and inheritance. Cambridge, Massachusetts: Belknap Press.

Menounos, B., G. Osborn, J. J. Clague, and B. H. Luckman. 2009. Latest Pleistocene and Holocene glacier fluctuations in western Canada. Quat. Sci. Rev. 28: 2049-2074.

Milne, I., F. Wright, G. Rowe, D. Marshall, D. Husmeier, and G. McGuire. 2004. TOPALi: software for automatic identification of recombinant sequences within DNA multiple alignments. Bioinformatics 20:1806-1807.

Mullen, L. M., and H. E. Hoekstra. 2008. Natural selection along an environmental gradient: a classic cline in mouse pigmentation. Evolution 62:1555-1570.

Nagorsen, D. W. 2005. Rodents & Lagomorphs of British Columbia. Royal British Columbia Museum, Victoria, British Columbia, Canada.

Nagorsen, D. W., and G. Keddie. 2002. Late Pleistocene mountain goats (*Oreamnos americanus*) from Vancouver Island: biogeographic implications. J. Mammal. 81:666-675.

Nagorsen, D. W., and A. Cardini. 2009. Tempo and mode of evolutionary divergence in modern and Holocene Vancouver Island marmots (*Marmota vancouverensis*) (Mammalia, Rodentia). J. Zool. Syst. Evol. Res. 47:258-267.

Nielsen, R., and J. Wakeley. 2001. Distinguishing migration from isolation: a Markov chain Monte Carlo approach. Genetics 158:885-896.

Palmer, G. H., J. L. Koprowski, and T. Pernas. 2007. Tree squirrels as invasive species: conservation and management implications. In: Managing vertebrate invasive species: proceedings of an international symposium (eds. G. L. Witmer, W. C. Pitt, and K. A. Fagerstone), pp. 273-282. United States Department of Agriculture, Animal and Plant Health Inspection Service Wildlife Services, National Wildlife Research Center, Fort Collins, Colorado.

Pearson, R. G., C. J. Raxworthy, M. Nakamura, and A. T. Peterson. 2007. Predicting species distributions from small numbers of occurrence records: A test case using cryptic geckos in Madagascar. J. Biogeogr. 34:102-117.

Peterson, A. T., J. Soberón, R. G. Pearson, R. P. Anderson , E. Martínez-Meyer, M.

Nakamura, and M. B. Araujo. 2011. Ecological Niches and Geographic Distributions (MPB-49) Princeton University Press. New Jersey.

Phillips, S. J., R. P. Anderson, R. E. Schapire. 2006. Maximum entropy modeling of species geographic distributions. Ecol. Modell. 190:231–259.

Phillips, S. J., and M. Dudík. 2008. Modeling of species distributions with Maxent: New extensions and a comprehensive evaluation. Ecography 21: 161-175.

Porter, S. C., and T. W. Swanson. 1998. Radiocarbon age constraints on rates of advance and retreat of the Puget Lobe of the cordilleran ice sheet during the last glaciation. Quatern. Res. 50:205-213.

Posada, D. 2008. jModelTest: phylogenetic model averaging. Mol. Biol. Evol. 25:1253–1256.

Pritchard, J. K., M. Stephens, and P. Donnelly. 2000. Inference of population structure using multilocus genotype data. Genetics 155:945-959.

Pritchard, J. K., W. Wen, and D. Falush. 2007. Documentation for STRUCTURE software: Version 2.3.2 Available from http://pritch.bsd.uchicago.edu.

R Development Core Team. 2012. R: A language and environment for statistical

computing. R Foundation for Statistical Computing, Vienna, Austria. http://www.R-project.org/.

Rambaut, A., and A. J. Drummond. 2007. Tracer v1.5. Available at http://beast.bio.ed.ac.uk/Tracer. Accessed 15 January 2010.

Richardson, B. A., S. J. Brunsfeld, and N. B. Klopfenstein. 2002. DNA from bird-dispersed seed and wind-disseminated pollen provides insights into postglacial colonization and population genetic structure of whitebark pine (*Pinus albicaulis*). Mol. Ecol. 11:215-227.

Riddihough, R. P. 1982. Contemporry movements and tectonics on Canada's west coast: A discussion. Tectonophysics 86:239-242.

Ritchie, J. C. 1987. The postglacial vegetation of Canada. Cambridge University Press, Cambridge.

Rozas, J., J. C. Sánchez-DelBarrio, X. Messeguer, and R. Rozas. 2003. DnaSP, DNA polymorphism analyses by the coalescent and other methods. Bioinformatics 19:2496–2497.

Rozen, S., and H. J. Skaletsky. 2000. Primer3 on the WWW for general users and for

biologist programmers. In: Krawetz S, Misener S (eds) Bioinformatics Methods and Protocols: Methods in Molecular Biology. Humana Press, Totowa, NJ, pp 365-386.

Shafer, A. B. A., C. I. Cullingham, S. D. Côté, and D. W. Coltman. 2010. Of glaciers and refugia: a decade of study sheds new light on the phylogeography of northwestern North America. Mol. Ecol. 19:4589-4621.

Sikes, R. S., W. L. Gannon, and the Animal Care and Use Committee of the American Society of Mammalogists. 2011. Guidelines of the American Society of Mammalogists for the use of wild mammals in research. J. Mammal. 92:235-253.

Slatkin, M. 1985. Gene flow in natural populations. Ann. Rev. Ecol. Syst 16:393-430.

Smith, C. C. 1968. The adaptive nature of social organization in the genus of three squirrels *Tamiasciurus*. Ecol. Monogr. 38:31-64.

Smith, C. C. 1970. The coevolution of pine squirrels (*Tamiasciurus*) and conifers. Ecol. Monogr. 40:349-371.

Smith, C. C. 1981. The indivisible niche of *Tamiasciurus*: an example of nonpartitioning of resources. Ecol. Monogr. 51:343–364.

Soberón, J. 2007. Grinnellian and Eltonian niches and geographic distributions of species.

Ecol. Lett. 10:1115-1123.

Steele, M. A. 1998. *Tamiasciurus hudsonicus*. Mammal. Species 586:1–9.

Steele, M. A. 1999. *Tamiasciurus douglasii*. Mammal. Species 630:1–8.

Stephens, M., N. Smith, and P. Donnelly. 2001. A new statistical method for haplotype reconstruction from population data. Am. J. Hum. Genet. 68:978-989.

Steppan, S. J., G. J. Kenagy, C. Zawadzki, R. Robles, E. A. Lyapunova, and R. S. Hoffmann. 2011. Molecular data resolve placement of the Olympic marmot and estimate dates of trans-Beringian interchange. J. Mammal. 92:1028-1037.

Sun, C. 1997. Dispersal of young in red squirrels (*Tamiasciurus hudsonicus*). Am. Midl. Nat. 138:252-259.

Swofford, D. L. 2003. PAUP∗. phylogenetic analysis using parsimony (∗and other methods). Ver 4.0b. Sinauer Associates, Sunderland, Massachusetts.

Thompson R. S., and R. F. Fleming. 1996. Middle Pliocene vegetation: reconstructions, paleoclimatic inferences, and boundary conditions for climate modeling. Mar. Micropaleontol. 27:27-49.

Thorington, R. W., Jr., and R. S. Hoffmann. 2005. Family Sciuridae. In: Mammal species of the world: a taxonomic and geographic reference (eds. D. E. Wilson and D. M. Reeder), pp. 754-818. 3rd ed. Johns Hopkins University Press, Baltimore, Maryland.

Thornton, I. 2007. Island colonization: the origin and development of island communities (ed. T. New). Cambridge University Press. New York.

Topp, C. M., and K. Winker. 2008. Genetic patterns of differentiation among five landbird species from the Queen Charlotte Islands, British Columbia. Auk 125:461-472.

Ward, B. C., M. C. Wilson, D. W. Nagorsen , D. E. Nelson, J. C. Driver, and R. J. Wigen. 2003. Port Eliza cave: North American west coast interstadial environment and implications for human migrations. Quat. Sci. Rev. 22:1383-1388.

Warren, D. L., and S. N. Seifert. 2011. Ecological niche modeling in Maxent: the importance of model complexity and the performance of model selection criteria. Ecol. Appl. 21:335-342.

Warren, D. L., R. E. Glor, and M. Turelli. 2008. Environmental niche equivalency versus conservatism: quantitative approaches to niche evolution. Evolution 62:2868-2883.

Warren, D. L., R. E. Glor, and M. Turelli. 2010. ENMTools: a toolbox for comparative studies of environmental niche models. Ecography 33:607-611.

Weckworth, B. V., N. G. Dawson, S. L. Talbot, M. J. Flamme, and J. A. Cook. 2011. Going coastal: shared evolutionary history between coastal British Columbia and Southeast Alaska wolves (*Canis lupus*). PloS ONE 6:e19582.

Whitlock, C. 1992. Vegetational and climatic history of the Pacific Northwest during the last 20,000 years: Implications for understanding present-day biodiversity. Northwest Environ. J. 8:5-28.

Williams, C. J., E. K. Mendell, J. Murphy, W. M. Court, A. H. Johnson, and S. L. Richter. 2008. Paleoenvironmental reconstruction of a Middle Miocene forest from the western Canadian Arctic. Palaeogeogr. Palaeoclim. Palaeoecol. 261:160-176.

Wilson, G. M., R. A. Den Bussche, K. McBee, L. A. Johnson, and C. A. Jones. 2005. Intraspecific phylogeography of red squirrels (*Tamiasciurus hudsonicus*) in the central rocky mountain region of North America. Genetica 125:141-154.

Wilson, M. C., S. M. Kenady, and R. F. Schalk. 2009. Late Pleistocene *Bison antiquus* from Orcas Island, Washington, and the biogeographic importance of an early postglacial land mammal dispersal corridor from the mainland to Vancouver Island. Quatern. Res. 71:49-61.

Wright, S. 1931. Evolution in Mendelian populations. Genetics 16:97-159.

Yang, Z. H., and B. Rannala. 2006. Bayesian estimation of species divergence times under a molecular clock using multiple fossil calibrations with soft bounds. Mol. Biol. Evol. 23:212–226.

Zazula, G. D., A. M. Telka, C. R. Harington, C. E. Schweger, and R. W. Mathewes. 2006. New spruce (*Picea* spp.) macrofossils from Yukon Territory: implications for late Pleistocene refugia in Eastern Beringia. Arctic 59:391-400.

Table 1. All 5 possible nested migration models within the full two-population IM model

Model Number	Model Description
1	migration not equal between pop1 and pop0
2	migration are equal between pop1 and pop0
3	migration asymmetrical: from pop1 into pop0 only
4	migration asymmetrical: from pop0 into pop1 only
5	migration equal to zero

Table 2. Summary of ranked model selection results from 'Load Geneologies Mode' in Ima2 for migration rates between the Vancouver Island population (Pop 0) and three different mainland populations (Pop 1): Interior Montane, Northern, and Pacific Coastal. All 5 nested models (Table 1) are shown for each pairwise migration analysis.

	Model No.	**Migration Rate Pop 0 → Pop 1**	**Migration Rate Pop 1 → Pop 0**	**log(P)**	***K***	**AIC**	Δ_i	ω_i	$E_{min/i}$
	5	0	0	-0.4571	3	6.914	0	0.49	1.00
Vancouver Island –	1	1.7442	3.2897	0.6034	5	8.793	1.879	0.19	2.56
Interior Montane	4	0.0001	0	-0.4571	4	8.914	2.000	0.18	2.72
	2	2.2881	2.2881	-1.286	4	10.572	3.658	0.08	6.23
	3	0	10.1878	-1.549	4	11.098	4.184	0.06	8.10
	1	0.5287	0.1894	2.639	5	4.722	0	0.27	1.00
Vancouver Island –	5	0	0	0.539	3	4.922	0.200	0.24	1.11
Northern	3	0.6568	0	1.433	4	5.134	0.412	0.22	1.23
	2	0.9788	0.9788	1.276	4	5.448	0.726	0.19	1.44
	4	0	3.1914	0.4588	4	7.082	2.360	0.08	3.26

	2	0.0628	0.0628	6.529	4	-5.058	0	0.62	1.00
Vancouver Island –	1	0.0421	0.0995	6.729	5	-3.458	1.600	0.28	2.23
Pacific Coastal	3	0	0.6214	4.684	4	-1.368	3.690	0.10	6.33
	4	0.0308	0	0.1027	4	7.795	12.853	0.00	617.88
	5	0	0	-11.53	3	29.060	34.118	0.00	>1000

'➔' direction of migration forward in time; '*K*' number of model parameters; 'Δ_i' difference in AIC; 'ω_i', Akaike weights; '$E_{min/i}$', evidence ratio.

Table S1. Localities and other identifying information of the 165 specimens of *Tamiasciurus douglasii* and *T. hudsonicus* used in this study. Also included are population assignment based on STRUCTURE analysis with nuclear DNA, as well as mtDNA phylogenetic inference.

Genus species	Museum Number	State Or Prov.	Lat. (dec.)	Long. (dec.)	TD-Baja Calif.	TD-Pacific Coastal	TH-North	TH-BC Coast	TH-VI	TH-Int. NW	TH-N. Rockies	TH-S. Rockies	TH-East	mtDNA Clade
Tamiasciurus hudsonicus	BYU_13761	Utah	38.45	-109.27			0.00	0.00	0.00	0.01	0.00	0.98	0.00	
Tamiasciurus douglasii	HSUVM_8218	California	41.63	-124.04	0.01	0.99								TD
Tamiasciurus douglasii	HSUVM_8220	California	41.49	-124.92	0.00	1.00								
Tamiasciurus douglasii	HSUVM_8235	California	41.03	-123.90	0.01	0.99								TD
Tamiasciurus douglasii	HSUVM_8237	California	41.02	-124.02	0.01	0.99								
Tamiasciurus hudsonicus	KU_120015	Yukon	61.45	-129.43			0.82	0.01	0.00	0.00	0.14	0.00	0.02	
Tamiasciurus douglasii	MSB_47459	Baja California	31.02	-115.53	0.94	0.06								TD
Tamiasciurus douglasii	MSB_47460	Baja California	31.02	-115.53	0.93	0.07								TD
Tamiasciurus douglasii	MSB_47461	Baja California	31.02	-115.53	0.98	0.02								TD
Tamiasciurus hudsonicus	MSB_62078	Arizona	34.11	-109.57			0.00	0.00	0.00	0.00	0.00	0.98	0.00	
Tamiasciurus hudsonicus	MSB_62079	Arizona	34.11	-109.57			0.01	0.01	0.00	0.00	0.01	0.95	0.01	
Tamiasciurus hudsonicus	MSB_66244	Alaska	65.29	-146.34			0.98	0.00	0.00	0.00	0.01	0.00	0.00	TH
Tamiasciurus hudsonicus	MSB_66245	Alaska	65.29	-146.34			0.98	0.00	0.00	0.00	0.01	0.00	0.00	
Tamiasciurus hudsonicus	MSB_70594	Maine	44.38	-68.25			0.01	0.00	0.00	0.00	0.00	0.00	0.99	TH
Tamiasciurus hudsonicus	MSB_73178	Ohio	41.23	-81.52			0.00	0.00	0.00	0.00	0.00	0.00	0.99	TH
Tamiasciurus hudsonicus	MSB_73420	Minnesota	48.26	-92.51			0.05	0.00	0.00	0.00	0.00	0.00	0.94	
Tamiasciurus hudsonicus	MSB_76659	Colorado	40.45	-106.00			0.00	0.00	0.00	0.00	0.00	0.99	0.00	TH
Tamiasciurus douglasii	MVZ_201566	California	37.75	-119.79	0.01	1.00								
Tamiasciurus douglasii	MVZ_201567	California	37.75	-119.80	0.01	0.99								TD
Tamiasciurus douglasii	MVZ_222808	California	39.42	-120.29	0.01	0.99								TD
Tamiasciurus douglasii	MVZ_222809	California	39.42	-120.29	0.00	1.00								
Tamiasciurus douglasii	MVZ_223974	California	36.75	-118.77	0.00	1.00								

Tamiasciurus douglasii	MVZ_223975	California	36.75	-118.77	0.00	1.00								
Tamiasciurus douglasii	MVZ_224506	California	36.77	-118.40	0.00	1.00								TD
Tamiasciurus douglasii	MVZ_224507	California	36.77	-118.40	0.01	0.99								
Tamiasciurus douglasii	MVZ_224633	California	39.30	-120.55	0.00	1.00								
Tamiasciurus douglasii	MVZ_224634	California	39.30	-120.55	0.01	0.99								
Tamiasciurus hudsonicus	NMMNH_17677	New Mexico	36.00	-106.29			0.00	0.00	0.00	0.00	0.00	0.98	0.00	TH
Tamiasciurus hudsonicus	NMMNH_17678	New Mexico	36.00	-106.29			0.00	0.00	0.00	0.00	0.00	0.98	0.00	
Tamiasciurus hudsonicus	PSM_13961	Alaska	63.57	-149.00			0.97	0.00	0.00	0.00	0.02	0.00	0.00	
Tamiasciurus hudsonicus	PSM_13962	Alaska	63.33	-150.55			0.89	0.01	0.00	0.00	0.09	0.00	0.01	
Tamiasciurus hudsonicus	PSM_13963	Alaska	63.72	-148.96			0.96	0.00	0.00	0.00	0.03	0.00	0.00	TH
Tamiasciurus hudsonicus	PSM_13964	Alaska	63.72	-148.96			0.96	0.01	0.00	0.00	0.02	0.00	0.00	
Tamiasciurus hudsonicus	PSM_4106	Alaska	68.13	-145.54			0.97	0.01	0.00	0.00	0.02	0.00	0.00	TH
Tamiasciurus hudsonicus	PSM_4107	Alaska	67.97	-151.60			0.97	0.00	0.00	0.00	0.02	0.00	0.00	
Tamiasciurus hudsonicus	RBCM_001938	British Columbia	51.56	-127.98			0.00	0.50	0.49	0.00	0.00	0.00	0.00	
Tamiasciurus hudsonicus	RBCM_001939	British Columbia	51.54	-127.95			0.00	0.56	0.32	0.11	0.00	0.00	0.00	
Tamiasciurus hudsonicus	RBCM_001941	British Columbia	51.54	-127.95			0.00	0.26	0.71	0.01	0.00	0.00	0.00	
Tamiasciurus hudsonicus	RBCM_001943	British Columbia	51.54	-127.95			0.00	0.41	0.58	0.01	0.00	0.00	0.00	
Tamiasciurus hudsonicus	RBCM_002900	British Columbia	52.60	-128.65			0.00	0.09	0.90	0.00	0.00	0.00	0.00	TH
Tamiasciurus hudsonicus	RBCM_002901	British Columbia	52.60	-128.65			0.01	0.24	0.74	0.00	0.00	0.00	0.00	
Tamiasciurus hudsonicus	RBCM_003176	British Columbia	53.56	-129.54			0.02	0.86	0.11	0.00	0.00	0.00	0.00	
Tamiasciurus hudsonicus	RBCM_003177	British Columbia	53.56	-129.54			0.02	0.85	0.13	0.00	0.00	0.00	0.00	TH
Tamiasciurus hudsonicus	RBCM_005433	British Columbia	52.18	-128.50			0.00	0.69	0.29	0.01	0.00	0.00	0.00	TH
Tamiasciurus hudsonicus	RBCM_005434	British Columbia	52.18	-128.50			0.00	0.79	0.19	0.01	0.00	0.00	0.00	TH
Tamiasciurus hudsonicus	RBCM_005853	British Columbia	50.10	-127.54			0.00	0.00	1.00	0.00	0.00	0.00	0.00	
Tamiasciurus hudsonicus	RBCM_005854	British Columbia	50.10	-127.54			0.00	0.00	0.98	0.00	0.01	0.00	0.00	
Tamiasciurus hudsonicus	RBCM_006660	British Columbia	49.15	-125.92			0.00	0.00	1.00	0.00	0.00	0.00	0.00	
Tamiasciurus hudsonicus	RBCM_006661	British Columbia	49.15	-125.92			0.00	0.00	0.99	0.00	0.00	0.00	0.00	
Tamiasciurus hudsonicus	RBCM_006793	British Columbia	49.16	-125.95			0.00	0.00	0.99	0.00	0.00	0.00	0.00	
Tamiasciurus hudsonicus	RBCM_007330	British Columbia	48.91	-125.09			0.00	0.00	1.00	0.00	0.00	0.00	0.00	TD
Tamiasciurus hudsonicus	RBCM_007331	British Columbia	48.91	-125.09			0.00	0.00	1.00	0.00	0.00	0.00	0.00	
Tamiasciurus hudsonicus	RBCM_007332	British Columbia	48.87	-125.17			0.00	0.00	0.99	0.00	0.00	0.00	0.00	
Tamiasciurus hudsonicus	RBCM_007334	British Columbia	48.91	-125.11			0.00	0.00	1.00	0.00	0.00	0.00	0.00	
Tamiasciurus hudsonicus	RBCM_007624	British Columbia	48.89	-125.13			0.00	0.00	0.99	0.01	0.00	0.00	0.00	
Tamiasciurus hudsonicus	RBCM_007680	British Columbia	57.72	-130.01			0.78	0.09	0.02	0.01	0.07	0.00	0.04	
Tamiasciurus hudsonicus	RBCM_009901	British Columbia	59.59	-133.69			0.96	0.01	0.00	0.00	0.03	0.00	0.01	

Tamiasciurus hudsonicus	RBCM_010488	British Columbia	59.59	-133.69			0.72	0.01	0.00	0.00	0.20	0.00	0.07	TH
Tamiasciurus hudsonicus	RBCM_010508	British Columbia	58.80	-121.98			0.94	0.00	0.00	0.00	0.04	0.00	0.00	TH
Tamiasciurus hudsonicus	RBCM_010510	British Columbia	58.80	-121.98			0.79	0.00	0.00	0.00	0.18	0.00	0.02	
Tamiasciurus hudsonicus	RBCM_010511	British Columbia	58.80	-121.98			0.89	0.01	0.00	0.00	0.09	0.00	0.01	
Tamiasciurus hudsonicus	RBCM_010800	British Columbia	59.64	-133.37			0.90	0.04	0.00	0.00	0.06	0.00	0.01	
Tamiasciurus hudsonicus	RBCM_010801	British Columbia	59.64	-133.37			0.94	0.02	0.00	0.00	0.03	0.00	0.01	
Tamiasciurus douglasii	RBCM_013116	British Columbia	50.23	-124.72	0.02	0.98								
Tamiasciurus douglasii	RBCM_013117	British Columbia	50.23	-124.72	0.00	1.00								
Tamiasciurus douglasii	RBCM_016992	British Columbia	50.15	-122.93	0.00	1.00								
Tamiasciurus hudsonicus	UAM_43102	Alaska	57.75	-136.28			0.92	0.01	0.01	0.00	0.04	0.00	0.01	TH
Tamiasciurus hudsonicus	UAM_51395	Alaska	64.87	-147.87			0.98	0.00	0.00	0.00	0.01	0.00	0.00	TH
Tamiasciurus hudsonicus	UBC_2482	British Columbia	52.49	-125.32			0.79	0.02	0.02	0.00	0.13	0.00	0.03	
Tamiasciurus hudsonicus	UBC_2483	British Columbia	52.49	-125.32			0.77	0.10	0.03	0.00	0.09	0.00	0.01	
Tamiasciurus hudsonicus	UMMZ_162427	Michigan	45.85	-84.71			0.01	0.01	0.00	0.00	0.00	0.00	0.98	TH
Tamiasciurus hudsonicus	UWBM_30055	Montana	45.56	-111.05			0.01	0.00	0.02	0.11	0.81	0.04	0.01	TH
Tamiasciurus hudsonicus	UWBM_30058	Alaska	58.71	-137.67			0.91	0.01	0.00	0.00	0.07	0.00	0.01	
Tamiasciurus hudsonicus	UWBM_30061	Alaska	58.64	-137.57			0.90	0.01	0.00	0.00	0.09	0.00	0.01	
Tamiasciurus hudsonicus	UWBM_30062	Alaska	58.37	-136.88			0.97	0.01	0.00	0.00	0.02	0.00	0.00	TH
Tamiasciurus hudsonicus	UWBM_32082	Alaska	64.94	-147.99			0.95	0.01	0.00	0.00	0.03	0.00	0.01	TH
Tamiasciurus hudsonicus	UWBM_32083	Alaska	64.94	-147.99			0.96	0.01	0.00	0.00	0.02	0.00	0.00	TH
Tamiasciurus hudsonicus	UWBM_35237	Michigan	42.35	-85.58			0.00	0.01	0.00	0.00	0.00	0.00	0.98	TH
Tamiasciurus hudsonicus	UWBM_38330	New York	42.63	-74.97			0.01	0.01	0.00	0.00	0.00	0.00	0.98	TH
Tamiasciurus douglasii	UWBM_41850	Washington	47.94	-122.40	0.01	0.99								
Tamiasciurus hudsonicus	UWBM_43180	Nova Scotia	46.70	-60.37			0.01	0.01	0.00	0.00	0.00	0.00	0.98	TH
Tamiasciurus hudsonicus	UWBM_43185	Alberta	50.74	-115.06			0.01	0.00	0.27	0.23	0.41	0.05	0.02	
Tamiasciurus hudsonicus	UWBM_43186	British Columbia	50.98	-118.31			0.01	0.01	0.08	0.36	0.52	0.02	0.01	
Tamiasciurus hudsonicus	UWBM_43188	British Columbia	51.95	-120.18			0.34	0.01	0.03	0.06	0.53	0.03	0.01	TH
Tamiasciurus hudsonicus	UWBM_43189	British Columbia	51.95	-120.18			0.04	0.01	0.02	0.04	0.83	0.01	0.06	
Tamiasciurus hudsonicus	UWBM_43200	Montana	48.66	-113.43			0.00	0.01	0.24	0.33	0.38	0.02	0.01	
Tamiasciurus hudsonicus	UWBM_43204	Utah	38.42	-109.25			0.00	0.02	0.01	0.01	0.01	0.95	0.00	TH
Tamiasciurus hudsonicus	UWBM_43225	Utah	41.84	-111.59			0.01	0.01	0.02	0.06	0.70	0.09	0.12	TH
Tamiasciurus hudsonicus	UWBM_43226	Utah	41.84	-111.59			0.01	0.00	0.03	0.03	0.86	0.07	0.01	TH
Tamiasciurus hudsonicus	UWBM_43245	Utah	40.64	-111.28			0.00	0.00	0.01	0.08	0.59	0.31	0.00	
Tamiasciurus hudsonicus	UWBM_43246	Utah	40.64	-111.28			0.01	0.00	0.02	0.06	0.29	0.61	0.01	
Tamiasciurus hudsonicus	UWBM_43254	Yukon	60.83	-136.95			0.92	0.01	0.00	0.00	0.05	0.00	0.01	
Tamiasciurus hudsonicus	UWBM_43255	Yukon	60.83	-136.95			0.91	0.01	0.00	0.00	0.07	0.00	0.01	TH

Tamiasciurus hudsonicus	UWBM_43256	Yukon	60.83	-136.95			0.85	0.00	0.00	0.00	0.14	0.00	0.01	
Tamiasciurus hudsonicus	UWBM_43257	Montana	46.83	-113.96			0.00	0.00	0.25	0.66	0.08	0.01	0.00	
Tamiasciurus hudsonicus	UWBM_43263	Yukon	60.83	-136.95			0.92	0.01	0.00	0.00	0.05	0.01	0.01	
Tamiasciurus hudsonicus	UWBM_43276	Wyoming	44.62	-110.08			0.01	0.00	0.02	0.12	0.71	0.12	0.02	TH
Tamiasciurus hudsonicus	UWBM_44442	Alaska	58.45	-135.88			0.97	0.01	0.00	0.00	0.01	0.00	0.00	
Tamiasciurus hudsonicus	UWBM_44943	Indiana	40.43	-86.96			0.00	0.00	0.00	0.00	0.00	0.00	0.99	TH
Tamiasciurus douglasii	UWBM_49091	Oregon	44.19	-121.69	0.01	0.99								
Tamiasciurus douglasii	UWBM_49092	Oregon	43.47	-121.86	0.00	1.00								
Tamiasciurus douglasii	UWBM_49093	Oregon	43.47	-121.86	0.00	1.00								
Tamiasciurus douglasii	UWBM_74107	Washington	47.98	-122.38	0.00	1.00								
Tamiasciurus douglasii	UWBM_74110	Washington	46.36	-121.73	0.00	1.00								TD
Tamiasciurus hudsonicus	UWBM_74113	West Virginia	38.98	-79.85			0.01	0.01	0.00	0.00	0.00	0.00	0.97	
Tamiasciurus douglasii	UWBM_74114	Washington	46.72	-121.89	0.00	1.00								
Tamiasciurus douglasii	UWBM_74139	Washington	46.53	-123.09	0.00	1.00								
Tamiasciurus douglasii	UWBM_75142	Washington	48.04	-123.25	0.00	1.00								TD
Tamiasciurus hudsonicus	UWBM_75455	British Columbia	50.03	-121.42	0.00	1.00								
Tamiasciurus hudsonicus	UWBM_75461	British Columbia	50.03	-121.42	0.00	1.00								
Tamiasciurus hudsonicus	UWBM_75493	British Columbia	49.14	-124.06			0.00	0.00	1.00	0.00	0.00	0.00	0.00	
Tamiasciurus hudsonicus	UWBM_75494	British Columbia	49.14	-124.06			0.00	0.00	1.00	0.00	0.00	0.00	0.00	
Tamiasciurus douglasii	UWBM_75828	Washington	48.08	-123.11	0.00	1.00								
Tamiasciurus hudsonicus	UWBM_76425	Alaska	56.41	-132.56			0.74	0.13	0.11	0.00	0.02	0.00	0.00	
Tamiasciurus hudsonicus	UWBM_76565	British Columbia	50.50	-127.17			0.00	0.00	1.00	0.00	0.00	0.00	0.00	
Tamiasciurus hudsonicus	UWBM_78088	Washington	48.42	-118.27			0.00	0.01	0.15	0.81	0.02	0.00	0.02	
Tamiasciurus hudsonicus	UWBM_78101	Washington	48.34	-118.43			0.01	0.01	0.11	0.75	0.09	0.00	0.04	
Tamiasciurus hudsonicus	UWBM_78125	Washington	48.50	-117.11			0.00	0.01	0.09	0.87	0.01	0.01	0.01	
Tamiasciurus hudsonicus	UWBM_78150	Washington	48.50	-117.11			0.00	0.00	0.17	0.73	0.04	0.00	0.05	
Tamiasciurus douglasii	UWBM_78345	Washington	46.23	-121.35	0.00	1.00								
Tamiasciurus douglasii	UWBM_78685	Washington	48.04	-123.06	0.00	1.00								
Tamiasciurus douglasii	UWBM_80404	Oregon	45.16	-121.44	0.01	0.99								
Tamiasciurus douglasii	UWBM_80630	Washington	48.08	-121.76	0.00	1.00								
Tamiasciurus douglasii	UWBM_80685	Oregon	45.30	-121.75	0.01	1.00								TD
Tamiasciurus hudsonicus	UWBM_81513	Oregon	44.80	-118.53			0.00	0.00	0.07	0.91	0.00	0.00	0.01	
Tamiasciurus hudsonicus	UWBM_81514	Oregon	44.80	-118.53			0.00	0.00	0.11	0.86	0.01	0.00	0.01	
Tamiasciurus hudsonicus	UWBM_81519	Oregon	45.29	-117.69			0.00	0.00	0.08	0.91	0.01	0.00	0.01	
Tamiasciurus hudsonicus	UWBM_81524	Oregon	45.29	-117.69			0.00	0.00	0.09	0.89	0.00	0.00	0.00	
Tamiasciurus hudsonicus	UWBM_81891	Washington	48.39	-119.88			0.00	0.02	0.19	0.77	0.01	0.00	0.01	

Tamiasciurus hudsonicus	UWBM_81892	Washington	48.44	-119.89			0.00	0.01	0.10	0.86	0.01	0.00	0.02	TH
Tamiasciurus hudsonicus	UWBM_81919	British Columbia	50.49	-126.99			0.00	0.00	1.00	0.00	0.00	0.00	0.00	TD
Tamiasciurus hudsonicus	UWBM_81920	British Columbia	50.49	-126.99			0.00	0.00	1.00	0.00	0.00	0.00	0.00	TD
Tamiasciurus hudsonicus	UWBM_81921	British Columbia	50.35	-126.16			0.00	0.00	0.99	0.01	0.00	0.00	0.00	TD
Tamiasciurus hudsonicus	UWBM_81922	British Columbia	49.74	-125.20			0.00	0.00	1.00	0.00	0.00	0.00	0.00	TD
Tamiasciurus hudsonicus	UWBM_81923	British Columbia	49.74	-125.20			0.00	0.00	1.00	0.00	0.00	0.00	0.00	
Tamiasciurus hudsonicus	UWBM_81924	British Columbia	49.74	-125.20			0.00	0.00	1.00	0.00	0.00	0.00	0.00	
Tamiasciurus hudsonicus	UWBM_81925	British Columbia	49.74	-125.20			0.00	0.00	1.00	0.00	0.00	0.00	0.00	
Tamiasciurus hudsonicus	UWBM_81926	British Columbia	49.74	-125.20			0.00	0.00	1.00	0.00	0.00	0.00	0.00	
Tamiasciurus hudsonicus	UWBM_81927	British Columbia	49.41	-124.75			0.00	0.00	0.99	0.00	0.00	0.00	0.00	TD
Tamiasciurus hudsonicus	UWBM_81928	British Columbia	49.41	-124.75			0.00	0.00	1.00	0.00	0.00	0.00	0.00	
Tamiasciurus hudsonicus	UWBM_81929	British Columbia	49.41	-124.75			0.00	0.00	1.00	0.00	0.00	0.00	0.00	
Tamiasciurus hudsonicus	UWBM_81930	British Columbia	49.41	-124.75			0.00	0.00	1.00	0.00	0.00	0.00	0.00	
Tamiasciurus hudsonicus	UWBM_81931	British Columbia	49.41	-124.75			0.00	0.00	1.00	0.00	0.00	0.00	0.00	
Tamiasciurus hudsonicus	UWBM_81932	British Columbia	48.76	-123.91			0.00	0.00	0.99	0.00	0.00	0.00	0.00	TD
Tamiasciurus hudsonicus	UWBM_81933	British Columbia	48.76	-123.91			0.00	0.00	0.99	0.00	0.00	0.00	0.00	
Tamiasciurus hudsonicus	UWBM_81934	British Columbia	48.76	-123.91			0.00	0.00	1.00	0.00	0.00	0.00	0.00	
Tamiasciurus hudsonicus	UWBM_81935	British Columbia	48.76	-123.91			0.00	0.00	0.99	0.00	0.00	0.00	0.00	
Tamiasciurus hudsonicus	UWBM_81936	British Columbia	49.16	-123.98			0.00	0.00	1.00	0.00	0.00	0.00	0.00	
Tamiasciurus hudsonicus	UWBM_81937	British Columbia	48.40	-123.98			0.00	0.00	1.00	0.00	0.00	0.00	0.00	TD
Tamiasciurus hudsonicus	UWBM_81938	British Columbia	48.40	-123.98			0.00	0.00	0.99	0.01	0.00	0.00	0.00	
Tamiasciurus douglasii	UWBM_81939	British Columbia	50.11	-124.96	0.00	1.00								TD
Tamiasciurus douglasii	UWBM_81940	British Columbia	50.11	-124.96	0.00	1.00								
Tamiasciurus douglasii	UWBM_81941	Washington	48.68	-121.76	0.01	0.99								
Tamiasciurus douglasii	UWBM_81942	Washington	48.68	-121.76	0.01	1.00								
Tamiasciurus douglasii	UWBM_82026	Washington	48.14	-122.28	0.00	1.00								
Tamiasciurus douglasii	UWBM_82029	Oregon	43.90	-123.87	0.01	0.99								TD
Tamiasciurus douglasii	UWBM_82030	Oregon	43.90	-123.87	0.00	1.00								
Tamiasciurus douglasii	UWBM_82048	Oregon	43.73	-122.70	0.01	0.99								
Tamiasciurus douglasii	UWBM_82049	Oregon	43.73	-122.70	0.02	0.98								TD
Tamiasciurus douglasii	UWBM_82058	Oregon	43.71	-121.33	0.00	1.00								
Tamiasciurus douglasii	UWBM_82059	Oregon	43.71	-121.33	0.00	1.00								
Tamiasciurus douglasii	UWBM_82091	Oregon	44.45	-119.94	0.01	0.99								
Tamiasciurus douglasii	UWBM_82092	Oregon	44.45	-119.94	0.02	0.98								
Tamiasciurus douglasii	UWBM_82110	Oregon	45.84	-123.96	0.02	0.98								
Tamiasciurus hudsonicus		Wyoming					0.01	0.00	0.02	0.14	0.75	0.04	0.03	TH

Table S2. Markers used in this study with summary statistics and laboratory conditions for PCR.

Locus Type	Name	Intron No.	ENSEMBL Code	Description	# of samples	Length (bp)	N_h	H_D	H_D SD (±)	π	π SD (±)	D	Subst. Model (AIC)	Primer Sequence -Forward	Primer Sequence -Reverse	Ta (°C)	MgCl2 (µl)
Nuclear	CARHSP1	1	ENSG00000153048	Calcium-regulated heat stable protein 1 (CARHSP1)	308	513	36	0.851	0.012	0.0077	0.0001	0.213	HKY+G	ACYCGCCGSACSAGGACCTTCT	GTRATGAAGCCRTGGCCCTTGGA	60	0.5
Nuclear	CLCN6	17	ENSG00000011021	Chloride channel protein 6 (CLCN6)	328	434	22	0.793	0.01	0.0055	0.0001	-0.713	HKY+G	ACACAGGCCAGAGTCCCTTT	AAGAGGAAGGGTCCTTGGTG	63	1
Nuclear	CSEIL	12	ENSG00000124207	Exportin-2 (CSE1L)	328	380	11	0.599	0.023	0.0021	0.0001	-0.987	HKY+G	TGTTATCCCCAGCTCTTACCA	GAAACCCACCTACCCCACTT	63	1
Nuclear	GABRP	3	ENSG00000094755	Gamma-aminobutyric-acid receptor subunit pi precursor (GABRP)	304	528	42	0.79	0.019	0.0094	0.0002	0.455	HKY+G	AATGATAAAAATGCAGTGGGAAACAGAATATCACA		63	1
Nuclear	GAD2	1	ENSG00000136750	Glutamate decarboxylase 2 (GAD2)	324	481	49	0.857	0.016	0.0135	0.0002	0.676	K80+G	CAGCAGGCGAGCTTTGTA	CCATCCCTCAGGTCATTGAT	63	1.5
Nuclear	GDAP1	1	ENSG00000104381	Ganglioside-induced differentiation-associated protein 1 (GDAP1)	310	790	40	0.881	0.011	0.0054	0.0001	-0.307	GTR+G	ACGCGGAGGTTAAGCTCATT	CGCATAAACCAAGGCTCATT	63	1
Nuclear	METTL11A	1	ENSG00000148335	UPF0351 protein C9orf32 (METTL11A)	304	664	28	0.868	0.011	0.0042	0.0001	-0.194	TrN+G	AGAGGTTCCTGAGGGTAGGC	ACCCTGTCACCACAGAGGAG	63	1
Nuclear	P4HA2	1	ENSG00000072682	Prolyl 4-hydroxylase alpha-2 subunit precursor (P4HA2)	328	704	30	0.83	0.011	0.0033	0.0000	-0.614	HKY+G	AGGCCGAGTTCTTCACCTCT	TGCACCAGGTCTTTCTCTGC	63	1
Nuclear	PIPOX	5	ENSG00000179797	Peroxisomal sarcosine	318	303	25	0.838	0.01	0.0104	0.0002	0.449	GTR+G	AGAGCAGTGTG	AAGGTGAGCAG	63	0.5

			61	oxidase (PIPOX)										GGCAGTGAT	AGAGGTGGA		
Nuclear	PNPO3	3	ENSG00000108439	Pyridoxine-5'-phosphate oxidase (PNPO)	330	489	19	0.821	0.011	0.0049	0.0001	0.062	HKY+G	AAGATTTCGCGCTTGTGGT	TGAGTCTTAGCTATTTCTGTCACTCAT	63	1
Nuclear	PPAN	2	ENSG00000130810	Suppressor of SWI4 1 homolog (PPAN)	330	422	22	0.797	0.013	0.0047	0.0001	-0.716	TrN+G	TCGGGTCATGGAACCAATTA	TTCAGCGAGTTCTTCTTACGG	60	1
Nuclear	SLC17A9	5	ENSG00000101194	Solute carrier family 17 member 9 (SLC17A9)	330	426	13	0.779	0.012	0.0055	0.0001	0.833	F81	CGTGTACAGGTACGTGCTGAG	AGGAGGAGGTCTGAGGGAAT	63	1
Nuclear	TBC1D21	9	ENSG00000167139	TBC1 domain family member 21 (TBC1D21)	330	265	39	0.862	0.012	0.0146	0.0004	0.754	TrN+G	GTAGGCCACCAGCACCTTT	AGCTTCCAGAACCTGCTTCA	63	1.5
Nuclear	THOC1	10	ENSG00000079134	THO complex subunit 1 (THOC1)	320	531	15	0.639	0.027	0.0038	0.0001	0.164	TrN+G	GGCACAATCTCCAGGAAAAA	GGCTACAGTCTTAGCACAGGAAA	63	1.5
Nuclear	TTR	1	ENSG00000118271	Transthyretin precursor (TTR)	328	446	6	0.244	0.031	0.0016	0.0002	-0.496	F81+G	TTCTGCCTCCAGACACATTG	GCATTAAGTCTGCCATGCCTA	63	1
Mitochondrial	Control Region	n/a	n/a	Right Domain of Control Region	159	353	75	0.963	0.008	0.0281	0.0007	-0.863	TrN+G	CCTTTAGCTGGCATAGGTA	CATTATATGGAGTGGAGAAGG	54	1

Table S3. Fossil and secondary calibrations used in this study.

Rodent-Lagomorph Species-Tree					
Node #	**Node**	**Minimum Hard Bound (Ma)**	**Fossil Justification for Minimum Bound**	**Maximum Soft Bound (Ma)**	**Justification for Maximum Bound**
1	Glires	61.5	*Heomys* (Rodentia) [1]	131.5	Absence of crown Glires during Cretaceous, estimate based on maximum paleontological estimate for Eomaia and Sindelphys (Archontoglires) [2]
2	Lagomorpha	30	*Vastan calcanei* (Leporidae, Lagomorpha) [3]	65.8	Absence of crown lagomorphs in early Paleocene [4]
3	Mus/Rattus	10.4	Karnimata (linage leading to Rattus) [5]	14.0	Absence of crown murines in early Miocene [5]
4	Sciuridae	26.9	*Douglassciurus jeffersoni* (earliest Sciurid) [6,7]	65.8	Absence of crown Sciurids in early Paleocene [6,7]
5	Sciurini	7.5	*Sciurus olsoni* (earliest Sciurini) [8]	13.6	Absence of crown Sciurines in early Miocene [8]

***Tamiasciurus* Species-Tree**				
Node #	**Node**	**Minimum Soft Bound (Ma)**	**Justification for Minimum and Maximum Bound**	**Maximum Soft Bound (Ma)**
1	*Tamiasciurus* root	0.1	2^{o} calibration estimate (95% HPD) from node representing split between *T. hudsonicus* and *T. douglasii* in Rodent-Lagormorph species-tree	0.81

References for Table S3

1 C.K. Li and S.Y. Ting. 1983. The Paleogene mammals of China. Bull. Carnagie Mus. Nat. His. 21:1–93.

2 M.J. Benton, P.C.J. Donoghue, and R.J. Asher. 2009. The Timetree of Life, chapter Calibrating and constraining molecular clocks, pages 35–86. Oxford University Press.

3 K.D. Rose, V.B. DeLeon, P. Missiaen, RS Rana, A. Sahni, L. Singh, and T. Smith. 2008. Early Eocene Lagomorph (Mammalia) from western India and the early diversification of Lagomorpha. Proc. Roy. Soc. B. 275:1203-1208.

4 R.J. Asher, J. Meng, J.R.Wible, M.C. McKenna, G.W. Rougier, D. Dashzeveg, and M.J. Novacek. 2005. Stem Lagomorpha and the antiquity of Glires. Science 307:1091-1094.

5 L.L. Jacobs, and L.J. Flynn. 2005. Interpreting the Past: Essays on Human, Primate, and Mammal Evolution in Honor of David Pilbeam, chapter Of mice ... again: the Siwalik rodent record, murine distribution, and molecular clocks, pages 63–80. Brill Academic Publishers.

6 R.J. Emry, and W.W. Korth. 1996. The Chadronian squirrel ‘‘*Sciurus*’’ *jeffersoni* Douglass, 1901: a new generic name, new material, and its bearing on the early evolution of Sciuridae (Rodentia). J. Vert. Paleontol. 16:775–780.

7 R.J. Emry, and W.W. Korth. 2001. *Douglassciurus*, new name for *Douglassia* Emry and Korth, 1996, not *Douglassia* Bartsch, 1934. J. Vert. Paleontol. 21:400.

8 R.J. Emry, W.W. Korth, and M.A. Bell. 2005. A tree squirrel (Rodentia, Sciuridae, Sciurini) from the Late Miocene (Clarendonian) of Nevada . J. Vert. Paleontol. 25:228–235.

Table S4. Model Selection

From ~16,000 museum records, we reduced our dataset to 350 localities of *Tamiasciurus hudsonicus* and 171 localities of *T. douglasii*. Splitting data into spatial subunits resulted in uneven splits for *T. hudsonicus* (249 for west and 101 for east) and *T. douglasii* (40 in the Sierra Nevada and 131 in the Cascades). Model selection procedures for all four spatial units suggested simpler models in Maxent were warranted (Table S5). In each case, the opposing spatial unit with a taxon was able to correct predict nearly all of the set in the opposing unit (Table S5), and model accuracy was better than random. Because we were able to predict well independent spatial data, we were comfortable with assumptions associated with transferring models to novel climate. Again, model selection suggested a reduced complexity for both species, which led to reasonably accurate models (Table S5). Localities withheld from the cross-validation were well represented by each of the models when thresholded (*T. douglasii* 35/35 correctly predicted by all models; *T. hudsonicus* 69 of 70 correctly predicted by all models).

Both Species

Species	Extent	Beta	Log Likelihood	Parameters	Sample Size	AIC score	AICc score
T. douglasii	All	1	-1360.75	52	136	2825.51	2891.919
	All	3	-1393.51	15	136	2817.019	2821.019
	All	5	-1400.87	12	136	2825.741	2828.278
	All	7	-1404.44	11	136	2830.886	2833.015
	All	9	-1408.3	10	136	2836.591	2838.351
	All	11	-1411.59	8	136	2839.181	2840.315
	All	13	-1414.15	6	136	2840.301	2840.952

	All	15	-1414.89	6	136	2841.772	2842.423
	All	17	-1415.77	6	136	2843.537	2844.189
	All	19	-1416.7	6	136	2845.4	2846.051
T. hudsonicus	All	1	-3356.39	67	280	6846.776	6889.757
	All	3	-3407.12	31	280	6876.246	6884.246
	All	5	-3421.98	17	280	6877.953	6880.289
	All	7	-3428.54	12	280	6881.073	6882.242
	All	9	-3432.89	9	280	6883.788	6884.454
	All	11	-3434.75	11	280	6891.498	6892.484
	All	13	-3437.15	12	280	6898.296	6899.465
	All	15	-3439.73	11	280	6901.47	6902.455
	All	17	-3442.2	11	280	6906.405	6907.39
	All	19	-3444.46	10	280	6908.929	6909.746
T. hudsonicus	East	1	-868.302	35	80	1806.603	1863.876
	East	3	-895.253	6	80	1802.505	1803.656
	East	5	-902.117	4	80	1812.235	1812.768
	East	7	-905.566	1	80	1813.132	1813.184
	East	9	-906.041	1	80	1814.081	1814.133
	East	11	-906.589	1	80	1815.178	1815.23
	East	13	-906.721	0	80	1813.442	1813.442
	East	15	-906.721	0	80	1813.442	1813.442
	East	17	-906.721	0	80	1813.442	1813.442
	East	19	-906.721	0	80	1813.442	1813.442
T. hudsonicus	West	1	-2287.65	50	199	4675.306	4709.765
	West	3	-2332.26	21	199	4706.511	4711.731
	West	5	-2339.19	13	199	4704.375	4706.343
	West	7	-2341.66	10	199	4703.321	4704.491
	West	9	-2345.06	10	199	4710.13	4711.3
	West	11	-2347.61	8	199	4711.222	4711.98
	West	13	-2350.1	7	199	4714.196	4714.782
	West	15	-2352.15	7	199	4718.299	4718.885

	West	17	-2354.13	7	199	4722.256	4722.842
	West	19	-2355.88	6	199	4723.754	4724.192
T. douglasii	Casc	1	-1020.12	49	104	2138.247	2228.988
	Casc	3	-1052.38	16	104	2136.761	2143.014
	Casc	5	-1063.46	11	104	2148.927	2151.796
	Casc	7	-1066.04	10	104	2152.085	2154.451
	Casc	9	-1068.95	9	104	2155.894	2157.808
	Casc	11	-1070.23	6	104	2152.465	2153.331
	Casc	13	-1071.03	6	104	2154.06	2154.926
	Casc	15	-1071.93	6	104	2155.856	2156.722
	Casc	17	-1072.93	6	104	2157.854	2158.72
	Casc	19	-1074.03	7	104	2162.053	2163.22
T. douglasii	Sierra	1	-266.383	18	32	568.7651	621.3805
	Sierra	3	-273.574	6	32	559.1486	562.5086
	Sierra	5	-276.158	6	32	564.3166	567.6766
	Sierra	7	-278.161	3	32	562.3212	563.1783
	Sierra	9	-279.48	3	32	564.9605	565.8177
	Sierra	11	-281.051	3	32	568.1014	568.9585
	Sierra	13	-282.891	3	32	571.781	572.6382
	Sierra	15	-285.036	3	32	576.0714	576.9285
	Sierra	17	-286.04	2	32	576.0803	576.4941
	Sierra	19	-286.889	2	32	577.7787	578.1925

Tamiasciurus douglasii

Extent	Beta	Log Likelihood	Parameters	Sample Size	AIC score	AICc score
All	1	-1360.75	52	136	2825.51	2891.919
All	3	-1393.51	15	136	2817.019	2821.019
All	5	-1400.87	12	136	2825.741	2828.278
All	7	-1404.44	11	136	2830.886	2833.015
All	9	-1408.3	10	136	2836.591	2838.351
All	11	-1411.59	8	136	2839.181	2840.315

All	13	-1414.15	6	136	2840.301	2840.952
All	15	-1414.89	6	136	2841.772	2842.423
All	17	-1415.77	6	136	2843.537	2844.189
All	19	-1416.7	6	136	2845.4	2846.051
Casc	1	-1020.12	49	104	2138.247	2228.988
Casc	3	-1052.38	16	104	2136.761	2143.014
Casc	5	-1063.46	11	104	2148.927	2151.796
Casc	7	-1066.04	10	104	2152.085	2154.451
Casc	9	-1068.95	9	104	2155.894	2157.808
Casc	11	-1070.23	6	104	2152.465	2153.331
Casc	13	-1071.03	6	104	2154.06	2154.926
Casc	15	-1071.93	6	104	2155.856	2156.722
Casc	17	-1072.93	6	104	2157.854	2158.72
Casc	19	-1074.03	7	104	2162.053	2163.22
Sierra	1	-266.383	18	32	568.7651	621.3805
Sierra	3	-273.574	6	32	559.1486	562.5086
Sierra	5	-276.158	6	32	564.3166	567.6766
Sierra	7	-278.161	3	32	562.3212	563.1783
Sierra	9	-279.48	3	32	564.9605	565.8177
Sierra	11	-281.051	3	32	568.1014	568.9585
Sierra	13	-282.891	3	32	571.781	572.6382
Sierra	15	-285.036	3	32	576.0714	576.9285
Sierra	17	-286.04	2	32	576.0803	576.4941
Sierra	19	-286.889	2	32	577.7787	578.1925

Tamiasciurus hudsonicus

Extent	Beta	Log Likelihood	Parameters	Sample Size	AIC score	AICc score
All	1	-3356.39	67	280	6846.776	6889.757
All	3	-3407.12	31	280	6876.246	6884.246
All	5	-3421.98	17	280	6877.953	6880.289
All	7	-3428.54	12	280	6881.073	6882.242

All	9	-3432.89	9	280	6883.788	6884.454
All	11	-3434.75	11	280	6891.498	6892.484
All	13	-3437.15	12	280	6898.296	6899.465
All	15	-3439.73	11	280	6901.47	6902.455
All	17	-3442.2	11	280	6906.405	6907.39
All	19	-3444.46	10	280	6908.929	6909.746
East	1	-868.302	35	80	1806.603	1863.876
East	3	-895.253	6	80	1802.505	1803.656
East	5	-902.117	4	80	1812.235	1812.768
East	7	-905.566	1	80	1813.132	1813.184
East	9	-906.041	1	80	1814.081	1814.133
East	11	-906.589	1	80	1815.178	1815.23
East	13	-906.721	0	80	1813.442	1813.442
East	15	-906.721	0	80	1813.442	1813.442
East	17	-906.721	0	80	1813.442	1813.442
East	19	-906.721	0	80	1813.442	1813.442
West	1	-2287.65	50	199	4675.306	4709.765
West	3	-2332.26	21	199	4706.511	4711.731
West	5	-2339.19	13	199	4704.375	4706.343
West	7	-2341.66	10	199	4703.321	4704.491
West	9	-2345.06	10	199	4710.13	4711.3
West	11	-2347.61	8	199	4711.222	4711.98
West	13	-2350.1	7	199	4714.196	4714.782
West	15	-2352.15	7	199	4718.299	4718.885
West	17	-2354.13	7	199	4722.256	4722.842
West	19	-2355.88	6	199	4723.754	4724.192

Table S5. ENM Summary

Species	Extent	β	Number Train Point	Number Test Points	Train AUC	Test AUC	St. Dev. Test AUC	Positive Predictive Value	Proportion of withheld predicted in all CV
T. douglasii	Cascades	3	104	27	0.75	0.769	0.029	0.95	
	Sierra	3	32	8	0.855	0.802	0.04	0.85	
	All	3	122/123	14/13	0.763	0.707	0.054		1.00
T. hudsonicus	East	3	80	21	0.675	0.615	0.057	1.00	
	West	7	199	50	0.743	0.733	0.032	1.00	
	All	5	252	28	0.712	0.688	0.057		0.99

Table S6. ENM Similarities

Map	Extent	Era	I	D	RR
Logistic	Full	Current	0.607	0.393	0.380
Logistic	V.I.	Current	0.973	0.826	0.594
Logistic	Restricted	Current	0.696	0.500	0.493
Thresholded	Full	Current	0.475	0.257	0.432
Thresholded	V.I.	Current	0.928	0.818	0.461
Thresholded	Restricted	Current	0.517	0.279	0.468
Logistic	Full	LGM (CCSM)	0.543	0.384	0.798
Logistic	Restricted	LGM (CCSM)	0.724	0.642	0.806
Thresholded	Full	LGM (CCSM)	0.456	0.299	0.840
Thresholded	Restricted	LGM (CCSM)	0.628	0.556	0.841
Logistic	Full	LGM (MIROC)	0.620	0.447	0.694
Logistic	Restricted	LGM (MIROC)	0.766	0.627	0.708
Thresholded	Full	LGM (MIROC)	0.561	0.377	0.734
Thresholded	Restricted	LGM (MIROC)	0.684	0.543	0.736
Logistic	Full	LIG	0.282	0.161	0.189
Logistic	V.I.	LIG	0.976	0.825	0.510
Logistic	Restricted	LIG	0.397	0.281	0.247
Thresholded	Full	LIG	0.195	0.082	0.378
Thresholded	V.I.	LIG	0.988	0.946	0.733
Thresholded	Restricted	LIG	0.315	0.178	0.399

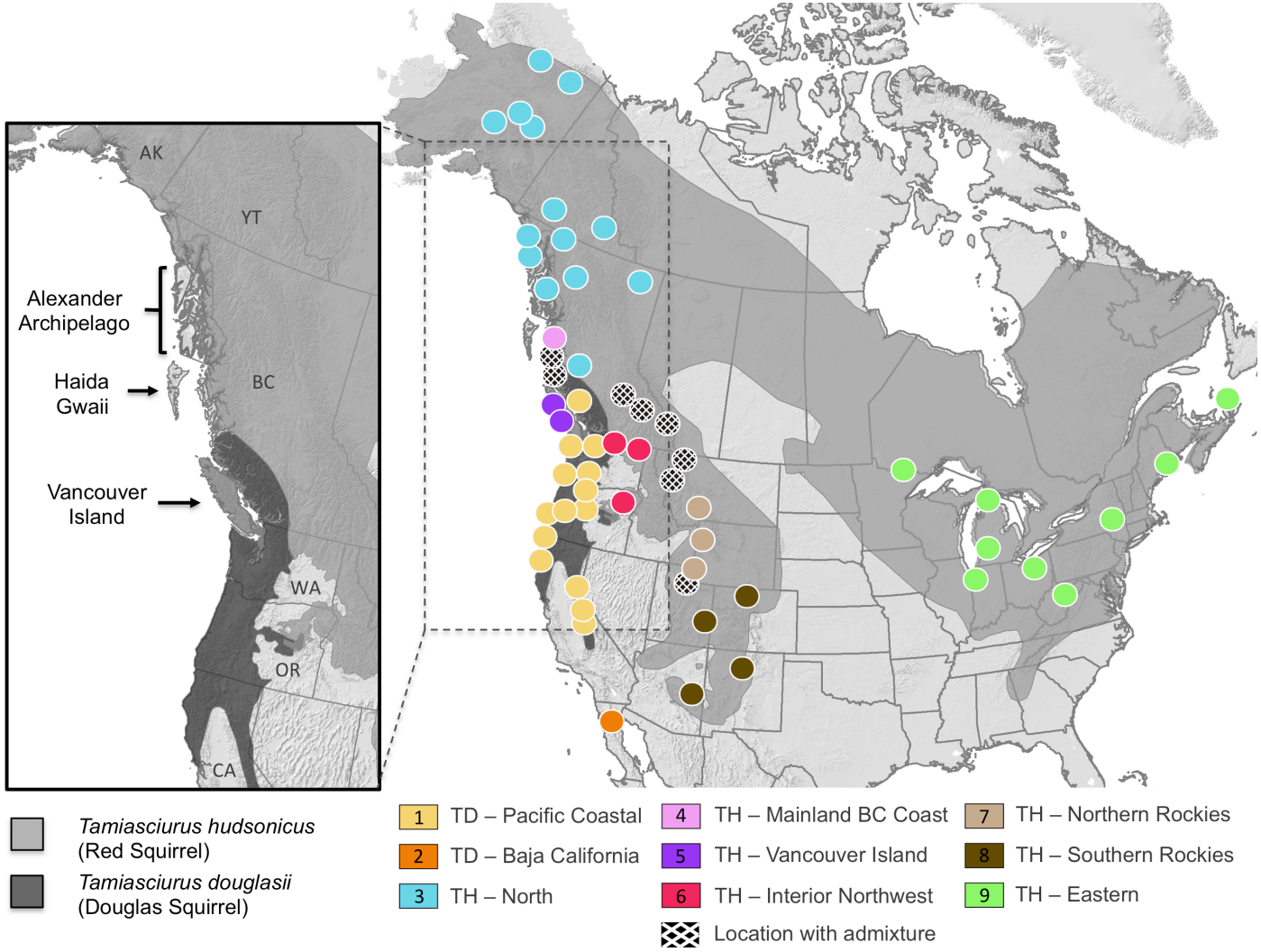

Figure 1. North American map depicting geographic ranges of pine squirrels (*Tamiasciurus*), with enlargement panel showing detail of Vancouver Island and other west-coast island groups. Dark gray on map indicates *T. douglasii* and medium gray is *T. hudsonicus*

(redrawn from Hall 1981; Nagorsen 2005). Colored circles mark 59 sampling localities, and associated color scheme indicates nine geographically discrete ancestral populations based on nuclear DNA using STRUCTURE. Numbered color codes and names of the nine populations are: (1) TD-Pacific Coastal: *Tamiasciurus douglasii*, Pacific coastal North America from southern British Columbia southward through California; (2) TD-Baja California: *T. douglasii (mearnsi),* San Pedro Martir mountains of Baja California; (3) TH-North: *Tamiasciurus hudsonicus* (TH)*,* Alaska, Yukon Territory, and northern British Columbia; (4) TH-Mainland BC Coast: coastal mountains of mainland British Columbia; (5) TH-Vancouver Island: Vancouver Island; (6) TH-Interior Northwest: southern interior British Columbia southward through eastern Washington and Oregon; (7) TH-Northern Rockies: northern Rocky Mountains region from Montana southward to northern Utah; (8) TH-Southern Rockies: southern Rocky Mountains from northern Utah to Arizona; (9) TH-Eastern: eastern North America. Checkered circles represent localities with populations containing individuals with an admixture of genotypes from adjacent areas (Table S1).

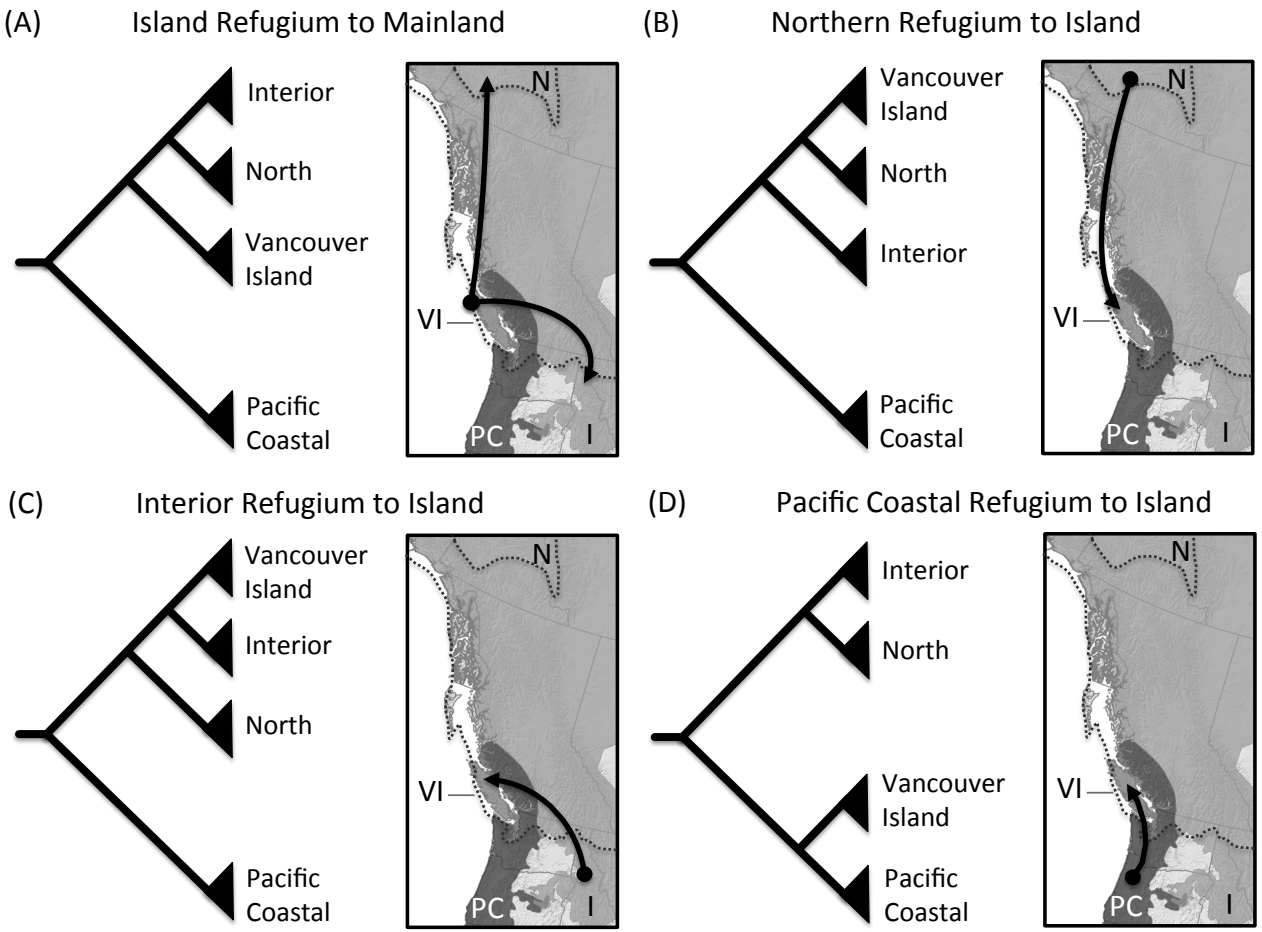

Figure 2. Phylogenetic hypotheses representing four alternative dispersal routes (arrows on maps) between Vancouver Island and mainland populations of pine squirrels (*T. hudsonicus* medium gray, *T. douglasii* dark gray). Dotted line represents approximate margin of the Cordilleran Ice Sheet during the LGM (Booth et al. 2003).

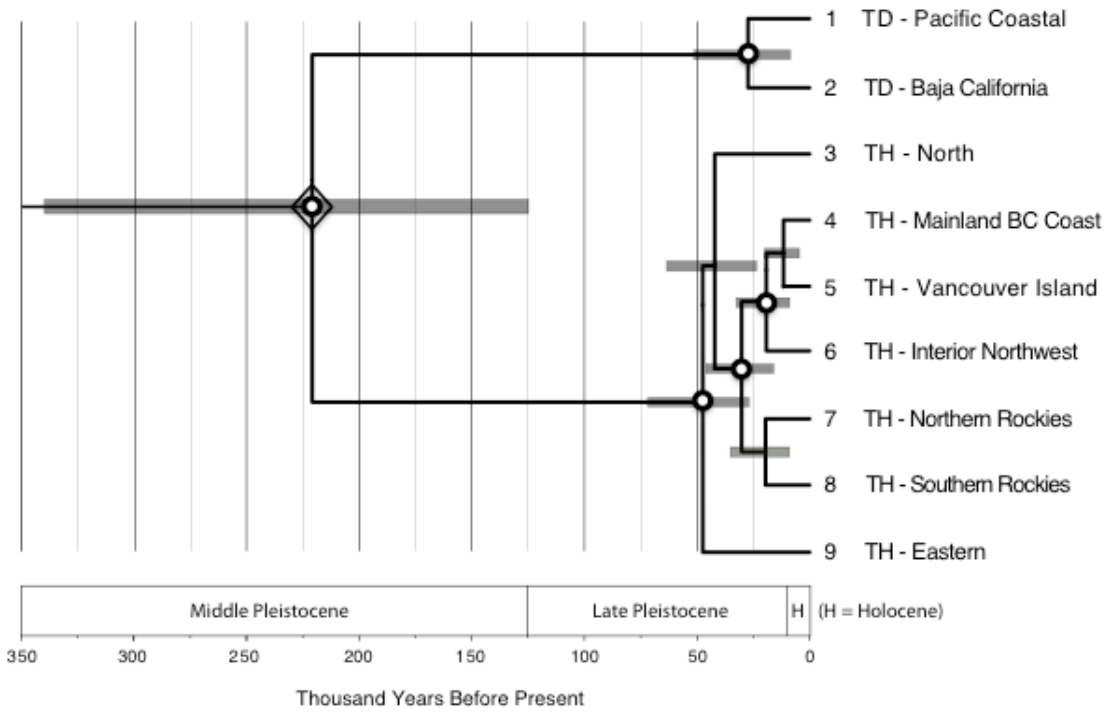

Figure 3. Time-calibrated species tree for the nine *Tamiasciurus* lineages based on 15 nuclear introns and computation with *BEAST. Nodes with white circles represent strong posterior probability (pp) support (pp ≥ 0.95). Gray-shaded bars represent 95% HPD of estimated node age. Diamond indicates secondary calibration (Table S3).

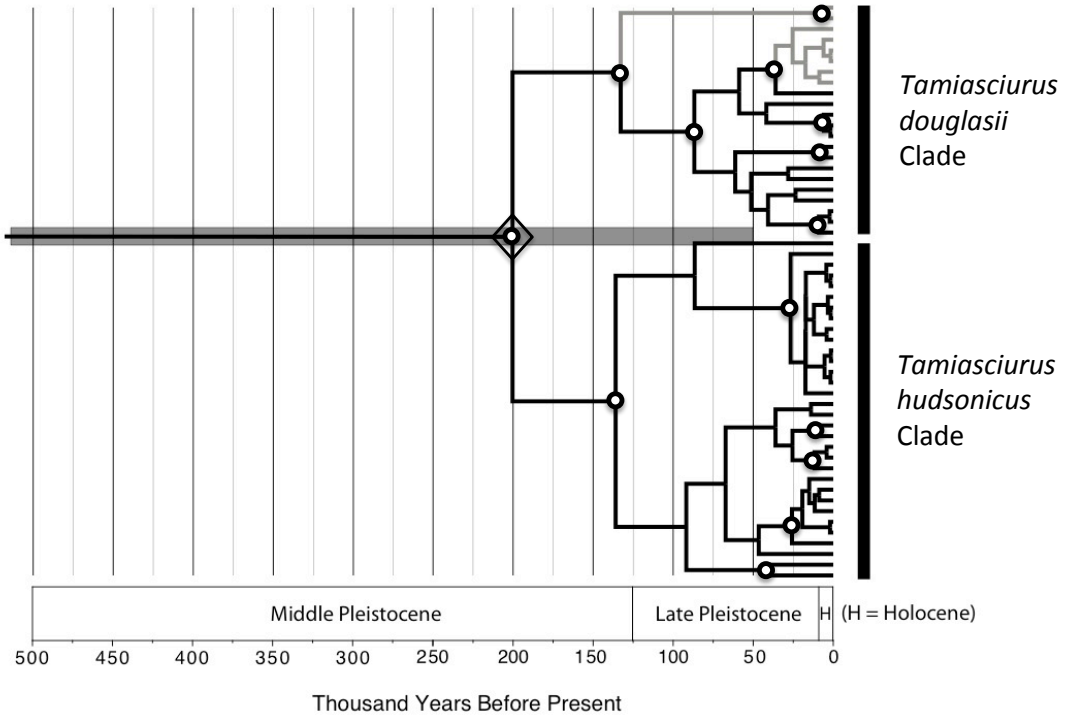

Figure 4. Time-calibrated Bayesian gene tree of 54 *Tamiasciurus* mtDNA haplotypes using BEAST. Analysis revealed strong support for two major clades corresponding to the two species, as indicated by vertical bars. All Vancouver Island lineages are shown in light grey shade and are nested within the *T. douglasii* clade. In contrast, all Vancouver Island samples were nested within a group of *T. hudsonicus* lineages in the nuclear intron species-tree analysis. White circles represents nodes with pp $\geq$ 0.95. Gray-shaded bar represent 95% HPD of estimated node age. Diamond indicates secondary calibration (Table S3).

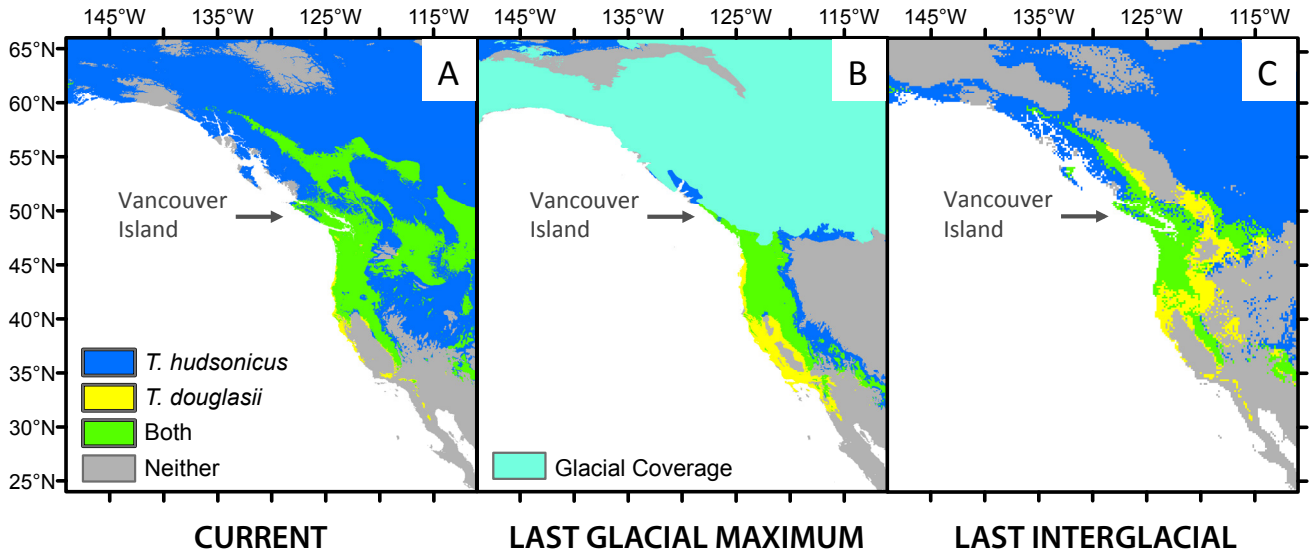

Figure 5. Bioclimatic envelope models for *T. hudsonicus* and *T. douglasii* under three historical climate scenarios, based on MAXENT: (A) Current, contemporary conditions; (B) Last Glacial Maximum (LGM; 18,000 years before present), and (C) Last Interglacial (LIG; 114,000-131,000 years before present). Potentially suitable climatic space is indicated by colors: *T. hudsonicus* only (blue), *T. douglasii* only (yellow), both species overlapping (green), neither species (gray).

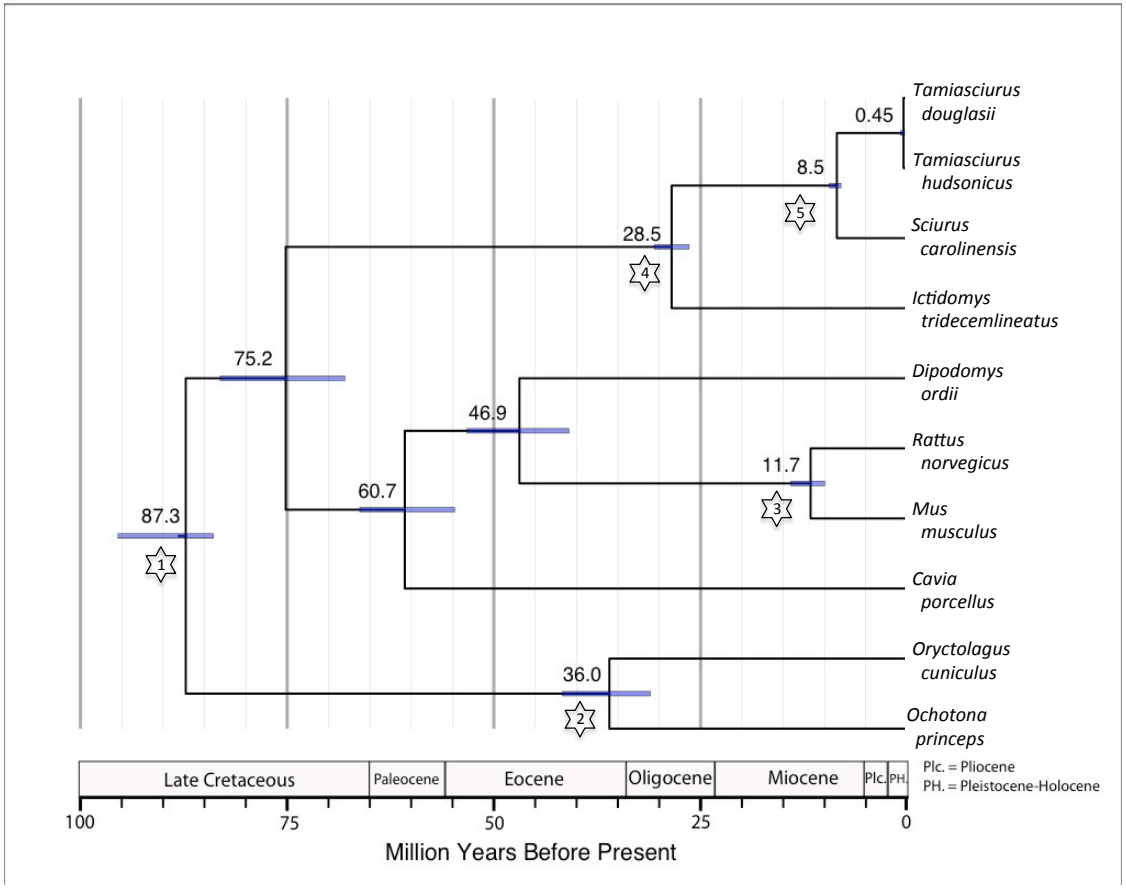

Figure S1. Time-calibrated species tree covering the Cenozoic history of lagomorphs and major groups of rodents, based on a dataset of the same 15 nuclear-intron markers used in our Tamiasciurus species-tree analysis, computed with *BEAST. Numbers on nodes represent posterior probability values. Stars with numbers indicate the location of the fossil calibration priors. (See **Materials and Methods**.)

CHAPTER 2

Genetic and phenotypic variation across a hybrid zone between ecologically divergent tree squirrels (*Tamiasciurus*)

Abstract

A hybrid zone along an environmental gradient should contain a clinal pattern of genetic and phenotypic variation. This occurs because divergent selection in the two parental habitats is typically strong enough to overcome the homogenizing effects of gene flow across the environmental transition. We studied hybridization between two parapatric tree squirrels (*Tamiasciurus spp*.) across a forest gradient over which the two species vary in coloration, cranial morphology, and body size. We sampled 397 individuals at 29 locations across a 600-km transect to seek genetic evidence for hybridization; upon confirming hybridization, we examined levels of genetic admixture in relation to maintenance of phenotypic divergence despite potentially homogenizing gene flow. Applying population assignment analyses to microsatellite data, we found that *T. douglasii* and *T. hudsonicus* form two distinct genetic clusters but also hybridize, mostly within transitional forest habitat. Overall, based on this nuclear analysis, 48% of the specimens were characterized as *T. douglasii*, 9% as hybrids, and 43% as *T. hudsonicus*. Hybrids appeared to be reproductively viable, as evidenced by the presence of later-generation hybrid genotypes. Observed clines in ecologically important phenotypic traits—fur coloration and cranial morphology—were sharper than the cline of putatively neutral mtDNA, which suggests that divergent selection may maintain phenotypic distinctiveness. The relatively recent divergence of these two species (probably late Pleistocene), apparent lack of pre-zygotic isolating mechanisms, and geographic coincidence of cline centers for both genetic and

phenotypic variation suggest that environmental factors play a large role in maintaining the distinctiveness of these two species across the hybrid zone.

Introduction

Geographic isolation and ecological adaptation have a powerful influence on the development of reproductive isolation in the process of speciation (Sobel et al. 2010). Limitations to gene flow are often initiated by the geographic separation of populations. Both the period of time over which populations are isolated and the evolution of divergent adaptations promote reproductive isolation through epistatic and pleiotropic effects (Dobzhansky 1937; Muller 1940, 1942; Coyne and Orr 2004). These effects can either be direct, as in the case of adaptation to a new habitat that leads to spatial isolation, or indirect, as when divergent selection for adaptive differences between populations creates divergent genomic backgrounds, which may hasten the generation of epistatic incompatibilities.

Zones of secondary contact between formerly allopatric species or divergent populations are often used as natural opportunities to study processes that are important in the early stages of speciation. The outcomes of secondary contact vary from system to system and typically depend on the duration of isolation and whether the two species in question evolved in ecologically different environments. At one extreme, populations are reproductively isolated from one another either because they cannot interbreed or, if they do, because they are unable to produce viable or fertile offspring. At the other extreme, divergent populations may freely interbreed and eventually fuse back to one population. Many secondary contact systems fall between these scenarios and result in narrow hybrid zones. This forms a tension zone, where the width of the zone is dependent upon a balance between dispersal and selection (Barton 1983; Barton and Hewitt 1985). In that case, populations still maintain their genetic distinctiveness over most of their distribution and may proceed toward reproductive isolation, even though some gene flow or diffusion of characters may still occur (Wu 2001).

Hybrid zone systems are also important for identifying ecologically important traits. This is especially true when a hybrid zone persists along an environmental gradient or an ecotone, because the divergent effects of natural selection are countered by the homogenizing effects of gene flow (Endler 1977; Barton and Hewitt 1985). One way to ascertain the ecological importance of traits is to compare clinal patterns of trait variation with patterns of neutrally evolving traits or markers (Gay et al. 2008). A trait or marker that is neutrally evolving is expected to have a greater cline width across the hybrid zone than a trait under strong divergent selection. Alternatively, a displaced cline may indicate that phenotypic traits of one species are beneficial to the other; thus a hybrid zone may be important for adaptive introgression (Grant et al. 2004; Martin et al. 2006; Whitney et al. 2006; Fitzpatrick et al. 2010). Here we examine clinal patterns of phenotypic variation in the face of hybridization between parapatric sister species of North American tree squirrels of the genus *Tamiasciurus*. These sibling species are good candidates for an investigation of the role of ecological factors in hybridization dynamics because they have been studied thoroughly in the field with regard to plant-animal interactions, behavioral ecology, and life history evolution (Smith 1968, 1970, 1978, 1981; Benkman 1995; Boutin et al. 2006; Digweed and Rendell 2009; Sanderson and Koprowski 2009).

Tamiasciurus is represented by only two species, the Douglas squirrel (*Tamiasciurus douglasii*) and the red squirrel (*T. hudsonicus*). Previous phylogenetic inference for *Tamiasciurus* using mitochondrial DNA (mtDNA) showed strong support for three major clades: a single "western" clade that is concordant with the taxonomic description for *T. douglasii,* and two other clades ("eastern" and "southwestern") that are associated with *T. hudsonicus* (Arbogast et al. 2001). Low levels of mtDNA sequence divergence between these three lineages (< 2.4%) suggest their divergence was relatively recent, probably during the Pleistocene. These squirrels

are distributed throughout boreal and montane coniferous forests across most of North America (Fig. 1), with T. *douglasii* in the Pacific Coastal region and *T. hudsonicus* more widespread across the continent, from the southern Appalachians northward in eastern North America, throughout the Rocky Mountains, and further northward into Alaska (Steele 1998, 1999). The ranges of these two species come into contact in a narrow transitional forest region of the northern Cascade Mountains of southern British Columbia and northern Washington (Smith 1968). *Tamiasciurus douglasii* inhabits dense, wet coastal forests on the west side of the Cascades, whereas *T. hudsonicus* inhabits open, dry interior forests on the east side of the Cascades. It has been proposed that secondary contact between these species occurred following the end of the Pleistocene, because this entire region was covered by continental ice during the last glacial maximum (Lindsay 1982; Smith 1981; Arbogast et al. 2001).

Tamiasciurus douglasii and *T. hudsonicus* are phenotypically distinct in coloration and skull morphology (Lindsay 1982; Smith 1981). *Tamiasciurus douglasii* is darker dorsally and has an orange ventral color and is slightly smaller than *T. hudsonicus,* which has a white ventral color. Smith (1981) argued that phenotypic differences in coloration and skull morphology result from local adaptation to variation in forest environments. For instance, the lighter ventral coloration of *T. hudsonicus* is an adaptation for background matching in an open canopy forest in order to reduce detection by predators. In addition, the stronger jaw musculature of *T. hudsonicus* is an adaptation for opening harder, closed pine cones that have evolved in an environment with a high frequency of fires. In the transitional forest habitat where these species are sympatric, individuals with intermediate coloration and vocalization frequencies have been recorded and are thought to be hybrids (Smith 1968; Stevens and Nellis 1974). However, Lindsay (1982) argued that these two species are reproductively isolated from one another and

that character convergence in the transitional forest habitat is an alternative explanation for the evolution of intermediate traits.

The goal of our study was to characterize environmental, genetic, and phenotypic variation across the secondary contact zone between these two squirrel taxa in order to assess whether species boundaries are being maintained and, if so, how. First, we undertook a population genetic analysis using microsatellite DNA to confirm the presence of hybridization. We also sought to verify the reproductive viability of hybrids by assessing the generation of hybrids with a multilocus analysis. Finally, we examined patterns of clinal variation in ventral coloration, cranial morphology, mtDNA clade assignment, and microsatellite genotype assignment in relation to the forest transition across the hybrid zone. Among these patterns we tested the general hypothesis that phenotypic traits under strong divergent selection should exhibit the sharpest cline patterns.

Materials and Methods

Sampling

We sampled 397 museum specimens of *Tamiasciurus douglasii* and *T. hudsonicus* from 29 localities along a nearly 600-km west-to-east study area across the northern Cascade Mountains region of northern Washington, southern British Columbia, and northern Idaho (Fig. 1; Table S1). These specimens were collected between 1920-1991, with a majority (60%) collected in the region of sympatry in two major sampling periods: 1963-65 by Smith (1968) and 1971-1973 by Stevens and Nellis (1974). All the specimens are accessioned at the Burke Museum, University of Washington (UWBM), and the University of Kansas Natural History Museum (KU).

Habitat associations across study area

Smith (1968) described the association of coniferous tree species and forest types with both *Tamiasciurus* species and the putative hybrids in the northern Cascade Mountains. *Tamiasciurus douglasii* is found on the western side of the north Cascade Mountains and mostly in western hemlock (*Tsuga heterophylla*) and Pacific silver fir (*Abies amabilis*) vegetation zones, whereas *T. hudsonicus* is found on the east side and mostly in ponderosa pine (*Pinus ponderosa*) and interior Douglas-fir (*Pseudotsuga menziesii*) vegetation zones. The squirrel species are sympatric near the crest of the northern Cascade Mountains in an approximately 25-km wide transitional-forest zone that includes a subalpine fir (*Abies lasiocarpa*) vegetation zone on the west side of the Cascade crest and an interior Douglas-fir vegetation zone also on the west side. These forest zones have been most recently defined by the Washington and Idaho GAP Analysis Programs (http://wdfw.wa.gov/conservation/gap/, http://www.wildlife.uidaho.edu/idgap/index.htm) and the British Columbia Biogeoclimatic Ecosystem Classification (BEC) and Ecology Research program (http://www.for.gov.bc.ca/hre/becweb/index.html), and are also in accord with Franklin and Dyrness (1973).

We designated the associated forests types according to the above habitat classification system for all 29 sampling localities by overlaying the center-most location of all individuals at each locality on current ecoregion maps (above URL's). We collapsed several specific forest types from these maps into the following three general forest zones from west to east: wet coastal forest, transitional forest, and dry interior forest. Localities 1-9 were in the wet coastal forest zone, 10-18 in the transitional forest zone, and 19-29 in the dry interior forest zone.

DNA extraction

We extracted genomic DNA from a 1.5 mm x 1.5 mm snippet of footpad tissue from each museum study specimen. Skin snippets were cleansed in an ethanol wash every 3 h for a 24-h period to remove salts and polymerase chain reaction (PCR) inhibitors that may have been inadvertently added during the preservation process of museum skins (Mullen and Hoekstra 2008). Following the washes, we used the prescribed protocol within the DNeasy Tissue Kit (Qiagen, Valencia, California) to extract genomic DNA. We undertook several steps during this process to avoid and detect any possible contamination. First, we used a new sterilized razor blade for snipping each sample. Second, we performed ethanol washes in a separate room from where PCR amplifications were performed. We also included negative extractions and PCR controls in the genotyping process. Finally, we repeated DNA extractions from 20 individuals using skin snippets from another part of the study specimen and compared their microsatellite genotype profiles with original samples.

Microsatellite amplifications and screening

We genotyped all 397 specimens at nine polymorphic microsatellite loci originally identified in *T. hudsonicus* by Gunn et al. (2005): Thu03, Thu08, Thu14, Thu21, Thu23, Thu25, Thu31, Thu41, and Thu42. Each 3.32 µl reaction mixture contained 1.0 µl of nuclease-free H_2O, 0.5 µl of 10X Bovine Serum Albumin (BSA), 0.5 µl of 10X PCR buffer, 4.5 mM $MgCl_2$, 0.286 mM of each dNTP, 0.75 µM of each primer, 0.31 U of JumpStart Taq DNA polymerase (Sigma, St. Louis, Missouri) and 1.68 µl of genomic DNA. We used a touchdown PCR protocol consisting of a denaturing step at 94^{o}C for 3 min; followed by 8 cycles (with a decreasing 1^{o}C annealing temperature after each cycle) of 94^{o}C for 15 s, 68^{o}C for 15 s, and 72^{o}C for 30 s; followed by 20 cycles of 94^{o}C for 45 s, 59^{o}C for 15 s, and 72^{o}C for 30 s; and with a final extension period of

72°C for 45 min. We diluted PCR amplification products by 1:10 with nuclease-free water. Individuals were genotyped on an ABI 3730 Genetic Analyzer in a 17-µl multiplex sample (3 primer-pair set) containing 3 µl of diluted PCR products (1 µl from each primer pair), 13.896 µl Hi-Di (ABI), and 0.104 µl GeneScan ROX400HD size standard. Allele sizes were visualized and scored using GeneMapper (ABI). We examined the data in Micro-checker (Van Oosterhout et al. 2004) to assess genotyping errors, such as allelic dropouts, stuttering, or null alleles, which may be elevated when using museum specimens that putatively contain partially degraded DNA. Micro-checker investigates the presence of null alleles when the combined probability test shows an overall significant excess of homozygotes evenly distributed across homozygote-classes. Our results detected no null alleles in any of the nine microsatellite loci.

Population structure and hybridization assignment

To determine the most probable number of genetic clusters that characterizes this secondary contact zone we analyzed our genotype data with two Bayesian assignment methods. STRUCTURE 2.3.3 is a model-based Markov chain Monte Carlo (MCMC) approach that clusters individuals to minimize Hardy-Weinberg disequilibrium and gametic phase disequilibrium between loci within groups (Pritchard et al. 2000). This method is useful for studying population structure in contact zones because it allows for the presence of admixed individuals in the sample. STRUCTURE requires a user-defined number of populations (K) to test for the true populations numbers. We set the model parameters to admixture with correlated allele frequencies among populations and performed 10 replicate runs for each value of K ranging from 1 to 10 with a burn-in of 2.5×10^4 followed by 1.25×10^5 repetitions. Each run estimated the 'log probability of data' (L(K)). We then estimated the number of clusters (K)

based on these likelihood values using the ad-hoc metric (ΔK) developed by Evanno et al. (2005). We chose this measure because Evanno et al. revealed with simulated data that STRUCTURE overestimates the numbers of populations in contact zone systems. This method is based on the rate of change in the log probability of data between successive K values. We also used STRUCTURAMA 2.0 to estimate the number of discrete genetic clusters (Huelsenbeck and Andolfatto 2007). In contrast to STRUCTURE, this program does not require a user-defined number of populations. The assignment of individuals to clusters and the number of clusters are treated as random variables under a Dirichlet process prior. We ran multiple analyses with different prior mean-numbers of populations [$E(K) = 2, 5, 10$] to explore whether the results remained consistent despite different priors. All MCMC analyses were run for 1×10^6 generations with a sample frequency of 1000 and the first 100 observations discarded as burn-in.

After determining the numbers of genetic clusters in the northern Cascade Mountains study area, we used STRUCTURE to estimate individual admixture proportions, *i.e.*, the estimated proportion of an individual's genotype originating from each of the parental populations. Following Vaha and Primmer (2006) we categorized individuals into three clusters, using a range of *q-values* between 0 - 0.10 as pure *T. hudsonicus*, 0.90 – 1.0 as pure *T. douglasii*, and 0.10 – 0.90 for admixed individuals. In addition, we used the program NEWHYBRIDS 1.1 to identify hybrid individuals (Anderson and Thompson 2002). This program is a more specific Bayesian method for identifying hybrids and can be used to identify individual assignment to various hybrid categories (F_1, F_2, backcross, pure, etc.). Unlike Structure, which treats q as a random continuous variable, NEWHYBRIDS treats q as a discrete variable with up to six genotype frequency classes. NEWHYBRIDS uses a MCMC sampling approach to acquire estimates from the posterior distribution that reflect the level of certainty that an individual

belongs to a certain hybrid class. We also included 16 individuals located 250 to 500 km away from the study area as reference samples representing pure genotypes of each species (Table S1). We performed 1×10^6 MCMC sweeps with a burn in of 1×10^4. We ran the analyses separately using the Uniform and Jeffreys-like priors because the Uniform prior can under-emphasize the influence of alleles that are rare in populations. However, neither prior should heavily influence the results of the analysis. A posterior probability value of 0.5 for the membership in a class was used as a threshold for assigning individuals to a specific class.

To assess the power of NEWHYBRIDS for detecting later-generation hybrids from our empirical dataset we performed assignment tests on a simulated dataset containing individuals with known hybrid identities and belonging different hybrid classes. Using HYBRIDLAB 1.0 (Nielsen et al. 2006) with this dataset, we generated ten simulated hybrids in each of the four hybrid classes: F_1, F_2, and F_1 backcrosses to each species. Next, we combined these 40 simulated hybrids into a dataset containing empirical data from 50 *T. douglasii* and 50 *T. hudsonicus* individuals that were identified to be pure from our STRUCTURE results, as well as eight *T. douglasii* and eight *T. hudsonicus* individuals located outside of the study area that were presumed to be pure representatives of each species to set as extra prior information for the analysis. We ran the simulated dataset in NEWHYBRIDS under the same settings and analyzed them separately under the Uniform and Jeffreys-like priors. Our results demonstrated that both analyses using different prior distributions performed well at inferring individuals belonging to the F_1 hybrid class. The analysis with the Uniform prior distribution accurately assigned all simulated F_1 individuals to the F_1 hybrid class, whereas the analysis with the Jeffreys-like priors distribution correctly assigned nine out of ten F_1 individuals to the F_1 hybrid class. However, our results were not as strong for the assignment of later generation hybrids to the right classes. The

analysis using the Jeffreys-like priors correctly assigned six out of ten simulated F_2 individuals to the F_2 hybrid class and the analysis using Uniform priors correctly assigned only one out of ten to the right class. Neither analysis was able to accurately assign simulated F_1 backcrosses to the right hybrid class. The inability of NEWHYBRIDS to correctly assign later generation hybrids class is likely due to a lack of sufficient loci (see Vähä and Primmer 2006). Therefore, our confidence in interpreting the NEWHYBRIDS results from the empirical dataset is strong for inferring the correct assignment of F_1 hybrids, but weak for the correct assignment of F_2 hybrids and F_1 backcrosses.

Mitochondrial DNA sequencing and analysis

We chose the mitochondrial DNA control region for simply determining individual assignment to mtDNA clades. The more geographically extensive work of Arbogast et al. (2001) with cytochrome-*b* has previously established mtDNA phylogenetic relationships. We amplified a 312-328 bp sequence of the control region using PCR with primers OSU5020L and OSU5021H (Wilson et al. 2005). We used a modified protocol to better amplify sequences due to possible degradation of DNA from museum specimens. The PCR was performed in 15 µl reaction volumes containing 4.74 µl of nuclease-free H2O, 1.5 µl of 10X BSA, 1.5 µl of 10X PCR buffer, 3 mM $MgCl_2$, 0.19 mM of each dNTP, 0.66 µM of each primer, 0.9375 U of JumpStart Taq DNA polymerase (Sigma, St. Louis, Missouri), and 1.8 µl of genomic DNA. We performed PCR amplifications in a GeneAmp PCR System 9700 thermocycler (Applied Biosystems, Foster City, California). The cycle conditions included a denaturing step at 94 ºC (3 min), followed by 35 cycles (45 s at 94ºC, 30 s at 54ºC, and 1 min at 72ºC) with a final extension period of 30 min at 72ºC. We treated all PCR products with ExoSapIT (USB Corp.) to remove unincorporated

nucleotides and primers. PCR samples were run on either ABI 3100 or 3730xl genetic analyzers (Applied Biosystems Inc.) with manual editing and alignment performed using Sequencher 4.6 (Gene Codes Corp.). Sequences were deposited in GenBank under accession numbers JF303085-JF303476 and JF308196-JF308209.

We used both maximum likelihood (ML) and Bayesian Inference (BI) methods to infer phylogenetic relationships of our mtDNA dataset. We estimated the Tamura-Nei (TrN; 1993) model of nucleotide substitution as the best-fitting model for our phylogenetic analyses using the Akaike Information Criterion in jModelTest v0.1.1 (Posada 2008). We also incorporated estimates of the proportion of invariable sites (0.6100) and gamma shape parameter (0.9020) into the analyses. The ML phylogeny was inferred using PHYML 3.0 (Guindon and Gascuel 2003) with 100 bootstrap replicates to evaluate nodal support for phylogenetic clades (Felsenstein 1985). The BI phylogenetic reconstructions were performed using MRBAYES 3.1 (Ronquist and Huelsenbeck 2003) using Markov Chain Monte Carlo (MCMC) sampling. Two different runs (each with 1 cold and 3 heated chains) were analyzed for 2×10^6 generations (with trees sampled every 100 generations), which was when the average standard deviation of the split frequencies became less than 0.10. The first 25% of sampled trees were discarded as burn-in after visual inspection using TRACER 1.5 (Rambaut and Drummond 2007) revealed that these initial samples had not reached stationarity. We sequenced one *T. hudsonicus mogollensis* specimen from Arizona (GenBank Accession JF303477) to serve as the outgroup, based on the previous determination that populations in that region belong to a divergent mitochondrial lineage (Arbogast et al. 2001). We also performed additional phylogenetic analyses across the broader geographic ranges of the two species, beyond the study area, to determine whether observed mismatches between mtDNA and species description are due to gene introgression or retention

of ancestral polymorphisms and to determine whether mtDNA markers are species-informative. These additional samples of *T. douglasii* (n=9) were from more northerly British Columbia, western Washington, and California; and those of *T. hudsonicus* (n=11) were from more northerly British Columbia, southern Idaho, Montana, Utah, Wyoming, and South Dakota (Table S1).

Color scoring

To quantify the readily apparent variation in ventral color of available museum specimens, we visually scored 388 individuals using a scale from 0 to 3 based on a reference set of four squirrels ranging as follows: white (0), light orange (1), medium orange (2), and dark orange (3). Scores of 0 are typical for pure *T. hudsonicus* in the Pacific Northwest, scores of 1 and 2 are typical of individuals with intermediate coloration between the two species, whereas a score of 3 is typical for pure *T. douglasii*. Next, to examine relationships between color score and genotype, we binned the specimens using the genotype assignment results from the STRUCTURE analysis into the following three categories: (1) pure *T. douglasii* (N = 185), (2) admixed ancestry between *T. douglasii* and *T. hudsonicus* (N = 35), and (3) pure *T. hudsonicus* (N = 168).

Analyses of cranial morphology

To examine differences in cranial morphology that may have resulted from either adaptive genetic divergence or phenotypic plasticity in response to different forest environments, we examined three cranial characters that seemed likely to serve important roles in modulating jaw strength and function (Smith 1981). Linear measurements were made to the nearest one hundredth millimeter using digital calipers (Mitutoyo Corp., Japan) as follows: (1) sagittal crest,

measured as distance between the temporal lines; (2) the angular moment arm (AMA), measured as distance between the mandibular notch to the angular process; (3) coronoid moment arm (CMA), measured as distance between the coronoid processes and the mandibular condyle.

Morphological traits typically scale with body size, which can obscure interesting differences in traits among species that differ in body size (Reist 1986). Because *T. hudsonicus* is slightly larger in body length than *T. douglasii* (Smith 1981), differences in cranial traits between the two species can be confounded by differences in overall body length. Accordingly, we used an Analysis of Covariance (ANCOVA) to eliminate the effects of body size (Berner *in press*). For this analysis we used body length (taken as total length minus tail length as measured at the original preparation of each museum specimen) as a covariate in the model. Each measurement was divided by the grand mean in order to preserve between-group differences (Berner *in press*). None of the three traits showed sexual dimorphism, and therefore sexes were pooled for each species (Fig S1). Species were binned into 3 microsatellite-genotype groups (pure *T. douglasii*, admixed, and pure *T. hudsonicus*) as assigned by our STRUCTURE analyses. These genotype groups were used as the factor variable in our ANCOVA model. For each trait, species always produced a significant effect at explaining the variance among data. However, the species-by-body-length interaction was never significant, which allowed us to reanalyze each ANCOVA without the interaction. We used the residuals from this model as our size-corrected data for the cline analyses. All analyses were carried out in JMP 7 (SAS Institute, Cary, NC).

Clinal analysis

To estimate the relationship between spatial position and clinal variation of genetic and phenotypic data, we fitted maximum likelihood clines to geographic variation of mtDNA

haplotype assignments, ventral color scores, principal component scores for cranial morphology, and microsatellite genotype assignments using CFIT-7 (Gay et al. 2008). CFIT uses a simulated annealing function that includes Metropolis algorithms to fit three-part clines that include a central sigmoid part and two exponential tails (Szymura and Barton 1986). For the mtDNA data, we compared allele frequency clines with different numbers of parameters: a simple sigmoid model (2 parameters), an asymmetric model (4 parameters), and a three-parts model with different positions of tails (6 parameters). We treated microsatellite genotype assignment, ventral color, and cranial morphology as quantitative characters and compared five different candidate models to find the best fitting curve: bimodal without introgression, bimodal, trimodal without introgression, trimodal, and unimodal. Bimodal distributions are characteristic of hybrid zones with very limited hybridization or introgression due to high dispersal of parental genotypes and very high selection against hybrids or high assortative mating. Most hybrid zones are characteristic of trimodal distributions, which can be described as having a pattern somewhere between a unimodal and a bimodal distribution (Gay et al. 2008). In this case, hybrids form a well identifiable group with intermediate allele frequences and often high phenotypic variation due to varying levels of introgression. Unimodal distributions are characteristic of situations where intermediate hybrid genotypes predominate (hybrid swarm) or of relatively weak disruptive selection (Jiggins and Mallet 2000). We first analyzed each character independently and used the Akaike Information Criterion (AIC) to rank the candidate models. We estimated cline width by measuring the geographic distance between 20% and 80% of the parental frequencies (Endler 1977). We performed pairwise comparisons of cline coincidence (center) and concordance (width) of each character with the geographical cline of the mtDNA clade assignment by constraining each character to have the same center or slope as the mtDNA cline.

We also performed a comparison of cline coincidence and concordance all three cranial characters, coloration, and microsatellite genotype assignment. We used the AIC to select the best model out of the constrained and unconstrained models. Evidence ratios were provided for each AIC model comparison to show the relative likelihood of the best model being correct when compared against other models. Different starting positions and an optimal number of chains were used for each analysis to ensure that the algorithms used in CFIT were adequately exploring parameter space. Data for each character were transformed to a scale of 1 – 0, with 1 representing *T. douglasii*-like character and 0 representing *T. hudsonicus*-like character.

For these cline analyses across the three forest zones, we reduced the spatial complexity of the 29 localities (Fig. 1) to a one-dimensional axis (transect) that follows a west-to-east orientation (Fig. 3). The topographical complexity of the hybrid zone in the northern Cascade Mountains presented a challenge in the transformation of the study area into a simple one-dimensional transect because of the uneven boundaries of the forest zones along the mountain axis. Therefore the distance values in our cline analyses (cline width and center) should be interpreted as relative values, rather than true distances. We binned each locality into one of three forest zones and measured straight west-to-east distances (km) from each locality to the boundary of the transitional forest zone. In the wet coastal forest zone, localities #1-9 were measured to the westernmost boundary of the transitional forest zone and in the dry interior forest zone, localities #19-29 were measured to the easternmost transitional forest boundary. For localities within the transitional forest zone (10-18) we measured a straight-line distance of each locality to the midpoint of this zone. To obtain a total distance across the entire transect, we assigned a distance value of zero to the westernmost locality (#1) and adjusted the remaining locality distances relative to this locality, resulting in a total distance of 467 km. The geographic

coordinates of each specimen and each locality (measured as the center-most individual of all individuals at each locality) are given in Table S1, along with the distance in km of each locality along the entire 467-km transect (as shown on the x-axis of Fig 4). In addition, not all samples from each locality were from exactly the same location. For localities close to the contact zone, we used watershed boundaries to delineate the spatial extent of the locality. For localities at or near the ends of the transect, we grouped samples from greater distances apart because we presumed these contained pure values for each species.

Results

Population genetic structure and genotypic identification of hybrids

All our analyses of genetic population structure indicate the existence of two population groups in the northern Cascade Mountains that correspond with the taxonomic descriptions of *T. douglasii* and *T. hudsonicus*. Bayesian clustering analyses using microsatellite genotype data revealed two such population groupings The ΔK statistic of Evanno et al. (2005) based on STRUCTURE likelihood estimates also showed that two genetic clusters best characterized this multilocus dataset (Table 1). All three STRUCTURAMA analyses using the Dirichlet process prior with population values of 2, 5, and 10 revealed that the highest posterior probability for the number of populations was also two (Table 1).

The assignment tests from STRUCTURE revealed the presence of hybrid individuals in our study area. About 9% (37 of 397) of all individuals from the entire study transect showed an admixed ancestry. Pure *T. douglasii* are represented by 48% (190 of 397) of all individuals and pure *T. hudsonicus* by 43% (170 of 397). Of all 37 admixed individuals, 28 (76%) were located in the transitional forest zone. These 28 individuals also represented 20% of all individuals from

the transitional forest zone. Results from NEWHYBRIDS indicated the presence of later-generation hybrids and thus reproductive viability among hybrids. From the analysis using the Jeffreys-like priors we could infer that all hybrids belonged to the F_2 hybrid class. However, because our analyses using simulated hybrids were only correct 60% of the time in identifying hybrids to the F_2 generation, it is possible that these hybrids actually belonged to other hybrid classes. Even so, we are confident that they were not F_1 hybrids, because our analyses with simulated hybrids showed a strong ability to correctly identify F_1 hybrids.

Relationship between mtDNA haplotype and microsatellite genotype

Phylogenetic inferences of mitochondrial sequence variation using Bayesian analyses (Fig. 2) and maximum likelihood (not shown) both revealed two major clades with strong nodal support corresponding to the two species. All mtDNA haplotypes belonging to the *T. douglasii* clade were distinguishable from those belonging to the *T. hudsonicus* clade by a 13-bp indel. Of 392 samples, 97 individuals had a mismatch between microsatellite genotype and mtDNA haplotype. In the *T. douglasii* mtDNA clade, 25 individuals had the pure microsatellite-genotype assignment of *T. hudsonicus* and 24 had admixed genotypes. In the *T. hudsonicus* clade, 35 individuals had the pure microsatellite genotype of *T. douglasii* and 13 had admixed genotypes. These mismatches may result from either the introgression of mtDNA haplotypes through admixture or from the retention of ancestral polymorphisms, which confounds the assignment of the two mtDNA clades to the two nominal species. To resolve this matter, we checked 20 additional mtDNA sequences from outside the study area (Table S1). None of these outside samples showed a mismatch between species designation and mitochondrial clade. We therefore conclude

that the most parsimonious explanation for the mismatched haplotypes in our study area is that they represent gene introgression rather than retention of ancestral polymorphisms.

Relationship between color and microsatellite genotype assignment

Our examination of the relationship between color scores and microsatellite genotype assignment showed a complex relationship between color and microsatellite genotype assignment. Not all individuals with demonstrably admixed genotypes possessed intermediate coloration and not all individuals with intermediate coloration had admixed genotypes (Table 2). This verifies previous speculation that squirrels with intermediate coloration include hybrid individuals (Smith 1968; Stevens and Nellis 1974), but also showed that not all squirrels showing intermediate coloration are hybrids.

Most of the squirrels with intermediate color (26 of 28) were located in the transitional forest zone. Of these 26 individuals, 13 had an admixed genotype, 10 had the pure *T. douglasii* genotype, and 3 had the pure *T. hudsonicus* genotype.

Clinal patterns of genetic and phenotypic variation

All clinal patterns—mtDNA clade assignment, microsatellite genotype assignment, coloration, and cranial morphology—possessed cline centers located within the transitional forest zone (Fig. 3). The clinal pattern for mtDNA variation (Fig. 3A) showed a pattern of bidirectional introgression, with the center occurring within the transitional forest zone. The center and width of this cline were estimated as 155 km and 27 km, respectively. The three-part model with six parameters showed the best fit for the clinal pattern of geographic variation in mtDNA clade assignments (Table 3). The geographic cline for microsatellite genotype assignment (Fig. 3B)

was steep, and all pure genotypes of each species were found only in their respective forest zone or in the transitional forest zone, but never in the forest zone inhabited by the other species. Furthermore, about 75% of the admixed genotypes were found in the transitional forest zone. Maximum likelihood estimates of the center and width of this cline were 150 km and 14 km, respectively. The trimodal distribution showed the best fit of the clinal pattern for microsatellite genotype assignment (Table 3), which is characteristic of hybrid zones that form a well identifiable group with intermediate allele frequencies and high variance due to varying levels of introgression. The geographic cline for fur coloration (Fig. 3C) was very steep and revealed that the typical fur color of each species was found only in its respective forest zone or in the transitional forest zone, but never in the forest zone inhabited by the other species. Furthermore, all but two of the intermediate color types were found in the transitional forest zone. Maximum likelihood estimates of the center and width of the cline in ventral color score were 150 km and 8 km, respectively. The trimodal distribution produced the best fit of the clinal pattern for this character (Table 3). The geographic cline for sagittal crest width (Fig. 3D) was best characterized by the bimodal-without-introgression model (Table 3), which is typical of relatively strong disruptive selection against intermediate forms. The center and width of this phenotypic cline were estimated as 148 km and 8 km, respectively. The geographic clines for both AMA and CMA (Fig. 3 E & F) were best characterized by the trimodal distribution (Table 3). For AMA, the center and width were estimated as 144 km and 12 km, respectively, and for CMA the center and width were 148 km and 3 km. Our pairwise comparisons of constrained versus unconstrained models found that none of the character clines could be constrained to share a common center or slope with the cline for the mtDNA marker (Table 4). The comparison of cline concordance and coincidence of all phenotypic characters and microsatellite genotype

assignment showed that clines could be constrained to share a common slope and center (Table 5).

Discussion

Identification of hybrids and their forest association

We have shown that *Tamiasciurus douglasii* and *T. hudsonicus* form distinct genetic clusters and hybridize in a secondary contact zone in the northern Cascades Mountains. Our genetic data suggest that the intermediate morphological phenotypes and behaviors previously observed by Smith (1968) and Stevens and Nellis (1974) resulted from this hybridization. We also found that most of the hybrids occurred in a relatively narrow band of ecotonal habitat. Although both species are ecologically dependent on coniferous forest habitat for food and shelter, each occupies a different forest type: *T. douglasii* in wet, western coastal forests and *T. hudsonicus* in dry, eastern interior forests. Smith (1968, 1970, 1978, 1981) found divergence of feeding efficiency, life history strategies, coloration, and vocalization across this east-west cline of forest environments. The transitional forest ecotone where we identified most of the hybrids is located slightly to the west of the crest of the Cascade Mountains and includes both a subalpine forest and an atypical, high-altitude Douglas-fir forest community. This special Douglas-fir community is unusual because it contains a complex and highly diverse mixture of coniferous tree species that are otherwise typical of both eastern dry forests (lodgepole and ponderosa pines) and western wet forests (western hemlock and western red cedar). The great breadth of the Cascade Mountain range in this region has created an exceptional rain shadow effect on the west side of the Cascade crest, which provides locally drier environmental conditions that support this unique forest assemblage (Franklin and Dyrness 1973). Moreover, this region is also near the area of

contact between two varieties of Douglas-fir trees, *Pseudotsuga menziesii* var. *menziesii* (coastal Douglas-fir) and *P. menziesii* var. *glauca* (interior Douglas-fir) which possess adaptive differences in phenology and growth rate (St. Clair et al. 2005). A recent phylogeographic analysis of these two tree varieties reveals that they represent divergent lineages of mtDNA and chloroplast-DNA that show genetic introgression and likely moved into secondary contact in the Cascade Mountains during the Holocene (Gugger et al. 2010). Douglas-fir is used extensively by both *T. douglasii* and *T. hudsonicus* for both food and shelter, and therefore it is likely that the postglacial secondary contact of these coniferous tree lineages facilitated secondary contact of the squirrel lineages.

Hybrid viability

Our genetic evidence based on microsatellite data demonstrated that hybrids are reproductively viable and able to backcross with both parental species. The assignment of all hybrids to a later generation hybrid class indicates that hybrids must have been reproductively viable to successfully breed beyond the F_1 generation. Hybrid viability is further supported by the fact that 19% of the pure *T. douglasii* specimens (based on microsatellite genotype assignment) and 15% of the pure *T. hudsonicus* specimens possessed a mtDNA haplotype belonging to the opposite species, which could only occur through multiple generations of hybrid backcrossing with both parental forms. This bidirectional pattern of mtDNA introgression suggests that species discrimination in mating, whether through male-male competition or female mate-choice, is not strong enough to maintain complete reproductive isolation in *Tamiasciurus*. In other mammalian taxa that hybridize, it has been suggested that prezygotic isolating mechanisms such as variation in bacular morphology and aggressive mating behavior have caused asymmetric introgression

patterns, i.e., mtDNA capture (Macholán et al. 2007; Good et al. 2008). However, unlike most members of the squirrel family (Wade and Gilbert 1940), male *Tamiasciurus* possess a minute os penis, or baculum, that is considered vestigial (Layne 1952), and thus this structure may not play an important role in reproductive isolation. Furthermore, interspecific copulations may be facilitated by a lack of overt mate choice by females, which would result in multi-male mating; this situation has been shown to occur in *Tamiasciurus* populations (Arbetan 1993; Lane et al. 2007; Bonanno and Schulte-Hostedde 2009). On the other hand, multi-male mating in *Tamiasciurus* may lead to sperm competition (Bonanno and Schulte-Hostedde 2009), which could promote interspecific assortative mating in a hybrid zone such as ours.

Phenotypic variation

The trimodal cline model for fur coloration supports a scenario in which hybridization has produced intermediate phenotypes, but in which these phenotypes do not spread outside the contact zone because of strong selection against them. The sharp cline for this trait and its position within the ecotonal forest zone suggest that divergent selection might be acting strongly on this variable and perhaps heritable trait. Fur coloration is ecologically important in mammals and under strong selection for cryptic protection from predators (Powell 1982; Kiltie 1992; Stoner et al. 2003; Hoekstra et al. 2005; Mullen and Hoekstra 2008). Most studies examining selection on fur color have focused on dorsal pelage and its match to ground color; however, the arboreal lifestyle of tree squirrels also makes their underside coloration a target of selection. Smith (1981) studied the ecology of both species of *Tamiasciurus* in this region and argued that reduced light intensity in the dense canopy forest (of the west) should favor a darker ventral fur color for protection against avian predators from the side or below, whereas the brighter

background sky in the more open canopy forest to the east should favor lighter ventral fur color. It would be interesting to assess with experimental selection studies whether these divergent phenotypes are being selected for greater matching to their respective forest environments (Kiltie 1992; Vignieri et al. 2010). It could also be argued that these species have not interbred for long enough for these traits to spread sufficiently across the hybrid zone. However, if this were the case then we might not have documented relatively deep introgression of the neutral mtDNA marker across the hybrid zone in both directions. Thus we conclude that ventral fur color appears to be an ecologically important trait.

Our cline analysis of three key, potentially adaptive cranial characters showed a lack of coincidence of cline centers and a lack of concordance of slopes with the putatively neutrally evolving mtDNA marker; we also found different clinal distributional patterns that are indicative of moderate to strong selection strength acting on these phenotypes. Both species of squirrels consume seeds from cones, as a primary food resource, after they have mechanically removed the scales from the cones (Smith 1968). *Tamiasciurus hudsonicus* lives in a dry forest environment where several species of coniferous trees have evolved harder and thicker cone scale tissue than the conifer species in the wetter forests where *T. douglasii* lives (Smith 1968). For example, lodgepole pine (*Pinus contorta*), an important food resource within the range of *T. hudsoncisus*, has evolved fire-mediated serotiny in its cones, which requires greater jaw force of squirrels to open than for cones of any of the tree species west of the Cascade Mountains. Mammals can produce different amounts of jaw force by modulations of their temporal and masseter jaw musculature (Turnbull 1970). Studies on jaw structure and feeding efficiency in *Tamiasciurus* have shown that *T. hudsonicus* is more powerful and faster than *T. douglasii* at chewing through harder cones (Smith 1970, 1981). Presence of a sagittal crest in mammals

generally indicates strong jaw muscles. The sagittal crest develops through the convergence of the temporal lines on the pariental bone and serves primarily as the origin of the temporalis muscle, one of the main chewing muscles. *Tamiasciurus hudsonicus* generally possess a large temporal muscle and a distinct sagittal crest, making them more efficient at chewing harder cones than *T. douglasii*, in which these characters are less pronounced (Smith 1981). Our demonstration of a bimodal clinal pattern of sagittal crest width and cline center in the transitional forest zone suggests that this trait is ecologically important and that it is responding to transitional variation in conifer species. Another important component of the temporalis muscle complex is the coronoid process, which is the insertion point for the temporalis muscle. The force applied along the temporal muscle is applied along the CMA, which is related to the length between the coronoid process and the mandibular condyle. Smith (1981) found that CMA is positively correlated with size of the temporal muscle in *Tamiasciurus* and accordingly is larger in *T. hudsonicus* than in *T. douglasii*. The angular moment arm (AMA) is related to the force applied along the masseter muscle and is another important trait involved in bite force in mammals. Both CMA and AMA exhibit trimodal clinal patterns and cline centers located within the transitional forest zone, which suggests that these traits are under moderately strong selection across the hybrid zone. All of these cranial features are subject to ontogenetic effects caused by environmental variation. However, it is beyond the scope of this study to ascertain the degree to which phenotypic variation is affected by underlying genetic variation versus phenotypic plasticity.

The occurrence of similar cline centers and widths of all phenotypic characters and the microsatellite genotype assignment within the narrow transitional forest zone demonstrates that ecological selection is possibly maintaining the geographic position of this hybrid zone system.

This could be due to the fact that selection is acting not only against a particular trait, but perhaps further against a correlated set of traits and associated loci. Strong statistical associations (linkage disequilibria) between genes, chromosomes, and morphological characters are generated by the continual diffusion of the combination of parental genes into the center of a hybrid zone (Barton and Hewitt 1989). Therefore, any disruptive selection that prohibits a particular trait from permeating through a hybrid zone may also be prohibiting other traits from permeating. If selection is strong, linkage disequilibrium between parental alleles becomes even stronger and pulls clines together (Slatkin 1975; Barton 2001).

Conclusion

The montane regions of northwestern North America contain "suture zones" for many pairs of terrestrial vertebrate species (Remington 1968, Swenson and Howard 2005). Pleistocene cycles of glaciation and associated historic north-south habitat shifts, together with the existence of prominent north-south montane axes (Cascade and Rocky Mountains), have played a major role in the vicariance and subsequent secondary contact of populations (Brunsfeld et al. 2001; Shafer et al. 2010). During colder intervals populations were forced into separate refugia (often eastward and westward), which resulted in allopatric divergence. The warming climate of the Holocene facilitated the spread of populations out of refugia and in some cases into secondary contact with previously segregated populations. The outcome of secondary contact varies among major vertebrate taxa, although most show limited hybridization in narrow regions of contact. These outcomes include directional asymmetries in introgression due to pre-mating behaviors (Krosby and Rowher 2009), limited hybridization due to post-mating factors (Irwin et al. 2009), and ancient, rather than contemporary hybridization (Good et al. 2008). Several wide-ranging

boreal mammals have similar distributions and apparent secondary contact zones similar to those of *Tamiasciurus* (Arbogast and Kenagy 2001), but hybridization has not been investigated in most of these taxa (Runck et al. 2009). The low mtDNA sequence divergence (1.0 – 2.4 %) between major *Tamiasciurus* lineages suggests that their divergence is very recent, perhaps dating only to the late Pleistocene (Arbogast et al. 2001). The recency of this divergence may explain why these two forms can still interbreed; perhaps not enough epistatic incompatibilities have developed between loci. This temporal perspective also provides a compelling argument that diversifying selection on the observed color phenotypes and skull morphology phenotypes in *Tamiasciurus* has been strong and that recently divergent lineages can remain separate units despite introgression.

Literature Cited

Anderson, E. C., and E. A. Thompson. 2002. A model-based method for identifying species hybrids using multilocus genetic data. Genetics 160:1217–1229.

Arbetan, P. T. 1993. The mating system of the red squirrel, (*Tamiasciurus hudsonicus*). M.S. thesis, University of Kansas, Lawrence, Kansas.

Arbogast, B. S., and G. J. Kenagy. 2001. Comparative phylogeography as an integrative approach to historical biogeography. J. Biogeogr. 28:819–825.

Arbogast, B. S., R. A. Browne, and P. D. Weigl. 2001. Evolutionary genetics and Pleistocene biogeography of North American tree squirrels (*Tamiasciurus*). J. Mammal. 82:302–319.

Barton, N. H., and G. M. Hewitt. 1985. Analysis of hybrid zones. Annu. Rev. Ecol. Evol. Syst. 16:113–148.

Barton, N. H., and G. M. Hewitt. 1989. Adaptation, speciation, and hybrid zones. Nature 341:497–503.

Barton, N. H. 2001. The role of hybridization in evolution. Mol. Ecol.10:551–568.

Benkman, C. W. 1995. The impact of tree squirrels (*Tamiasciurus*) on limber pine seed dispersal

adaptations. Evolution 49:585–592.

Berner, D. 2011. Size correction in biology: how reliable are approaches based on (common) principal component analysis? Oecologia 166:961–971.

Bonanno, V.L., and A. I. Schulte-Hostedde. 2009. Sperm competition and ejaculate investment in red squirrels (*Tamiasciurus hudsonicus*). Behav. Ecol. Sociobiol. 63:835–846.

Boutin, S., L. A. Wauters, A. G. McAdam, M. M. Humphries, G. Tosi, and A. A. Dhondt. 2006. Anticipatory reproduction and population growth in seed predators. Science 314:1928–1930.

Brunsfeld, S.J., J. Sullivan, D. E. Soltis, and P. S. Soltis. 2001. Comparative phylogeography of northwestern North America: a synthesis. In: *Integrating Ecological and Evolutionary Processes in a Spatial Context* (eds. J. Silvertown, and J. Antonovics), pp. 319–339. Blackwell Science, Oxford.

Coyne, J. A., and H. A. Orr. 2004. Speciation. Sinauer Associates, Inc., Sunderland, Massachusetts.

Digweed, S. M., and D. Rendall. 2009. Predator-associated vocalizations in North American red squirrels, *Tamiasciurus hudsonicus*: are alarm calls predator specific? Anim. Behav. 78:1135–1144.

Endler, J. 1977. Geographical variation, speciation, and clines. Princeton University Press, Princeton, New Jersey.

Evanno, G., S. Regnaut, and J. Goudet. 2005. Detecting the number of clusters of individuals using the software STRUCTURE: a simulation study. Mol. Ecol. 14:2611–2620.

Felsenstein, J. 1985. Phylogenies and the comparative method. Am. Nat. 125:1–15.

Fitzpatrick, B. M., J. R. Johnson, D. K. Kump, J. J. Smith, S. R. Voss, and H. B. Shaffer. 2010. Rapid spread of invasive genes into a threatened native species. Proc. Natl. Acad. Sci. U.S.A. 107:3606–3610.

Franklin, J. F., and C. T. Dyrness. 1973. Natural vegetation of Oregon and Washington. Oregon State University Press, Corvallis, Oregon.

Gay, L., P. A. Crochet, D. A. Bell, and T. Lenormand. 2008. Comparing clines on molecular and phenotypic traits in hybrid zones: a window on tension zone models. Evolution 62:2789–2806.

Good, J., S. Hird, N. Reid, J. Demboski, S. Steppan, T. Martin-Nims, and J. Sullivan. 2008. Ancient hybridization and mitochondrial capture between two distantly related species of chipmunks (*Tamias*: Rodentia). Mol. Ecol. 17:1313–1327.

Grant, P. R., B. R. Grant, J. A. Markert, L. F. Keller, and K. Petren. 2004. Convergent evolution of Darwin's finches caused by introgressive hybridization and selection. Evolution 58:1588–1599.

Gugger, P. F., S. Shinya, and J. Cavender-Bares. 2010. Phylogeography of Douglas-fir based on mitochondrial and chloroplast DNA sequences: testing hypotheses from the fossil record. Mol. Ecol. 19:1877–1897.

Guindon, S., and O. Gascuel. 2003. A simple, fast, and accurate algorithm to estimate large phylogenies by maximum likelihood. Syst. Biol. 52:696–704.

Gunn, M. R., D. A. Dawson, A. Leviston, K. Hartnup, C. S. Davis, C. Strobeck, J. Slate, and D. W. Coltman. 2005. Isolation of 18 polymorphic microsatellite loci from the North American red squirrel, *Tamiasciurus hudsonicus* (Sciuridae, Rodentia), and their cross-utility in other species. Mol. Ecol. Notes 5:650–653.

Hoekstra, H. E., J. G. Krenz, and M. W. Nachman. 2005. Local adaptation in the rock pocket mouse (*Chaetodipus intermedius*): natural selection and phylogenetic history of populations. Heredity 94:217–228.

Irwin, D. E., A. Brelsford, D. P. L. Toews, C. MacDonald, and M. Phinney. 2009. Extensive

hybridization in a contact zone between MacGillivray's warblers *Oporornis tolmiei* and mourning warblers *O. philadelphia* detected using molecular and morphological analyses. J. Avian Biol. 40:539–552.

Jiggins, C. D., and J. Mallet. 2000. Bimodal hybrid zones and speciation. Trends Ecol. Evol. 15:250–255.

Kiltie, R. A. 1992. Tests of hypotheses on predation as a factor maintaining polymorphic melanism in coastalplain fox squirrels (*Sciurus niger* L.). Biol. J. Linn. Soc. Lond. 45:17–37.

Krosby, M., and S. Rowher. 2009. A 2000 km genetic wake yields evidence for northern glacial refugia and hybrid zone movement in a pair of songbirds. Proc. R. Soc. Lond., B, Biol. Sci. 276:615–621.

Lane, J. E., S. Boutin, M. R. Gunn, J. Slate, and D. W. Coltman (2007) Genetic relatedness of mates does not predict patterns of parentage in North American red squirrels. Anim. Behav. 74:611–619.

Layne, J. N. 1952. The os genitale of the red squirrel, *Tamiasciurus*. J. Mammal. 33:457–459.

Lindsay, S. L. 1982. Systematic relationship of parapatric tree squirrel species (Tamiasciurus) in the Pacific Northwest. Can. J. Zool. 60:2149–2156.

Macholán, M., P. Munclinger, M. Šugerková, P. Dufková, B. Bímová, E. Božíková, J. Zima, and J. Piálek. 2007. Genetic analysis of autosomal and X-linked markers across a mouse hybrid zone. Evolution 61:746–771.

Martin, N. H., A. C. Bouck, and M. L. Arnold. 2006. Detecting adaptive trait introgression between *Iris fulva* and *I. brevicaulis* in highly selective field conditions. Genetics 172:2481–2489.

Mullen L. M., H. E. Hoekstra. 2008. Natural selection along an environmental gradient: a classic cline in mouse pigmentation. Evolution 62:1555–1570.

Nielsen, E. E., L. A. Bach, and P. Kotlicki. 2006. HYBRIDLAB (VERSION 1.0): a program for generating simulated hybrids from population samples. Mol. Ecol. Notes 6:971–973.

Posada, D. 2008. JMODELTEST: Phylogenetic Model Averaging. Mol. Biol. Evol. 25:1253–1256.

Powell, R. A. 1982. Evolution of black-tipped tails in weasels: predator confusion. Am. Nat. 119:126–131.

Pritchard, J. K., M. Stephens, and P. Donnelly. 2000. Inference of population structure using multilocus genotype data. Genetics 155:945–959.

Rambaut, A., A. J. Drummond. 2007. TRACER v.1.4, Available from http://beast.bio.ed.ac.uk/Tracer.

Reist, J. D. 1986. An empirical evaluation of coefficients used in residual and allometric adjustments of size covariation. Can. J. Zool. 64:1363–1368.

Remington, C. L. 1968. Suture-zones of hybrid interaction between recently joined biotas. In: Evolutionary biology (eds. T. Dobzhansky, M. K. Hecht, and W. C. Steere), pp. 321–428. Plenum Press, New York.

Ronquist, F., and J. P. Huelsenbeck (2003) MRBAYES 3: Bayesian phylogenetic inference under mixed models. Bioinformatics 19:1572–1574.

Runck, A. M., M. D. Matocq, and J. A. Cook. 2009. Historic hybridization and persistence of a novel mito-nuclear combination in red-backed voles (genus *Myodes*). BMC Evol. Biol. 9:114.

Sanderson, H. R., and J. L. Koprowski. 2009. The last refuge of the Mt. Graham red squirrel. University of Arizona Press, Tucson, Arizona.

Shafer, A. B. A., C. I. Cullingham, S. D. Cote, and D. W. Coltman. 2010. Of glaciers and refugia: a decade of study sheds new light on the phylogeography of northwestern North America. Mol. Ecol. 19:4589–4621.

Slatkin, M. 1975. Gene flow and selection in a two-locus system. Genetics 81:787–802.

Smith, C. C. 1968. The adaptive nature of social organization in the genus of three squirrels *Tamiasciurus*. Ecol. Monogr. 38:31–64.

Smith, C. C. 1970 The coevolution of pine squirrels (*Tamiasciurus*) and conifers. Ecol. Monogr. 40:349–371.

Smith, C. C. 1978. Structure and function of the vocalizations of tree squirrels (*Tamiasciurus*). J. Mammal. 59:793–808.

Smith, C. C. 1981. The indivisible niche of *Tamiasciurus*: an example of nonpartitioning of resources. Ecol. Monogr. 51:343–364.

Sobel, J. M., G. F. Chen, L. R. Watt, and D. W. Schemske. 2010. The biology of speciation. Evolution 64:295–315.

St. Clair J. B., N. L. Mandel, and K. W. Vance-Borland. 2005. Genecology of Douglas-fir in western Oregon and Washington. Ann. Bot. 96:1199–1214.

Steele, M. A. 1998. *Tamiasciurus hudsonicus*. Mamm. Species 586:1–9.

Steele, M. A. 1999. *Tamiasciurus douglasii*. Mamm. Species 630:1–8.

Stevens, W. F., and C. H. Nellis. 1974. Notes on the hybridization of three mammals in the Ross Lake Basin: squirrel, deer, and deermouse. Appendix H. In: Biotic survey of Ross Lake Basin, report for January 1973-April 1974 (ed. R. D. Taber), pp. 1–12. College of Forest Resources, University of Washington, Seattle, Washington.

Stoner, C. J., O. R. Bininda-Emonds, and T. Caro. 2003. The adaptive significance of coloration in lagomorphs. Biol. J. Linn. Soc. Lond. 79:309–328.

Swenson, N. G., and D. J. Howard. 2005. Clustering of contact zones, hybrid zones, and phylogeographic breaks in North America. Am. Nat. 166:581–591.

Szymura, J., and N. Barton. 1986. Genetic analysis of a hybrid zone between the fire-bellied toads, *Bombina bombina* and *Bombina variegata*, near Cracow in southern Poland. Evolution 40:1141–1159.

Tamura, K., and M. Nei. 1993. Estimation of the number of nucleotide substitution in the control region of mitochondrial DNA in humans and chimpanzees. Mol. Biol. Evol. 10:512–526.

Turnbull, W. D. 1970. Mammalian masticatory apparatus. Fieldiana. Geology 18:149–356.

Vähä, J. P., and C. R. Primmer. 2006. Efficiency of model-based Bayesian methods for detecting

hybrid individuals under different hybridization scenarios and with different numbers of loci. Mol. Ecol. 15:63–72.

Van Oosterhout, C., W. F. Hutchinson, D. P. M. Wills, and P. Shipley. 2004. MICRO-CHECKER: software for identifying and correcting genotyping errors in microsatellite data. Mol. Ecol. Notes 4:535–538.

Vignieri, S. N., J. G. Larson, and H. E. Hoekstra. 2010. The selective advantage of crypsis in mice. Evolution 64:2153–2158.

Wade, O., and P. T. Gilbert. 1940. The baculum of some Sciuridae and its significance in determining relationships. J. Mammal. 21:52–63.

Whitney, K. D., R. A. Randell, and L. H. Rieseberg. 2006. Adaptive introgression of herbivore resistance traits in the weedy sunflower Helianthus annuus. Am Nat. 167:794–807.

Wilson, G. M., R. A. Den Bussche, K. McBee, L. A. Johnson, and C. A. Jones. 2005. Intraspecific phylogeography of red squirrels (*Tamiasciurus hudsonicus*) in the central rocky mountain region of North America. Genetica 125:141–154.

Wu, C-I. 2001. The genic view of the process of speciation. J. Evol. Biol. 14:851–865.

Table 1. Estimates of population number (*K*) from STRUCTURE and STRUCTURAMA analyses using nine microsatellite loci. The number of populations with the highest Δ*K* value estimated from STRUCTURE and the highest posterior probability estimated from STRUCTURAMA is *K*=2 (shown in bold).

No. of populations	STRUCTURE ad-hoc statistic	STRUCTURAMA posterior probability distributions		
K	Δ*K*	*E*(*K*) = 2	*E*(*K*) = 5	*E*(*K*) = 10
1	–	0.09	–	–
2	**103.53**	**0.91**	**1.00**	**0.99**
3	1.99	–	–	0.01
4	5.71	–	–	–
5	0.63	–	–	–
6	0.24	–	–	–
7	4.46	–	–	–
8	2.01	–	–	–
9	0.21	–	–	–
10	6.69	–	–	–

Table 2. Numbers of individuals in a sample of 388 scored for both microsatellite genotype assignment and ventral coloration. Color scores are 0 for lightest, 3 for darkest, and 2 or 3 for "intermediate."

		Genotype-Assignment Category		
		Tamiasciurus douglasii	Admixed	*Tamiasciurus hudsonicus*
Color score	0	-	10	162
	1	-	8	3
	2	8	6	3
	3	177	11	-

Table 3. Comparison of hybrid zone models using the Akaike Information Criteria (AIC) for clinal variation in microsatellite genotype assignment, mtDNA clade assignment, ventral color score, and three cranial features. The best model for each cline is in bold. Evidence ratios (AIC weight of the best model divided by the AIC weight of the listed model) for each character shows the relative likelihood of the best model being correct.

	Model	Parameters	AIC_c	Δ_{AIC}	AIC weights	Evidence Ratio
mtDNA clade assignment	**3-Part**	**6**	**380.0937**	**0**	**0.8018**	
	Asymmetric	4	382.8901	2.7964	0.1981	4.0
	Simple sigmoid	2	397.1475	17.1170	~0	>10
Microsatellite genotype assignment	Unimodal	11	3046.0065	1298.8263	~0	>10
	Trimodal	**18**	**1747.1802**	**0**	**0.7575**	
	Trimodal No Introgression	16	1749.4579	2.2778	0.2425	3.1
	Bimodal	12	2737.7096	990.5294	~0	>10
	Bimodal No Introgression	10	2764.0177	1016.8375	~0	>10
Ventral color score	Unimodal	11	-1262.2427	2796.6596	~0	>10
	Trimodal	**18**	**-4058.9023**	**0**	**0.6753**	
	Trimodal No Introgression	16	-4057.4381	1.4643	0.3247	2.1
	Bimodal	12	-2338.0259	1720.8764	~0	>10
	Bimodal No Introgression	10	-2167.6486	1891.2537	~0	>10
Sagittal Crest Width	Unimodal	11	-238.4167	50.3278	~0	>10
	Trimodal	18	-279.2470	9.4975	0.0074	>10
	Trimodal No Introgression	16	-283.8755	4.8690	0.0751	>10
	Bimodal	12	-283.4637	5.2807	0.0611	>10
	Bimodal No Introgression	**10**	**-288.7445**	**0**	**0.8564**	

CMA	Unimodal	11	-108.1881	9.3547	0.0092	>10
	Trimodal	**18**	**-117.5428**	**0**	**0.9883**	
	Trimodal No Introgression	16	-96.5462	20.9966	~0	>10
	Bimodal	12	-105.5160	12.0269	0.0024	>10
	Bimodal No Introgression	10	-95.4318	22.1110	~0	>10
AMA	Unimodal	11	-104.9091	4.9642	0.0836	>10
	Trimodal	**18**	**-109.8733**	**0**	**~1**	
	Trimodal No Introgression	16	-93.2671	16.6061	~0	>10
	Bimodal	12	-104.5430	5.3303	0.0696	>10
	Bimodal No Introgression	10	-89.4879	20.3853	~0	>10

Table 4. Pairwise comparisons of hybrid-zone models for coincidence and concordance of each character cline with the putatively neutral mtDNA cline using the AIC. The best model for each cline is in bold. Evidence ratios (AIC weight of the best model divided by the AIC weight of the listed model) for each character shows the relative likelihood of the best model being correct.

Character	Hybrid-zone Models	Parameters	AIC_c	Δ_{AIC}	AIC weights	Evidence Ratio
Ventral Color	Center Constraint	23	-3634.152	41.454	0.000	>10
	Slope Constraint	23	-811.489	2864.116	0.000	>10
	Slope and Center Constraints	22	-1056.912	2618.694	0.000	>10
	Unconstrained	**24**	**-3675.606**	**0**	**~1**	
Sagittal Crest Width	Center Constraint	15	102.586	7.342	0.025	>10
	Slope Constraint	15	218.959	123.715	~0	>10
	Slope and Center Constraints	14	217.741	122.497	~0	>10
	Unconstrained	**16**	**95.244**	**0**	**0.975**	
CMA	Center Constraint	23	296.423	26.910	~0	>10
	Slope Constraint	23	404.442	134.929	~0	>10
	Slope and Center Constraints	22	402.978	133.465	~0	>10
	Unconstrained	**24**	**269.513**	**0**	**~1**	
AMA	Center Constraint	23	299.834	18.349	~0	>10
	Slope Constraint	23	411.934	130.448	~0	>10
	Slope and Center Constraints	22	411.974	130.488	~0	>10
	Unconstrained	**24**	**281.486**	**0**	**~1**	
Microsatellite Genotype Assignment	Center Constraint	21	1904.322	45.876	~0	>10
	Slope Constraint	21	3728.995	1870.549	~0	>10
	Slope and Center Constraints	20	3733.619	1875.172	~0	>10
	Unconstrained	**22**	**1858.446**	**0**	**~1**	

Table 5. Comparison of hybrid-zone models for coincidence and concordance of clines of the microsatellite genotype assignment, ventral color, and all three cranial characters using the AIC. The best model is in bold.

Hybrid-zone Models	Parameters	AIC_c	Δ_{AIC}	AIC weights	Evidence Ratio
Center Constraint	78	-3095.712	48.048	~0	>10
Slope Constraint	78	-3111.901	31.859	~0	>10
Slope and Center Constraints	**74**	**-3143.760**	**0**	**~1**	
Unconstrained	82	-2997.069	34.907	~0	>10

Table S1. Localities and other identifying information for the northern Cascade Mountains study area of 397 museum specimens of *Tamiasciurus douglasii* and *T. hudsonicus* used in this study.

Taxonomic Description	Museum Number	mtDNA Haplotype Number	mtDNA GenBank Number	Three Forest Zones	State or Province	Lat (dec)	Long (dec)
Tamiasciurus douglasii	UWBM43832	Td_13	JF303085	Wet Coastal Forest	BC	50.09	-123.75
Tamiasciurus douglasii	UWBM43833	Td_19	JF303086	Wet Coastal Forest	BC	49.75	-124.17
Tamiasciurus douglasii	UWBM43834	Td_19	JF303087	Wet Coastal Forest	BC	50.09	-123.75
Tamiasciurus douglasii	UWBM43836	Td_19	JF303088	Wet Coastal Forest	BC	50.09	-123.75
Tamiasciurus douglasii	UWBM18652	Td_10	JF303089	Wet Coastal Forest	WA	48.85	-122.59
Tamiasciurus douglasii	UWBM18654			Wet Coastal Forest	WA	48.72	-122.36
Tamiasciurus douglasii	UWBM18656			Wet Coastal Forest	WA		
Tamiasciurus douglasii	UWBM18657			Wet Coastal Forest	WA	48.76	-122.49
Tamiasciurus douglasii	UWBM18658	Td_10	JF303090	Wet Coastal Forest	WA	48.76	-122.49
Tamiasciurus douglasii	UWBM18659	Td_10	JF303091	Wet Coastal Forest	WA	48.76	-122.49
Tamiasciurus douglasii	UWBM18660	Td_10	JF303092	Wet Coastal Forest	WA	48.76	-122.49
Tamiasciurus douglasii	UWBM43827	Td_33	JF303093	Wet Coastal Forest	WA	48.42	-122.65
Tamiasciurus douglasii	UWBM43828	Td_33	JF303094	Wet Coastal Forest	WA	48.42	-122.66
Tamiasciurus douglasii	UWBM43829	Th_13	JF303095	Wet Coastal Forest	WA	48.42	-122.66
Tamiasciurus douglasii	UWBM44395	Th_13	JF303096	Wet Coastal Forest	WA	48.51	-122.61
Tamiasciurus douglasii	UWBM44396	Td_10	JF303097	Wet Coastal Forest	WA	48.51	-122.61
Tamiasciurus douglasii	UWBM44405	Td_10	JF303098	Wet Coastal Forest	WA	48.76	-122.49
Tamiasciurus douglasii	UWBM76286	Td_19	JF303099	Wet Coastal Forest	WA	48.73	-122.43
Tamiasciurus douglasii	UWBM76361	Td_10	JF303100	Wet Coastal Forest	WA	48.68	-122.43
Tamiasciurus douglasii	UWBM76381	Td_19	JF303101	Wet Coastal Forest	WA	48.52	-122.18
Tamiasciurus douglasii	UWBM76384	Td_19	JF303102	Wet Coastal Forest	WA	48.70	-122.48
Tamiasciurus douglasii	UWBM76408	Td_34	JF303103	Wet Coastal Forest	WA	48.67	-122.47
Tamiasciurus douglasii	UWBM18653	Td_10	JF303104	Wet Coastal Forest	WA	48.99	-122.07
Tamiasciurus douglasii	UWBM18655	Td_10	JF303105	Wet Coastal Forest	WA	48.91	-122.22
Tamiasciurus douglasii	UWBM76302	Td_3	JF303106	Wet Coastal Forest	WA	48.97	-122.18
Tamiasciurus douglasii	UWBM76409	Td_1	JF303107	Wet Coastal Forest	WA	48.75	-122.15

Tamiasciurus douglasii	UWBM30817	Td_10	JF303108	Wet Coastal Forest	WA	48.84	-121.58
Tamiasciurus douglasii	UWBM43831	Td_10	JF303109	Wet Coastal Forest	WA	48.72	-121.62
Tamiasciurus douglasii	UWBM44365	Td_11	JF303110	Wet Coastal Forest	WA	48.71	-121.71
Tamiasciurus douglasii	UWBM44368	Th_13	JF303111	Wet Coastal Forest	WA	48.71	-121.71
Tamiasciurus douglasii	UWBM44369	Td_10	JF303112	Wet Coastal Forest	WA	48.70	-121.73
Tamiasciurus douglasii	UWBM44370	Td_19	JF303113	Wet Coastal Forest	WA	48.70	-121.73
Tamiasciurus douglasii	UWBM73457	Td_10	JF303114	Wet Coastal Forest	WA	48.90	-121.70
Tamiasciurus douglasii	UWBM32852	Th_13	JF303115	Wet Coastal Forest	WA	48.50	-121.49
Tamiasciurus douglasii	KU141381	Td_19	JF303116	Wet Coastal Forest	WA	48.61	-121.38
Tamiasciurus douglasii	KU141382	Td_10	JF303117	Wet Coastal Forest	WA	48.61	-121.38
Tamiasciurus douglasii	KU141383	Th_13	JF303118	Wet Coastal Forest	WA	48.61	-121.38
Tamiasciurus douglasii	KU141384	Td_28	JF303119	Wet Coastal Forest	WA	48.61	-121.38
Tamiasciurus douglasii	KU141385	Th_13	JF303120	Wet Coastal Forest	WA	48.61	-121.38
Tamiasciurus douglasii	KU141386	Td_28	JF303121	Wet Coastal Forest	WA	48.61	-121.38
Tamiasciurus douglasii	KU141387	Td_19	JF303122	Wet Coastal Forest	WA	48.61	-121.38
Tamiasciurus douglasii	KU141388	Td_28	JF303123	Wet Coastal Forest	WA	48.61	-121.38
Tamiasciurus douglasii	KU141389	Td_28	JF303124	Wet Coastal Forest	WA	48.61	-121.38
Tamiasciurus douglasii	KU141390	Td_19	JF303125	Wet Coastal Forest	WA	48.61	-121.38
Tamiasciurus douglasii	KU141404	Td_29	JF303126	Wet Coastal Forest	WA	48.68	-121.27
Tamiasciurus douglasii	KU141405	Td_29	JF303127	Wet Coastal Forest	WA	48.68	-121.27
Tamiasciurus douglasii	KU141406	Td_29	JF303128	Wet Coastal Forest	WA	48.68	-121.27
Tamiasciurus douglasii	KU141407	Th_13	JF303129	Wet Coastal Forest	WA	48.68	-121.27
Tamiasciurus douglasii	KU141409	Td_17	JF303130	Wet Coastal Forest	WA	48.68	-121.27
Tamiasciurus douglasii	KU141410	Td_17	JF303131	Wet Coastal Forest	WA	48.68	-121.27
Tamiasciurus douglasii	KU141411	Td_19	JF303132	Wet Coastal Forest	WA	48.68	-121.27
Tamiasciurus douglasii	KU141412	Td_17	JF303133	Wet Coastal Forest	WA	48.68	-121.27
Tamiasciurus douglasii	KU141413	Td_17	JF303134	Wet Coastal Forest	WA	48.68	-121.27
Tamiasciurus douglasii	UWBM20785	Td_11	JF303135	Wet Coastal Forest	BC	49.60	-121.50
Tamiasciurus douglasii	UWBM20787	Td_16	JF303136	Wet Coastal Forest	BC	49.60	-121.50
Tamiasciurus douglasii	UWBM20788	Td_19	JF303137	Wet Coastal Forest	BC	49.60	-121.50
Tamiasciurus douglasii	UWBM20789	Td_12	JF303138	Wet Coastal Forest	BC	49.60	-121.50
Tamiasciurus douglasii	UWBM20792	Td_18	JF303139	Wet Coastal Forest	BC	49.62	-121.50
Tamiasciurus douglasii	UWBM20793	Td_18	JF303140	Wet Coastal Forest	BC	49.62	-121.50
Tamiasciurus douglasii	UWBM20794	Th_13	JF303141	Wet Coastal Forest	BC	49.62	-121.50
Tamiasciurus douglasii	UWBM20795	Td_11	JF303142	Wet Coastal Forest	BC	49.55	-121.45
Tamiasciurus douglasii	UWBM20796	Td_12	JF303143	Wet Coastal Forest	BC	49.57	-121.43

Tamiasciurus douglasii	UWBM20899	Td_10	JF303144	Wet Coastal Forest	BC	49.60	-121.50
Tamiasciurus hudsonicus	UWBM20900	Th_13	JF303145	Wet Coastal Forest	BC	49.60	-121.50
Tamiasciurus douglasii	UWBM20901	Td_10	JF303146	Wet Coastal Forest	BC	49.60	-121.50
Tamiasciurus douglasii	UWBM20907	Td_19	JF303147	Wet Coastal Forest	BC	49.60	-121.50
Tamiasciurus douglasii	UWBM20908	Td_25	JF303148	Wet Coastal Forest	BC	49.60	-121.50
Tamiasciurus douglasii	UWBM20909	Td_10	JF303149	Wet Coastal Forest	BC	49.60	-121.50
Tamiasciurus douglasii	UWBM20910	Td_19	JF303150	Wet Coastal Forest	BC	49.60	-121.50
Tamiasciurus douglasii	UWBM20912	Td_19	JF303151	Wet Coastal Forest	BC	49.60	-121.50
Tamiasciurus douglasii	UWBM20913	Td_23	JF303152	Wet Coastal Forest	BC	49.57	-121.47
Tamiasciurus douglasii	UWBM20915	Td_16	JF303153	Wet Coastal Forest	BC	49.60	-121.45
Tamiasciurus douglasii	UWBM20916	Td_22	JF303154	Wet Coastal Forest	BC	49.60	-121.45
Tamiasciurus douglasii	UWBM20917	Td_10	JF303155	Wet Coastal Forest	BC	49.60	-121.45
Tamiasciurus douglasii	UWBM20918	Td_11	JF303156	Wet Coastal Forest	BC	49.55	-121.45
Tamiasciurus douglasii	UWBM20919	Td_5	JF303157	Wet Coastal Forest	BC	49.60	-121.45
Tamiasciurus douglasii	UWBM20926	Td_10	JF303158	Wet Coastal Forest	BC	49.60	-121.50
Tamiasciurus douglasii	UWBM20927	Td_10	JF303159	Wet Coastal Forest	BC	49.60	-121.50
Tamiasciurus douglasii	UWBM32830	Td_19	JF303160	Wet Coastal Forest	WA	48.68	-121.09
Tamiasciurus douglasii	UWBM32831	Td_19	JF303161	Wet Coastal Forest	WA	48.68	-121.09
Tamiasciurus douglasii	UWBM32832	Td_10	JF303162	Wet Coastal Forest	WA	48.68	-121.09
Tamiasciurus douglasii	UWBM32833	Td_10	JF303163	Wet Coastal Forest	WA	48.68	-121.09
Tamiasciurus douglasii	UWBM32834	Td_10	JF303164	Wet Coastal Forest	WA	48.68	-121.09
Tamiasciurus douglasii	KU141391	Td_10	JF303165	Wet Coastal Forest	WA	48.70	-121.10
Tamiasciurus douglasii	KU141392	Th_13	JF303166	Wet Coastal Forest	WA	48.70	-121.10
Tamiasciurus douglasii	KU141393	Th_13	JF303167	Wet Coastal Forest	WA	48.70	-121.10
Tamiasciurus douglasii	KU141394	Td_18	JF303168	Wet Coastal Forest	WA	48.70	-121.10
Tamiasciurus douglasii	KU141395	Td_19	JF303169	Wet Coastal Forest	WA	48.70	-121.10
Tamiasciurus douglasii	KU141396	Td_19	JF303170	Wet Coastal Forest	WA	48.70	-121.10
Tamiasciurus douglasii	KU141397	Th_13	JF303171	Wet Coastal Forest	WA	48.70	-121.10
Tamiasciurus douglasii	KU141398	Td_10	JF303172	Wet Coastal Forest	WA	48.70	-121.10
Tamiasciurus douglasii	KU141399	Td_10	JF303173	Wet Coastal Forest	WA	48.70	-121.10
Tamiasciurus douglasii	KU141400	Td_19	JF303174	Wet Coastal Forest	WA	48.70	-121.10
Tamiasciurus douglasii	KU141401	Td_18	JF303175	Wet Coastal Forest	WA	48.70	-121.10
Tamiasciurus douglasii	KU141402	Th_15	JF303176	Wet Coastal Forest	WA	48.70	-121.10
Tamiasciurus douglasii	KU141403	Td_19	JF303177	Wet Coastal Forest	WA	48.70	-121.10
Tamiasciurus douglasii	UWBM20790	Td_10	JF303178	Wet Coastal Forest	BC	49.20	-120.99
Tamiasciurus douglasii	UWBM20929	Td_15	JF303179	Wet Coastal Forest	BC	49.20	-120.99

Tamiasciurus douglasii	UWBM20935	Td_33	JF303180	Wet Coastal Forest	BC	49.20	-120.99
Tamiasciurus douglasii	UWBM20930	Td_10	JF303181	Wet Coastal Forest	BC	49.20	-120.99
Tamiasciurus douglasii	UWBM20931	Td_29	JF303182	Wet Coastal Forest	BC	49.20	-120.99
Tamiasciurus douglasii	UWBM20933	Td_29	JF303183	Wet Coastal Forest	BC	49.20	-120.99
Tamiasciurus douglasii	UWBM20934	Th_13	JF303184	Wet Coastal Forest	BC	49.20	-120.99
Tamiasciurus douglasii	UWBM20936	Td_33	JF303185	Wet Coastal Forest	BC	49.17	-120.95
Tamiasciurus douglasii	UWBM20937	Td_10	JF303186	Wet Coastal Forest	BC	49.20	-120.99
Tamiasciurus douglasii	UWBM20783	Th_16	JF303187	Transitional Forest	BC	49.87	-121.50
Tamiasciurus douglasii	UWBM20784	Td_19	JF303188	Transitional Forest	BC	49.87	-121.50
Tamiasciurus douglasii	UWBM20786	Td_8	JF303189	Transitional Forest	BC	49.87	-121.50
Tamiasciurus douglasii	UWBM20791	Th_13	JF303190	Transitional Forest	BC	49.87	-121.50
Tamiasciurus douglasii	UWBM20797	Td_27	JF303191	Transitional Forest	BC	49.87	-121.50
Tamiasciurus douglasii	UWBM20897	Td_12	JF303192	Transitional Forest	BC	49.87	-121.50
Tamiasciurus douglasii	UWBM20898	Td_10	JF303193	Transitional Forest	BC	49.87	-121.50
Tamiasciurus douglasii	UWBM20902	Td_29	JF303194	Transitional Forest	BC	49.87	-121.50
Tamiasciurus douglasii	UWBM20903			Transitional Forest	BC	49.87	-121.50
Tamiasciurus douglasii	UWBM20904	Th_16	JF303195	Transitional Forest	BC	49.87	-121.50
Tamiasciurus douglasii	UWBM20905	Td_10	JF303196	Transitional Forest	BC	49.87	-121.50
Tamiasciurus douglasii	UWBM20906	Td_10	JF303197	Transitional Forest	BC	49.87	-121.50
Tamiasciurus douglasii	UWBM20914	Td_10	JF303198	Transitional Forest	BC	49.87	-121.50
Tamiasciurus douglasii	UWBM20920	Th_13	JF303199	Transitional Forest	BC	49.87	-121.50
Tamiasciurus douglasii	UWBM20921	Td_6	JF303200	Transitional Forest	BC	49.87	-121.50
Tamiasciurus douglasii	UWBM20922	Td_19	JF303201	Transitional Forest	BC	49.87	-121.50
Tamiasciurus douglasii	UWBM20923	Th_27	JF303202	Transitional Forest	BC	49.87	-121.50
Tamiasciurus douglasii	UWBM20924	Td_31	JF303203	Transitional Forest	BC	49.87	-121.50
Tamiasciurus douglasii	UWBM20925	Td_6	JF303204	Transitional Forest	BC	49.87	-121.50
Tamiasciurus douglasii	UWBM20928	Td_11	JF303205	Transitional Forest	BC	49.87	-121.50
Tamiasciurus douglasii	UWBM20938	Th_13	JF303206	Transitional Forest	BC	49.87	-121.50
Tamiasciurus hudsonicus	UWBM20997	Td_10	JF303207	Transitional Forest	BC	49.80	-121.47
Tamiasciurus hudsonicus	UWBM21016	Th_13	JF303208	Transitional Forest	BC	49.85	-121.45
Tamiasciurus hudsonicus	UWBM21034	Td_10	JF303209	Transitional Forest	BC	49.85	-121.45
Tamiasciurus hudsonicus	UWBM21056	Td_7	JF303210	Transitional Forest	BC	49.85	-121.45
Tamiasciurus hudsonicus	UWBM21057	Th_16	JF303211	Transitional Forest	BC	49.85	-121.45
Tamiasciurus hudsonicus	UWBM21058	Th_13	JF303212	Transitional Forest	BC	49.85	-121.45
Tamiasciurus hudsonicus	UWBM21059	Th_33	JF303213	Transitional Forest	BC	49.85	-121.45
Tamiasciurus douglasii	UWBM20812	Td_10	JF303214	Transitional Forest	BC	49.05	-121.07

Tamiasciurus douglasii	UWBM20813	Th_13	JF303215	Transitional Forest	BC	49.05	-121.07
Tamiasciurus douglasii	UWBM20814	Td_19	JF303216	Transitional Forest	BC	49.05	-121.07
Tamiasciurus douglasii	UWBM20815	Td_10	JF303217	Transitional Forest	BC	49.05	-121.07
Tamiasciurus douglasii	UWBM20816	Td_10	JF303218	Transitional Forest	BC	49.05	-121.07
Tamiasciurus douglasii	UWBM20817	Td_25	JF303219	Transitional Forest	BC	49.05	-121.07
Tamiasciurus douglasii	UWBM20818	Td_24	JF303220	Transitional Forest	BC	49.05	-121.07
Tamiasciurus douglasii	UWBM20819	Th_19	JF303221	Transitional Forest	BC	49.05	-121.07
Tamiasciurus douglasii	UWBM20820	Td_6	JF303222	Transitional Forest	BC	49.05	-121.07
Tamiasciurus douglasii	UWBM20822	Td_32	JF303223	Transitional Forest	BC	49.05	-121.07
Tamiasciurus douglasii	UWBM30031	Th_16	JF303224	Transitional Forest	WA	49.02	-121.07
Tamiasciurus douglasii	UWBM30016	Td_19	JF303225	Transitional Forest	WA	48.79	-121.07
Tamiasciurus douglasii	UWBM30021	Td_29	JF303226	Transitional Forest	WA	48.79	-121.07
Tamiasciurus douglasii	UWBM30022	Td_10	JF303227	Transitional Forest	WA	48.78	-121.06
Tamiasciurus douglasii	UWBM30023	Td_6	JF303228	Transitional Forest	WA	49.00	-121.07
Tamiasciurus douglasii	UWBM30025	Td_10	JF303229	Transitional Forest	WA	48.74	-121.07
Tamiasciurus douglasii	UWBM30026	Th_13	JF303230	Transitional Forest	WA	48.78	-121.07
Tamiasciurus douglasii	UWBM30027	Td_29	JF303231	Transitional Forest	WA	48.78	-121.07
Tamiasciurus douglasii	UWBM30029	Th_13	JF303232	Transitional Forest	WA	48.74	-121.07
Tamiasciurus douglasii	UWBM30030	Th_13	JF303233	Transitional Forest	WA	48.80	-121.09
Tamiasciurus douglasii	UWBM30033	Td_10	JF303234	Transitional Forest	WA	48.78	-121.06
Tamiasciurus douglasii	UWBM30034	Td_11	JF303235	Transitional Forest	WA	48.78	-121.06
Tamiasciurus douglasii	UWBM30035	Th_19	JF303236	Transitional Forest	WA	48.79	-121.04
Tamiasciurus douglasii	UWBM30036	Td_10	JF303237	Transitional Forest	WA	48.78	-121.06
Tamiasciurus douglasii	UWBM30045	Td_19	JF303238	Transitional Forest	WA	48.75	-121.03
Tamiasciurus douglasii	UWBM30047	Td_19	JF303239	Transitional Forest	WA	48.80	-121.15
Tamiasciurus douglasii	UWBM30048	Td_19	JF303240	Transitional Forest	WA	48.80	-121.15
Tamiasciurus douglasii	UWBM30049	Th_13	JF303241	Transitional Forest	WA	48.80	-121.16
Tamiasciurus hudsonicus	UWBM30051	Th_34	JF303242	Transitional Forest	WA	48.78	-121.06
Tamiasciurus douglasii	UWBM30064	Td_10	JF303243	Transitional Forest	WA	48.77	-121.08
Tamiasciurus douglasii	UWBM30065	Td_29	JF303244	Transitional Forest	WA	48.77	-121.07
Tamiasciurus douglasii	UWBM30066	Th_13	JF303245	Transitional Forest	WA	48.80	-121.15
Tamiasciurus douglasii	UWBM30067	Td_29	JF303246	Transitional Forest	WA	48.78	-121.06
Tamiasciurus douglasii	UWBM30068	Td_18	JF303247	Transitional Forest	WA	48.78	-121.06
Tamiasciurus douglasii	UWBM30069	Td_14	JF303248	Transitional Forest	WA	48.78	-121.06
Tamiasciurus douglasii	UWBM30070	Th_13	JF303249	Transitional Forest	WA	48.78	-121.06
Tamiasciurus douglasii	UWBM20798	Td_10	JF303250	Transitional Forest	BC	49.93	-121.57

Tamiasciurus douglasii	UWBM20799	Td_31	JF303251	Transitional Forest	BC	49.93	-121.57
Tamiasciurus douglasii	UWBM20805	Td_26	JF303252	Transitional Forest	BC	49.97	-121.52
Tamiasciurus douglasii	UWBM20806	Td_10	JF303253	Transitional Forest	BC	49.97	-121.52
Tamiasciurus douglasii	UWBM20807	Td_20	JF303254	Transitional Forest	BC	49.97	-121.52
Tamiasciurus douglasii	UWBM20808	Th_13	JF303255	Transitional Forest	BC	49.97	-121.52
Tamiasciurus douglasii	UWBM20809	Td_19	JF303256	Transitional Forest	BC	49.97	-121.52
Tamiasciurus douglasii	UWBM20810	Td_20	JF303257	Transitional Forest	BC	49.97	-121.52
Tamiasciurus douglasii	UWBM20811	Td_19	JF303258	Transitional Forest	BC	49.97	-121.52
Tamiasciurus hudsonicus	UWBM30054	Th_35	JF303259	Transitional Forest	WA	48.72	-120.91
Tamiasciurus douglasii	UWBM32849	Td_19	JF303260	Transitional Forest	WA	48.71	-120.97
Tamiasciurus douglasii	UWBM32850	Td_19	JF303261	Transitional Forest	WA	48.69	-120.96
Tamiasciurus douglasii	UWBM32851	Th_37	JF303262	Transitional Forest	WA	48.69	-120.96
Tamiasciurus douglasii	KU141414	Td_10	JF303263	Transitional Forest	WA	48.71	-120.99
Tamiasciurus douglasii	KU141415	Th_13	JF303264	Transitional Forest	WA	48.71	-120.99
Tamiasciurus douglasii	KU141416	Td_10	JF303265	Transitional Forest	WA	48.71	-120.99
Tamiasciurus douglasii	KU141417	Td_19	JF303266	Transitional Forest	WA	48.71	-120.99
Tamiasciurus douglasii	KU141418	Td_9	JF303267	Transitional Forest	WA	48.71	-120.99
Tamiasciurus douglasii	UWBM30017	Td_10	JF303268	Transitional Forest	WA	48.78	-121.02
Tamiasciurus douglasii	UWBM30018	Td_10	JF303269	Transitional Forest	WA	48.78	-121.02
Tamiasciurus douglasii	UWBM30020	Td_10	JF303270	Transitional Forest	WA	48.77	-120.98
Tamiasciurus douglasii	UWBM30028	Th_13	JF303271	Transitional Forest	WA	48.78	-121.01
Tamiasciurus douglasii	UWBM30032	Td_10	JF303272	Transitional Forest	WA	48.78	-121.02
Tamiasciurus douglasii	UWBM30039	Td_29	JF303273	Transitional Forest	WA	48.74	-121.02
Tamiasciurus douglasii	UWBM30046	Td_19	JF303274	Transitional Forest	WA	48.73	-121.02
Tamiasciurus hudsonicus	UWBM30050	Th_13	JF303275	Transitional Forest	WA	48.74	-121.02
Tamiasciurus hudsonicus	UWBM30052	Th_20	JF303276	Transitional Forest	WA	48.74	-121.04
Tamiasciurus douglasii	UWBM30019	Td_29	JF303277	Transitional Forest	WA	48.91	-121.02
Tamiasciurus douglasii	UWBM30024	Td_35	JF303278	Transitional Forest	WA	48.88	-121.00
Tamiasciurus douglasii	UWBM30037	Td_21	JF303279	Transitional Forest	WA	48.88	-121.01
Tamiasciurus douglasii	UWBM30038	Td_29	JF303280	Transitional Forest	WA	48.88	-121.00
Tamiasciurus douglasii	UWBM30040	Td_19	JF303281	Transitional Forest	WA	48.88	-121.01
Tamiasciurus hudsonicus	UWBM30041	Th_13	JF303282	Transitional Forest	WA	48.88	-121.01
Tamiasciurus douglasii	UWBM30042	Th_13	JF303283	Transitional Forest	WA	48.92	-121.04
Tamiasciurus douglasii	UWBM30043	Th_13	JF303284	Transitional Forest	WA	48.92	-121.04
Tamiasciurus douglasii	UWBM30044	Td_3	JF303285	Transitional Forest	WA	48.88	-121.01
Tamiasciurus douglasii	UWBM30053	Td_33	JF303286	Transitional Forest	WA	48.88	-121.01

Tamiasciurus douglasii	UWBM30063	Td_19	JF303287	Transitional Forest	WA	48.88	-121.00
Tamiasciurus hudsonicus	UWBM20746	Td_10	JF303288	Transitional Forest	BC	49.93	-121.45
Tamiasciurus hudsonicus	UWBM20747	Th_7	JF303289	Transitional Forest	BC	49.93	-121.45
Tamiasciurus hudsonicus	UWBM20752	Th_13	JF303290	Transitional Forest	BC	49.93	-121.45
Tamiasciurus douglasii	UWBM20800	Td_12	JF303291	Transitional Forest	BC	50.00	-121.48
Tamiasciurus hudsonicus	UWBM20993	Th_16	JF303292	Transitional Forest	BC	50.00	-121.48
Tamiasciurus hudsonicus	UWBM20994	Th_13	JF303293	Transitional Forest	BC	50.00	-121.48
Tamiasciurus hudsonicus	UWBM20995	Th_16	JF303294	Transitional Forest	BC	50.00	-121.48
Tamiasciurus hudsonicus	UWBM20996	Th_16	JF303295	Transitional Forest	BC	50.00	-121.48
Tamiasciurus hudsonicus	UWBM20998	Th_28	JF303296	Transitional Forest	BC	49.97	-121.47
Tamiasciurus hudsonicus	UWBM20999	Th_13	JF303297	Transitional Forest	BC	49.97	-121.47
Tamiasciurus hudsonicus	UWBM21000	Th_13	JF303298	Transitional Forest	BC	49.97	-121.47
Tamiasciurus hudsonicus	UWBM21001	Th_19	JF303299	Transitional Forest	BC	50.00	-121.48
Tamiasciurus hudsonicus	UWBM21012	Th_31	JF303300	Transitional Forest	BC	50.00	-121.48
Tamiasciurus hudsonicus	UWBM21013	Td_16	JF303301	Transitional Forest	BC	49.93	-121.40
Tamiasciurus hudsonicus	UWBM21023	Th_6	JF303302	Transitional Forest	BC	49.97	-121.47
Tamiasciurus hudsonicus	UWBM21026	Th_16	JF303303	Transitional Forest	BC	49.97	-121.47
Tamiasciurus hudsonicus	UWBM21054	Th_13	JF303304	Transitional Forest	BC	49.97	-121.47
Tamiasciurus hudsonicus	UWBM21055	Td_19	JF303305	Transitional Forest	BC	50.00	-121.48
Tamiasciurus hudsonicus	UWBM21060	Td_10	JF303306	Transitional Forest	BC	49.93	-121.40
Tamiasciurus hudsonicus	UWBM21061	Td_10	JF303307	Transitional Forest	BC	49.93	-121.40
Tamiasciurus hudsonicus	UWBM21062	Td_19	JF303308	Transitional Forest	BC	50.00	-121.48
Tamiasciurus hudsonicus	UWBM21063	Td_10	JF303309	Transitional Forest	BC	49.93	-121.40
Tamiasciurus hudsonicus	UWBM21065	Td_10	JF303310	Transitional Forest	BC	49.97	-121.47
Tamiasciurus hudsonicus	UWBM21066	Td_29	JF303311	Transitional Forest	BC	49.93	-121.40
Tamiasciurus hudsonicus	UWBM21067	Th_13	JF303312	Transitional Forest	BC	49.93	-121.40
Tamiasciurus hudsonicus	UWBM21068	Td_29	JF303313	Transitional Forest	BC	49.91	-121.43
Tamiasciurus hudsonicus	UWBM21069	Th_13	JF303314	Transitional Forest	BC	49.93	-121.40
Tamiasciurus hudsonicus	UWBM21070	Td_19	JF303315	Transitional Forest	BC	50.00	-121.48
Tamiasciurus hudsonicus	UWBM21071	Td_19	JF303316	Transitional Forest	BC	50.00	-121.48
Tamiasciurus hudsonicus	UWBM21072	Td_4	JF303317	Transitional Forest	BC	49.97	-121.47
Tamiasciurus hudsonicus	UWBM21073	Td_10	JF303318	Transitional Forest	BC	49.97	-121.47
Tamiasciurus hudsonicus	UWBM21074	Td_4	JF303319	Transitional Forest	BC	49.97	-121.47
Tamiasciurus hudsonicus	UWBM21075	Td_4	JF303320	Transitional Forest	BC	49.97	-121.47
Tamiasciurus hudsonicus	UWBM21076	Th_13	JF303321	Transitional Forest	BC	49.93	-121.40
Tamiasciurus hudsonicus	UWBM21077	Td_34	JF303322	Transitional Forest	BC	49.93	-121.40

Tamiasciurus hudsonicus	UWBM21078	Td_19	JF303323	Transitional Forest	BC	50.00	-121.48
Tamiasciurus hudsonicus	UWBM21053	Th_13	JF303324	Transitional Forest	WA	48.37	-120.66
Tamiasciurus douglasii	UWBM38389	Td_36	JF303325	Transitional Forest	WA	48.34	-120.72
Tamiasciurus douglasii	UWBM38419	Td_19	JF303326	Transitional Forest	WA	48.36	-120.75
Tamiasciurus douglasii	UWBM38465	Th_13	JF303327	Transitional Forest	WA	48.34	-120.72
Tamiasciurus hudsonicus	UWBM21015	Th_16	JF303328	Dry Interior Forest	BC	49.18	-120.53
Tamiasciurus hudsonicus	UWBM20743	Td_30	JF303329	Dry Interior Forest	BC	49.10	-120.70
Tamiasciurus hudsonicus	UWBM20764	Th_16	JF303330	Dry Interior Forest	BC	49.18	-120.53
Tamiasciurus hudsonicus	UWBM21002	Td_10	JF303331	Dry Interior Forest	BC	49.15	-120.60
Tamiasciurus hudsonicus	UWBM21004	Td_10	JF303332	Dry Interior Forest	BC	49.18	-120.53
Tamiasciurus hudsonicus	UWBM21014	Th_6	JF303333	Dry Interior Forest	BC	49.13	-120.62
Tamiasciurus hudsonicus	UWBM21017	Th_18	JF303334	Dry Interior Forest	BC	49.18	-120.53
Tamiasciurus hudsonicus	UWBM21018	Td_10	JF303335	Dry Interior Forest	BC	49.18	-120.57
Tamiasciurus hudsonicus	UWBM21019	Th_18	JF303336	Dry Interior Forest	BC	49.18	-120.53
Tamiasciurus hudsonicus	UWBM21033	Th_12	JF303337	Dry Interior Forest	BC	49.18	-120.53
Tamiasciurus hudsonicus	UWBM21039	Th_13	JF303338	Dry Interior Forest	BC	49.15	-120.57
Tamiasciurus hudsonicus	UWBM32836	Th_13	JF303339	Dry Interior Forest	WA	48.58	-120.48
Tamiasciurus hudsonicus	UWBM32837	Th_13	JF303340	Dry Interior Forest	WA	48.58	-120.48
Tamiasciurus hudsonicus	UWBM32838	Td_10	JF303341	Dry Interior Forest	WA	48.58	-120.48
Tamiasciurus hudsonicus	UWBM32839	Th_2	JF303342	Dry Interior Forest	WA	48.58	-120.48
Tamiasciurus hudsonicus	UWBM32840	Th_11	JF303343	Dry Interior Forest	WA	48.58	-120.48
Tamiasciurus hudsonicus	UWBM32841	Th_13	JF303344	Dry Interior Forest	WA	48.58	-120.48
Tamiasciurus hudsonicus	UWBM32842	Th_13	JF303345	Dry Interior Forest	WA	48.58	-120.48
Tamiasciurus hudsonicus	UWBM32843	Th_14	JF303346	Dry Interior Forest	WA	48.58	-120.48
Tamiasciurus hudsonicus	UWBM32844	Th_13	JF303347	Dry Interior Forest	WA	48.58	-120.48
Tamiasciurus hudsonicus	UWBM32845	Th_13	JF303348	Dry Interior Forest	WA	48.58	-120.48
Tamiasciurus hudsonicus	UWBM32846	Th_36	JF303349	Dry Interior Forest	WA	48.58	-120.48
Tamiasciurus hudsonicus	UWBM32847	Td_6	JF303350	Dry Interior Forest	WA	48.58	-120.48
Tamiasciurus hudsonicus	UWBM32848	Th_13	JF303351	Dry Interior Forest	WA	48.58	-120.48
Tamiasciurus hudsonicus	UWBM35509	Th_16	JF303352	Dry Interior Forest	WA	48.58	-120.47
Tamiasciurus hudsonicus	UWBM39169	Th_10	JF303353	Dry Interior Forest	WA	48.70	-120.64
Tamiasciurus hudsonicus	KU141371	Th_13	JF303354	Dry Interior Forest	WA	48.64	-120.48
Tamiasciurus hudsonicus	KU141372	Th_14	JF303355	Dry Interior Forest	WA	48.64	-120.48
Tamiasciurus hudsonicus	KU141373	Th_14	JF303356	Dry Interior Forest	WA	48.64	-120.48
Tamiasciurus hudsonicus	KU141374	Th_13	JF303357	Dry Interior Forest	WA	48.64	-120.48
Tamiasciurus hudsonicus	KU141375	Th_14	JF303358	Dry Interior Forest	WA	48.64	-120.48

Tamiasciurus hudsonicus	KU141376	Th_13	JF303359	Dry Interior Forest	WA	48.64	-120.48
Tamiasciurus hudsonicus	KU141377	Th_13	JF303360	Dry Interior Forest	WA	48.64	-120.48
Tamiasciurus hudsonicus	KU141378	Th_13	JF303361	Dry Interior Forest	WA	48.64	-120.48
Tamiasciurus hudsonicus	KU141379	Th_14	JF303362	Dry Interior Forest	WA	48.64	-120.48
Tamiasciurus hudsonicus	KU141380	Td_12	JF303363	Dry Interior Forest	WA	48.64	-120.48
Tamiasciurus hudsonicus	UWBM20740	Th_13	JF303364	Dry Interior Forest	BC	49.22	-120.57
Tamiasciurus hudsonicus	UWBM20741	Th_16	JF303365	Dry Interior Forest	BC	49.20	-120.57
Tamiasciurus hudsonicus	UWBM20742	Th_13	JF303366	Dry Interior Forest	BC	49.20	-120.57
Tamiasciurus hudsonicus	UWBM20744	Th_23	JF303367	Dry Interior Forest	BC	49.20	-120.57
Tamiasciurus hudsonicus	UWBM20745	Th_13	JF303368	Dry Interior Forest	BC	49.20	-120.57
Tamiasciurus hudsonicus	UWBM20748	Th_24	JF303369	Dry Interior Forest	BC	49.20	-120.57
Tamiasciurus hudsonicus	UWBM20749	Th_13	JF303370	Dry Interior Forest	BC	49.20	-120.57
Tamiasciurus hudsonicus	UWBM20750	Th_17	JF303371	Dry Interior Forest	BC	49.20	-120.57
Tamiasciurus hudsonicus	UWBM20751	Th_13	JF303372	Dry Interior Forest	BC	49.20	-120.57
Tamiasciurus hudsonicus	UWBM20753	Th_14	JF303373	Dry Interior Forest	BC	49.20	-120.57
Tamiasciurus hudsonicus	UWBM20754	Th_13	JF303374	Dry Interior Forest	BC	49.20	-120.57
Tamiasciurus hudsonicus	UWBM20755	Th_13	JF303375	Dry Interior Forest	BC	49.22	-120.57
Tamiasciurus hudsonicus	UWBM20756	Th_13	JF303376	Dry Interior Forest	BC	49.28	-120.57
Tamiasciurus hudsonicus	UWBM20757	Td_10	JF303377	Dry Interior Forest	BC	49.28	-120.57
Tamiasciurus hudsonicus	UWBM20758	Th_13	JF303378	Dry Interior Forest	BC	49.22	-120.57
Tamiasciurus hudsonicus	UWBM20759	Th_13	JF303379	Dry Interior Forest	BC	49.20	-120.57
Tamiasciurus hudsonicus	UWBM20760	Th_23	JF303380	Dry Interior Forest	BC	49.22	-120.57
Tamiasciurus hudsonicus	UWBM20761	Th_13	JF303381	Dry Interior Forest	BC	49.22	-120.57
Tamiasciurus hudsonicus	UWBM20762	Td_10	JF303382	Dry Interior Forest	BC	49.22	-120.57
Tamiasciurus hudsonicus	UWBM20763	Th_13	JF303383	Dry Interior Forest	BC	49.22	-120.57
Tamiasciurus hudsonicus	UWBM20765	Th_25	JF303384	Dry Interior Forest	BC	49.25	-120.57
Tamiasciurus hudsonicus	UWBM20766	Th_13	JF303385	Dry Interior Forest	BC	49.22	-120.57
Tamiasciurus hudsonicus	UWBM20767	Th_13	JF303386	Dry Interior Forest	BC	49.32	-120.57
Tamiasciurus hudsonicus	UWBM20768	Th_13	JF303387	Dry Interior Forest	BC	49.32	-120.57
Tamiasciurus hudsonicus	UWBM20769	Th_26	JF303388	Dry Interior Forest	BC	49.32	-120.57
Tamiasciurus hudsonicus	UWBM21003	Th_13	JF303389	Dry Interior Forest	BC	49.22	-120.57
Tamiasciurus hudsonicus	UWBM21005	Th_13	JF303390	Dry Interior Forest	BC	49.22	-120.57
Tamiasciurus hudsonicus	UWBM21006	Th_29	JF303391	Dry Interior Forest	BC	49.22	-120.57
Tamiasciurus hudsonicus	UWBM21007	Th_29	JF303392	Dry Interior Forest	BC	49.22	-120.57
Tamiasciurus hudsonicus	UWBM21008	Td_10	JF303393	Dry Interior Forest	BC	49.22	-120.57
Tamiasciurus hudsonicus	UWBM21009	Td_10	JF303394	Dry Interior Forest	BC	49.22	-120.57

Tamiasciurus hudsonicus	UWBM21010	Th_30	JF303395	Dry Interior Forest	BC	49.22	-120.57
Tamiasciurus hudsonicus	UWBM21011	Th_13	JF303396	Dry Interior Forest	BC	49.22	-120.57
Tamiasciurus hudsonicus	UWBM21020	Th_16	JF303397	Dry Interior Forest	BC	49.22	-120.57
Tamiasciurus hudsonicus	UWBM21021	Td_10	JF303398	Dry Interior Forest	BC	49.22	-120.57
Tamiasciurus hudsonicus	UWBM21022	Td_10	JF303399	Dry Interior Forest	BC	49.22	-120.57
Tamiasciurus hudsonicus	UWBM21024	Th_9	JF303400	Dry Interior Forest	BC	49.22	-120.57
Tamiasciurus hudsonicus	UWBM21025	Td_15	JF303401	Dry Interior Forest	BC	49.22	-120.57
Tamiasciurus hudsonicus	UWBM21027	Th_13	JF303402	Dry Interior Forest	BC	49.22	-120.57
Tamiasciurus hudsonicus	UWBM21028	Th_13	JF303403	Dry Interior Forest	BC	49.22	-120.57
Tamiasciurus hudsonicus	UWBM21029	Th_13	JF303404	Dry Interior Forest	BC	49.22	-120.57
Tamiasciurus hudsonicus	UWBM21030	Th_13	JF303405	Dry Interior Forest	BC	49.22	-120.57
Tamiasciurus hudsonicus	UWBM21031	Th_13	JF303406	Dry Interior Forest	BC	49.22	-120.57
Tamiasciurus hudsonicus	UWBM21032	Th_16	JF303407	Dry Interior Forest	BC	49.22	-120.57
Tamiasciurus hudsonicus	UWBM21035	Th_14	JF303408	Dry Interior Forest	BC	49.22	-120.57
Tamiasciurus hudsonicus	UWBM21036	Th_16	JF303409	Dry Interior Forest	BC	49.22	-120.57
Tamiasciurus hudsonicus	UWBM21037	Th_13	JF303410	Dry Interior Forest	BC	49.22	-120.57
Tamiasciurus hudsonicus	UWBM21038	Th_32	JF303411	Dry Interior Forest	BC	49.22	-120.57
Tamiasciurus hudsonicus	UWBM43323	Th_13	JF303412	Dry Interior Forest	WA	48.47	-120.17
Tamiasciurus hudsonicus	KU63944	Th_16	JF303413	Dry Interior Forest	WA	48.36	-120.34
Tamiasciurus hudsonicus	KU63945	Th_13	JF303414	Dry Interior Forest	WA	48.36	-120.34
Tamiasciurus hudsonicus	KU63946	Th_16	JF303415	Dry Interior Forest	WA	48.36	-120.34
Tamiasciurus hudsonicus	KU63947	Th_21	JF303416	Dry Interior Forest	WA	48.36	-120.34
Tamiasciurus hudsonicus	KU63948	Td_17	JF303417	Dry Interior Forest	WA	48.36	-120.34
Tamiasciurus hudsonicus	KU63919	Td_19	JF303418	Dry Interior Forest	WA	48.64	-120.29
Tamiasciurus hudsonicus	KU63920	Td_19	JF303419	Dry Interior Forest	WA	48.64	-120.29
Tamiasciurus hudsonicus	KU63921	Td_19	JF303420	Dry Interior Forest	WA	48.64	-120.29
Tamiasciurus hudsonicus	KU63922	Th_14	JF303421	Dry Interior Forest	WA	48.64	-120.29
Tamiasciurus hudsonicus	KU63923	Th_13	JF303422	Dry Interior Forest	WA	48.72	-120.29
Tamiasciurus hudsonicus	KU63924	Th_13	JF303423	Dry Interior Forest	WA	48.72	-120.29
Tamiasciurus hudsonicus	KU63925	Th_13	JF303424	Dry Interior Forest	WA	48.72	-120.29
Tamiasciurus hudsonicus	UWBM32081	Th_21	JF303425	Dry Interior Forest	WA	48.09	-120.03
Tamiasciurus hudsonicus	UWBM32502	Th_13	JF303426	Dry Interior Forest	WA	48.25	-120.12
Tamiasciurus hudsonicus	UWBM32504	Th_13	JF303427	Dry Interior Forest	WA	48.19	-120.12
Tamiasciurus hudsonicus	UWBM32611	Th_16	JF303428	Dry Interior Forest	WA	48.24	-119.97
Tamiasciurus hudsonicus	UWBM33265	Th_13	JF303429	Dry Interior Forest	WA	48.70	-119.75
Tamiasciurus hudsonicus	UWBM33266	Th_8	JF303430	Dry Interior Forest	WA	48.70	-119.75

Tamiasciurus hudsonicus	UWBM39167	Th_17	JF303431	Dry Interior Forest	WA	48.66	-119.94
Tamiasciurus hudsonicus	UWBM39168	Td_29	JF303432	Dry Interior Forest	WA	48.61	-120.08
Tamiasciurus hudsonicus	UWBM39170	Th_13	JF303433	Dry Interior Forest	WA	48.65	-119.97
Tamiasciurus hudsonicus	UWBM39171	Th_26	JF303434	Dry Interior Forest	WA	48.65	-119.97
Tamiasciurus hudsonicus	UWBM39172	Th_11	JF303435	Dry Interior Forest	WA	48.66	-119.94
Tamiasciurus hudsonicus	UWBM39173	Th_13	JF303436	Dry Interior Forest	WA	48.66	-119.94
Tamiasciurus hudsonicus	UWBM39174	Th_34	JF303437	Dry Interior Forest	WA	48.66	-119.94
Tamiasciurus hudsonicus	UWBM39175	Th_14	JF303438	Dry Interior Forest	WA	48.66	-119.94
Tamiasciurus hudsonicus	KU63926	Th_13	JF303439	Dry Interior Forest	WA	48.42	-119.65
Tamiasciurus hudsonicus	KU63927	Th_13	JF303440	Dry Interior Forest	WA	48.42	-119.65
Tamiasciurus hudsonicus	KU63928	Th_13	JF303441	Dry Interior Forest	WA	48.38	-119.78
Tamiasciurus hudsonicus	KU63929	Th_14	JF303442	Dry Interior Forest	WA	48.38	-119.78
Tamiasciurus hudsonicus	KU63930			Dry Interior Forest	WA	48.38	-119.78
Tamiasciurus hudsonicus	KU63931	Td_2	JF303443	Dry Interior Forest	WA	48.38	-119.78
Tamiasciurus hudsonicus	KU63932	Td_2	JF303444	Dry Interior Forest	WA	48.38	-119.78
Tamiasciurus hudsonicus	KU63933	Th_38	JF303445	Dry Interior Forest	WA	48.38	-119.78
Tamiasciurus hudsonicus	KU63934	Th_13	JF303446	Dry Interior Forest	WA	48.36	-119.87
Tamiasciurus hudsonicus	KU63935	Th_13	JF303447	Dry Interior Forest	WA	48.36	-119.87
Tamiasciurus hudsonicus	KU63936	Th_39	JF303448	Dry Interior Forest	WA	48.36	-119.87
Tamiasciurus hudsonicus	KU63937	Th_13	JF303449	Dry Interior Forest	WA	48.36	-119.87
Tamiasciurus hudsonicus	KU63938	Th_13	JF303450	Dry Interior Forest	WA	48.36	-119.87
Tamiasciurus hudsonicus	KU63939	Th_13	JF303451	Dry Interior Forest	WA	48.36	-119.87
Tamiasciurus hudsonicus	KU63940	Th_13	JF303452	Dry Interior Forest	WA	48.36	-119.87
Tamiasciurus hudsonicus	KU63941	Th_13	JF303453	Dry Interior Forest	WA	48.36	-119.87
Tamiasciurus hudsonicus	KU63942	Th_13	JF303454	Dry Interior Forest	WA	48.36	-119.87
Tamiasciurus hudsonicus	KU63943	Th_13	JF303455	Dry Interior Forest	WA	48.36	-119.87
Tamiasciurus hudsonicus	UWBM12811	Th_13	JF303456	Dry Interior Forest	WA	48.65	-118.15
Tamiasciurus hudsonicus	UWBM15051	Th_1	JF303457	Dry Interior Forest	WA	47.66	-117.43
Tamiasciurus hudsonicus	UWBM18926	Th_13	JF303458	Dry Interior Forest	WA	48.65	-118.91
Tamiasciurus hudsonicus	UWBM18927	Th_9	JF303459	Dry Interior Forest	WA	48.65	-118.91
Tamiasciurus hudsonicus	UWBM18928	Th_13	JF303460	Dry Interior Forest	WA	48.65	-118.91
Tamiasciurus hudsonicus	UWBM18929	Th_13	JF303461	Dry Interior Forest	WA	48.89	-118.33
Tamiasciurus hudsonicus	UWBM32503	Th_13	JF303462	Dry Interior Forest	WA	48.79	-119.06
Tamiasciurus hudsonicus	UWBM39196	Th_12	JF303463	Dry Interior Forest	WA	48.75	-118.16
Tamiasciurus hudsonicus	UWBM39197	Th_13	JF303464	Dry Interior Forest	WA	48.71	-118.41
Tamiasciurus hudsonicus	UWBM39198	Th_13	JF303465	Dry Interior Forest	WA	48.75	-118.16

Tamiasciurus hudsonicus	UWBM39199	Th_13	JF303466	Dry Interior Forest	WA	48.71	-118.16
Tamiasciurus hudsonicus	UWBM39200	Th_13	JF303467	Dry Interior Forest	WA	48.71	-118.41
Tamiasciurus hudsonicus	UWBM39201	Th_9	JF303468	Dry Interior Forest	WA	48.71	-118.41
Tamiasciurus hudsonicus	KU41460	Th_3	JF303469	Dry Interior Forest	ID	48.92	-116.67
Tamiasciurus hudsonicus	UWBM43181	Th_4	JF303470	Dry Interior Forest	WA	48.82	-117.32
Tamiasciurus hudsonicus	UWBM43182	Th_5	JF303471	Dry Interior Forest	WA	48.65	-118.15
Tamiasciurus hudsonicus	KU41461	Th_13	JF303472	Dry Interior Forest	ID	47.75	-116.50
Tamiasciurus hudsonicus	KU41462	Th_16	JF303473	Dry Interior Forest	ID	47.75	-116.50
Tamiasciurus hudsonicus	KU41463	Th_13	JF303474	Dry Interior Forest	ID	47.75	-116.50
Tamiasciurus hudsonicus	KU41465	Th_13	JF303475	Dry Interior Forest	ID	47.75	-116.50
Tamiasciurus hudsonicus	KU57260	Th_22	JF303476	Dry Interior Forest	ID	47.62	-116.50
Tamiasciurus hudsonicus	UWBM15272	T.h.m.	JF303477		AZ	35.31	-111.65
Samples from outside of study transect used for mtDNA phylogenetic analysis							
Tamiasciurus hudsonicus	UWBM43200		JF308196		MT	48.66	-113.43
Tamiasciurus hudsonicus	UWBM30055		JF308197		MT	45.56	-111.05
Tamiasciurus hudsonicus			DQ74118U		UT	42.00	-111.52
Tamiasciurus hudsonicus			DQ74116I		ID	42.37	-111.55
Tamiasciurus hudsonicus			DQ74090W		WY	43.86	-110.26
Tamiasciurus hudsonicus	UWBM43189		JF308198		BC	51.95	-120.18
Tamiasciurus hudsonicus	UWBM43232		JF308199		BC	49.88	-119.30
Tamiasciurus hudsonicus	UWBM43186		JF308200		BC	50.98	-118.31
Tamiasciurus hudsonicus			DQ74122W		WY	42.44	-105.84
Tamiasciurus hudsonicus			DQ74105W		WY	44.98	-109.84
Tamiasciurus hudsonicus			DQ74077S		SD	43.82	-103.85
Tamiasciurus douglasii	UWBM44407		JF308201		WA	48.06	-123.81
Tamiasciurus douglasii	UWBM36019		JF308202		WA	46.82	-121.55
Tamiasciurus douglasii	UWBM34154		JF308203		WA	47.42	-122.50
Tamiasciurus douglasii	UWBM15062		JF308204		WA	47.10	-122.43
Tamiasciurus douglasii	UWBM44390		JF308205		WA	47.38	-121.86
Tamiasciurus douglasii	UWBM44403		JF308206		CA	39.39	-122.77
Tamiasciurus douglasii	UWBM44397		JF308207		WA	46.51	-123.88
Tamiasciurus douglasii	UWBM43835		JF308208		BC	50.92	-124.83
Tamiasciurus douglasii	UWBM34412		JF308209		WA	45.85	-121.97

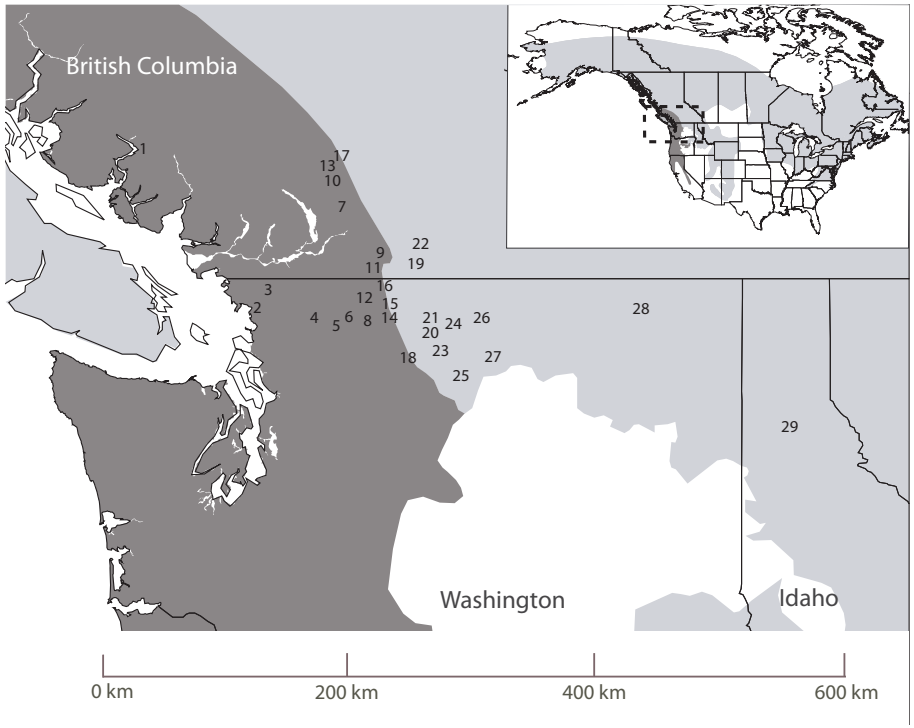

Figure 1. Maps of geographic distribution and sampling localities of *T. douglasii* (dark shading) and *T. hudsonicus* (light shading). The small inset shows the entire distribution of both species across North America (Steele 1998, 1999) and the dashed box indicates the position of the northern Cascade Mountains study area. The study area consists of 29 sampling localities (**Table S1**) across the forest gradient representing westerly allopatric populations of *Tamiasciurus douglasii*, easterly allopatric populations of *Tamiasciurus hudsonicus*, and an intermediate zone of contact between the two in the northern Cascade Mountains.

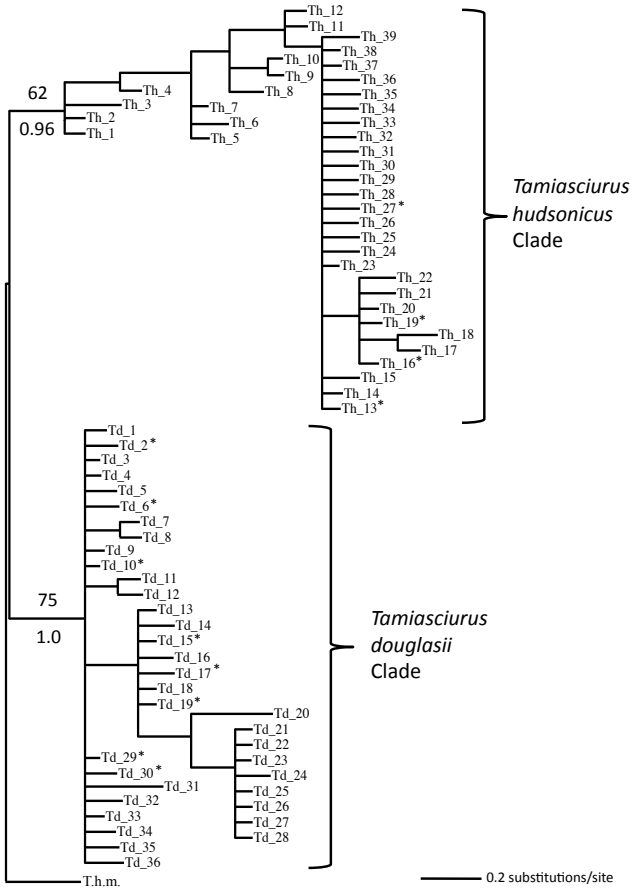

Figure 2. Bayesian gene tree of 392 samples inferred for *T. douglasii* and *T. hudsonicus* across the northern Cascade Mountains study area (**Table S1**), based on 327 base pairs of the mitochondrial control region. Bayesian posterior probabilities are shown below each major node and maximum likelihood bootstrap values above. The haplotypes in the *T. hudsonicus* clade are labeled "Th" and numbered 1-39, and the haplotypes in the *T. douglasii* clade are labeled "Td" and numbered 1-36. Stars represent 17 haplotypes containing 97 individuals assigned as either admixed genotype or a mismatch between microsatellite genotype assignment and mtDNA haplotype assignment. Outgroup sequence is *T. hudsonicus mogollonensis* from Arizona (T.h.m.).

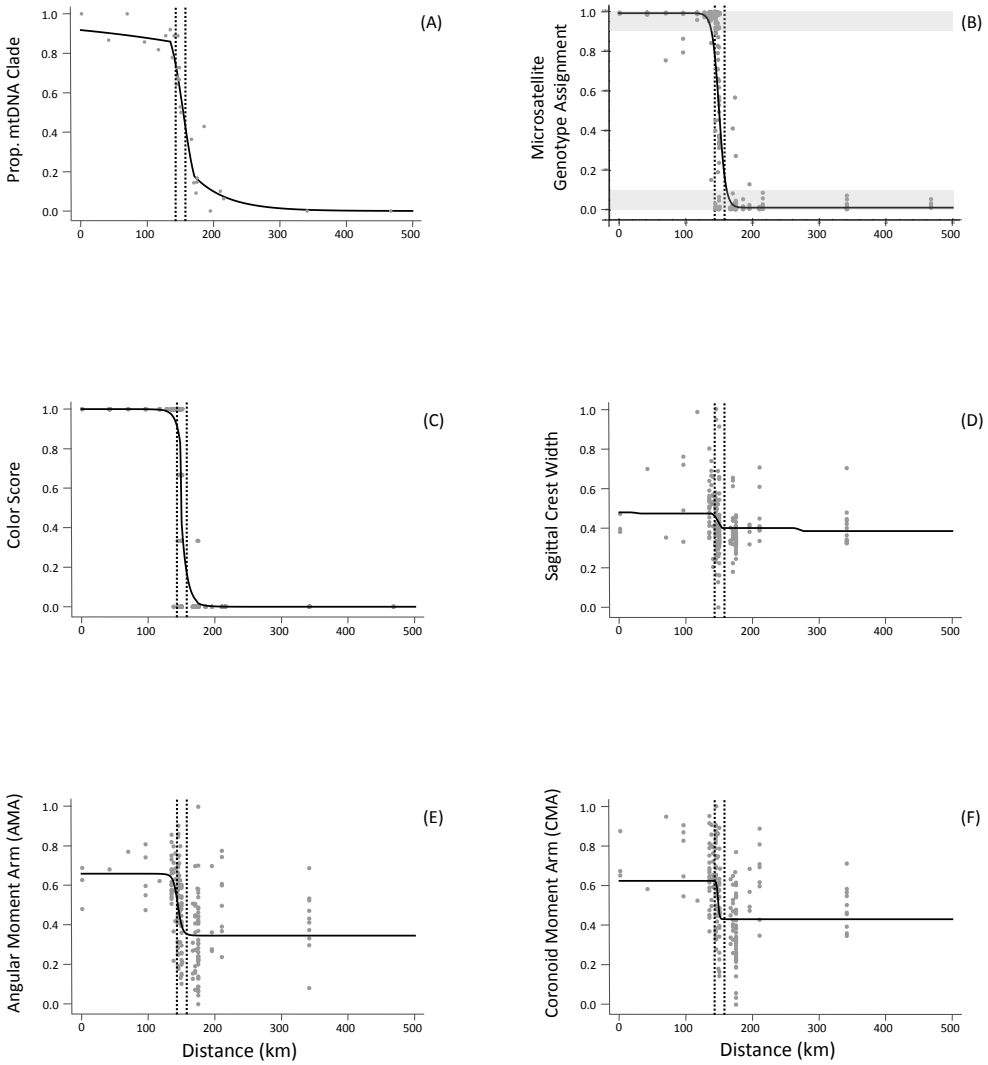

Figure 3. Clinal patterns of variation among individuals at 29 localities in the three forest zones across the west-to-east study transect. Derivation of the 467-km transect (x-axis) is described in **Materials and Methods,** and the distance of each locality is given in Table S1. Dotted vertical lines represent limits between the three forest zones. The area west (left) of the dotted lines represents the wet coastal forest zone, between the lines is the transitional forest zone, and the area east (right) of the dotted lines represents the dry interior forest zone. (A) Proportion of individuals belonging to the two mtDNA clades, where 1.0 = *T. douglasii* and 0.0 = T. hudsonicus. (B) Genotype assignment proportions

(*q*-values) based on microsatellite data of 397 individuals as determined by STRUCTURE. We have categorized these values as pure *T. douglasii* genotype (upper 10% shaded; extreme = 1.0), pure *T. hudsonicus* genotype (lower 10% shaded; extreme = 0.0), and admixed genotype (middle 80%). Only 37 of the 397 individuals (9%) were admixed. (C) Ventral color scores of 388 individuals, ranging over four shades from darkest (1.0) to lightest (0.0). (D) Sagittal crest residual values for 207 individuals. (E) Angular moment arm (AMA) residual values for 192 individuals. (F) Coronoid moment arm (CMA) residual values for 192 individuals. The values for all three cranial characters (D-F) represent size-corrected values determined by the ANCOVA.

Figure S1. Results from the ANCOVA showing effect tests for each of the three cranial characters. Scatterplot showing the relationship of all three cranial characters against the covariate of body length for each of the three microsatellite genotype groups: pure *T. douglasii* (red), admixed (green), pure *T. hudsonicus* (blue). The effect tests are also shown for each character.

(a)

Response Sagittal Crest Width Whole Model Regression Plot

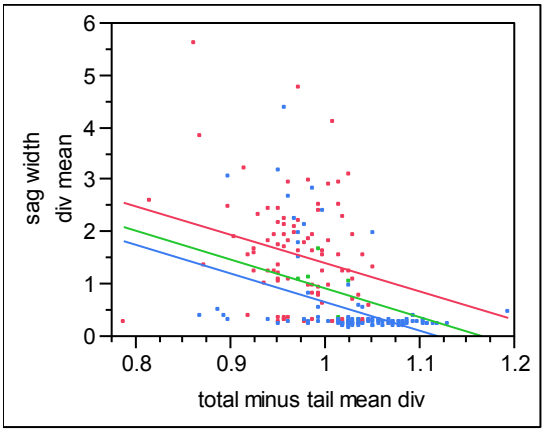

***Tamiasciurus douglasii* (n=87)**
Admixed (n=6)
***Tamiasciurus hudsonicus* (n=114)**

Effect Tests

Source	Nparm	DF	Sum of Squares	F Ratio	Prob > F
Species	2	2	20.338533	14.7802	<.0001
Body Length	1	1	16.034956	23.3054	<.0001

(b)

Response Angular Moment Arm (AMA) Whole Model Regression Plot

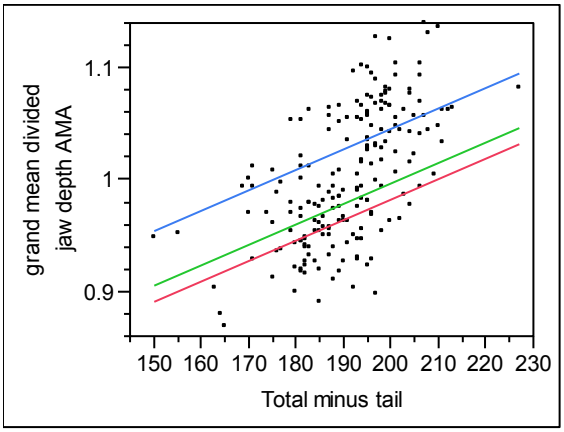

Tamiasciurus douglasii **(n=79)**
Admixed (n=7)
Tamiasciurus hudsonicus **(n=106)**

Effect Tests

Source	Nparm	DF	Sum of Squares	F Ratio	Prob > F
Species	2	2	0.14229251	46.5236	<.0001
Body Length	1	1	0.06147612	40.2001	<.0001

(c)
Response Coronoid Moment Arm (CMA) Whole Model Regression Plot

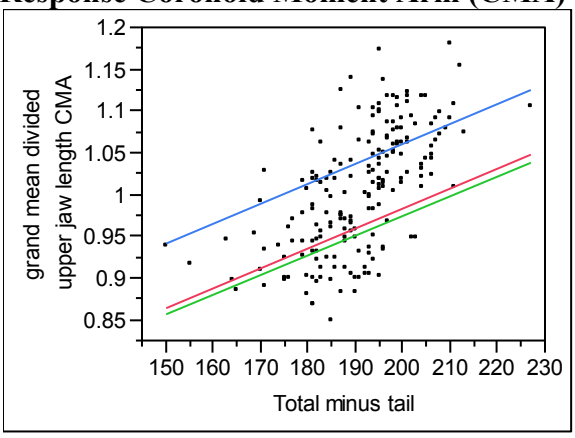

Tamiasciurus douglasii **(n=79)**
Admixed (n=7)
Tamiasciurus hudsonicus **(n=106)**

Effect Tests

Source	Nparm	DF	Sum of Squares	F Ratio	Prob > F
Species	2	2	0.22779847	53.3131	<.0001
Body Length	1	1	0.10379445	48.5834	<.0001

CHAPTER 3

Clinal Phenotypic Variation within a Panmictic Population of Douglas squirrels (*Tamiasciurus douglasii*) across an Ecological Gradient

Abstract

Patterns of clinal variation in phenotypic characters provide a significant opportunity to explore the interrelation of natural selection and gene flow in nature. We have examined clinal variation in several ecologically important traits of Douglas squirrels, including fur coloration and cranial morphology associated with bite force, to examine whether phenotypic clines correspond with ecological transitions in forest structure and ecology. Ventral fur color showed a moderate transition from deep orange in the coastal region to a whitish-yellow on the eastern side of the Cascade Mountains. Interestingly, the center of this transition (cline) coincided with a transition in tree canopy openness. In contrast, cranial morphology varied continuously and gradually and did not show any sharp transitions, which is surprising given the abrupt changes in size and hardness of their primary food source, the cones from which they extract seeds. Our study provides an indication of the contemporary processes of selection and gene flow that shape phenotypic variation and result in local adaptation.

Introduction

The ubiquity of ecogeographic patterns of phenotypic variation within continuously distributed animal populations (e.g., Rules of Bergmann, Gloger, Allen) suggests that local adaptation is common in nature. The development of these geographic patterns is often generated by spatial differences in the selective environments of continuous populations (Endler 1977). Local adaptation is the consequence of different selection pressures favoring alternative traits in local populations (demes) that are living in different environments, even in the presence of the homogenizing effects of gene flow (Kawecki and Ebert 2004). Ecological selection is not only important for adaptation, but for speciation, as divergent selection favors the prevalence of locally beneficial alleles and other closely linked loci (Maynard Smith and Haigh 1974; Barton 2000; Nosil et al 2009; Lenormand 2012), which may include loci that contribute to reproductive incompatibilities between genetically divergent populations (Felsenstein 1981).

Huxley (1938) coined the term "cline" to describe geographic gradations of phenotypes (but this can also include allele frequencies [see Slatkin 1985]) within or between species. One of the best ways to measure the strength of selection in nature is to measure the rate of change in gene or phenotype frequencies across a cline (Slatkin 1973). Early mathematical treatments by Fisher (1937) and Haldane (1948) showed how the balance between selection and gene flow maintains clines. Gene flow will push distinct populations towards genetic homogeneity and potentially remove clinal variation. However, disruptive selection can counter the effects of gene flow and accentuate the distinction of traits or allele frequencies between populations. The tension between these

evolutionary forces revealed by clines generally suggests that both forces are ongoing. Therefore, studies of local adaptation can provide evolutionary biologists with important opportunities to understand the central issue that drives ecogeographic patterns of phenotypic variation and ultimately speciation.

One of the challenges to studying patterns of clinal variation is determining whether its formation was due to primary intergradation (selection within a continuous population) or from secondary contact between genetically divergent populations. Both of these processes can produce similar clinal patterns over similar time courses (Endler 1977; Barton and Hewitt 1989). One approach for dealing with this is to incorporate historical evidence from genetic or paleontological studies to aid in the interpretation of cline formation (Thorpe 1984; Barton and Hewitt 1985).

The Douglas squirrel (*Tamiasciurus douglasii*) is a good species to study the role of selection and gene flow in phenotypic clines because it possesses striking variation in several ecologically important traits. Members of this genus (*Tamiasciurus*) have coevolved with conifers in North America due to their specialization on conifers for food and shelter (Smith 1970; Elliot 1974; Benkman 1995, but see Wheatley 2007). In Oregon, the ventral fur color of Douglas squirrels continuously varies from a reddish-orange in coastal populations to a whitish-yellow in interior populations located on the eastern side of the Cascade Mountains (Verts and Carraway 1998). Fur coloration can be an important adaptive trait in small mammals to avoid predation (Vignieri et al 2010). Smith (1981) argued that differentiation in ventral fur color in *Tamiasciurus* could have evolved for better matching with different forest canopy backgrounds. Similarly, cranial characters in Douglas squirrels that are associated with bite force show wide geographic variation and

are believed to vary geographically with differences in size and hardness of conifer cones, which itself has evolved in response to differences of forest fire regimes (Lindsay 1986, Smith 1970).

The environment in the Pacific Northwest (PNW) has given rise to ecological gradients in forest communities that potentially exert different selective pressures on fur coloration and cranial morphology in *T. douglasii*. This region's climate and ecology is largely shaped by the interactions that occur between seasonally varying weather patterns and the region's mountain ranges, primarily the north-to-south spanning Cascade Mountains. The coastal forest region west of the Cascade Mountains experiences a maritime climate that is characterized by heavy winter rainfall (ranging from 75-300 cm per year) and mild year-round temperatures (Franklin and Dyrness 1973). The Cascade Mountains create a strong rain shadow effect and the eastern side experiences minimal precipitation (~20 cm per year) with stronger fluctuations between winter and summer temperatures. Correspondingly, coastal forests are typically very dense in structure and allow little penetration of light through the forest canopy. Whereas, the canopy structure in interior forests is much less dense, which allows for a brighter environment. Furthermore, forest fires are frequent in interior forests and many pine tree species have evolved the production of hard serotinous cones that generally only open during periods of forest fires.

For this study, we investigated patterns variation in fur color and skull morphology of Douglas squirrels (*T. douglasii*) along an environmental gradient using cline models with phenotypic data. We tested the hypotheses that cline patterns of ecologically important traits (fur coloration and skull traits associated with bite force)

will show greater sharp patterns of clinal transition that corresponds with transitions between forest types. We also performed population genetic analyses to investigate whether clines were formed by primary or secondary intergradation.

Materials and Methods

Sampling

We collected 92 specimens of *Tamiasciurus douglasii* from 9 localities along a 440-km west-to-east transect in Oregon (Fig. 1; Table 1). Douglas squirrels are closely associated with coniferous forests and so we designed the one-dimensional survey transect to span along a forest gradient from the coastal region to a dry interior forest in the central part of the state. The forest gradient spanned from the wet coastal forest to a dry interior forest found on the eastern side of the Cascade Mountains that continue eastward into the geographically distinct Blue Mountains. The coastal forest consists primarily of the sitka spruce (*Picea sitchensis*), coastal Douglas Fir (*Pseudotsuga menziesii* var. *menziesii*) forest zones, whereas the dry interior forests are comprised primarily of ponderosa pine (*Pinus ponderosa*)/lodgepole pine (*Pinus contorta*), mountain lodgepole pine, and interior Douglas-fir (*P. m. glauca*) vegetation zones (Fig. 1: Franklin and Dyrness 1973; Kiilsgaard and Barrett 1999). All squirrel specimens are accessioned at the Burke Museum, University of Washington (UWBM).

Percent Canopy Openness

To document variation in openness of forest canopy across the ecological gradient, we acquired percent tree canopy cover at each sampling location from digitized images in the

National Land Cover Database (NLCD) (Homer et al 2012) using ArcGIS (ESRI, Inc., Redlands, CA). The NLCD is a Landsat-based, 30-meter resolution, land cover database for the United States. The percent tree canopy layer quantifies per pixel tree canopy fraction as a continuous variable from 1 to 100 percent. We used a quadrat-sampling method for obtaining an average percent cover value for each sampling location. This was performed by randomly selecting 10 points within a 0.08 km^2 area, which is nearly equivalent to the size of 10 Douglas squirrel territories (Smith 1968). Four our analyses we converted the percent canopy cover to percent canopy openness by subtracting each value from 100 percent.

Molecular Methods

We extracted whole genomic DNA from liver tissue using the prescribed protocol of DNeasy Tissue Kit (Qiagen, Valencia, California). We genotyped all 467 specimens at 18 polymorphic microsatellite loci originally developed for *T. hudsonicus* by Gunn et al. (2005): Thu03, Thu08, Thu14, Thu21, Thu23, Thu25, Thu31, Thu32, Thu33, Thu37, Thu38, Thu40, Thu41, Thu42, Thu49, Thu50, Thu55, and Thu59. Polymerase chain reactions (PCRs) were carried out in 4.0-µL reaction volumes that included 2.03 µL of nuclease-free H2O, 0.2 mg/ml of Bovine Serum Albumin, 0.33 × PCR buffer, 0.83 mM of $MgCl_2$, 0.067 mM of each dNTP, 0.167 µM of each primer, and 0.35 U of Taq DNA polymerase and 30 ng of genomic DNA template. We used a touchdown PCR protocol consisting of a denaturing step at 94 ^oC for 3 min; followed by eight cycles (with a decreasing 1 ^oC annealing temperature after each cycle) of 94 ^oC for 15 s, 68 ^oC for 15 s and 72 ^oC for 30 s; followed by 20 cycles of 94 ^oC for 45 s, 59 ^oC for 15 s and 72 ^oC for

30 s; and with a final extension period of 72 ^{o}C for 45 min. We diluted PCR amplicons by 1:15 with nuclease-free water prior to fragment analysis on an ABI 3730 Genetic Analyzer (Applied Biosystems). Individual samples were multiplexed in three primer-pair sets in a 17-μL volume consisting of 3 μL of diluted PCR products (1 μL from each primer pair), 13.896 μL Hi-Di (ABI) and 0.104 lL GeneScan ROX400HD size standard. Allele sizes were visualized and scored using GeneMapper (ABI). We examined the data in Micro-checker (Van Oosterhout et al. 2004) to assess genotyping errors, such as allelic dropouts, stuttering or null alleles. Our results detected no null alleles in any of the 18 microsatellite loci.

Population Structure

We used the program STRUCTURE 2.3.4 (Pritchard et al. 2000) with data from 18 microsatellite loci to infer historical lineages through clustering of similar genotypes using STRUCTURE 2.3.4 (Pritchard et al 2000). This analysis assessed the most probable number of genetic clusters that characterizes samples from this transect and assigned individuals to populations. STRUCTURE is a model-based algorithm method that uses Bayesian statistics and Markov chain Monte Carlo (MCMC) to make cluster assignments using genetic data. We used the 'admixture' model with correlated allele frequencies among populations and performed 3 replicate runs for each value of K ranging from 1 to 6 with a burn-in of 1.0×10^4 followed by 2.0×10^4 repetitions. Each run estimated the 'log probability of data' (L(K)). We recorded the ln Prob(Data) for each run and averaged the ln Prob(Data) across runs for each value of K.

Analysis of Population Demography

We assessed evidence of historical fluctuations in population size using data from 18 microsatellite loci with LAMARC 2.1.8 (Kuhner 2006). LAMARC estimates a population-growth parameter, g, by using the coalescent and a Markov-chain Monte Carlo genealogy sampler. The exponential growth parameter, g, can be defined by the equation $\theta_{t(\text{time before present})} = \theta_{t(\text{present time})}^{-gt}$ where the time parameter t is measured in units of mutations. Positive values of g indicate a growing population and negative values represent shrinking populations. A g of zero represents constant size. We used the 99% confidence intervals for g to test for significant difference from zero. For each maximum likelihood run, we used 20 short chains of 10,000 steps and two long chains with 200,000 steps. The number of short chains was based on when parameter estimates appeared to be stabilized. We used a Brownian-Motion model for the mutation model, which is a statistical approximation of the stepwise model. Each run was replicated 3 times with different starting seeds and with 3 simultaneously heating searches.

Migration Patterns Between Coastal and Interior Populations

We used the coalescence-based program MIGRATE-N 3.2.6. (Beerli 2006; Beerli and Felsenstein 2001; Beerli and Palczewski 2010) from 18 microsatellite loci to test for and estimate gene flow between populations. We estimated effective population sizes (Ne) and migration rates among populations using Bayesian inference and the Brownian motion mutation model. The model allows for mutation rates differing among loci by using the number of alleles per locus to estimate locus specific relative mutation rate modifiers. We evaluated four migration models: (1) a full model with two population

sizes and two migration rates (between coastal and interior populations); (2) a model with two population sizes and one migration rate (gene flow only to the coastal population); (3) a model with two population sizes and one migration rate (gene flow only to the interior population); (4) a model assuming one panmictic population. The model comparison was done using Bayes factors with the marginal likelihood values from each model. Runs were carried out multiple times with varying parameter settings to achieve convergence. The final MCMC parameters were four long chains with 100,000-recorded steps and a 100-step increment with a burn in of 10,000. The total number of sampled parameter values was ten million with a uniform distribution for theta (0.0 – 100) and for migration (0.0–1,000).

Color Scoring

The ventral region of *T. douglasii* contains the most striking differences in fur color from coastal and interior populations. Thus, we measured spectral reflectance of the ventral region spectral from prepared museum specimens using a USB2000 (Ocean Optics, Dunedin, FL) spectrophotometer with a dual deuterium and halogen light source. The probe was held at a 45^{o} angle to the surface of the body. Spectral reflectance wavelengths were recorded using the program Spectrasuite (Ocean Optics).

Analyses of Cranial Morphology

To examine differences in cranial morphology that may have resulted from either adaptive genetic divergence or phenotypic plasticity in response to different forest environments, we examined three cranial characters that are reasonable proxies for

measures of bite force and function (Smith 1981), as well as one trait not known to be directly related to bite force (width of foramen magnum). Linear measurements were made to the nearest one hundredth millimeter using digital calipers (Mitutoyo Corp., Japan) for the following skull traits: (i) sagittal crest, measured as distance between the temporal lines; (ii) the angular moment arm (AMA), measured as distance between the mandibular notch to the angular process; (iii) coronoid moment arm (CMA), measured as distance between the coronoid processes and the mandibular condyle; (iv) foramen magnum, measured as the transverse distance of the foramen magnum.

Morphological traits typically scale with body size, which can obscure interesting differences in traits among populations that differ in body size (Reist 1986). Because populations of *T. douglasii* are known to be larger in body size in eatern Oregon than western Oregon (Verts and Carraway 1998), differences in cranial traits between populations can be confounded by differences in overall body size. Accordingly, we made ratios of each skull character against skull length. Furthermore, a previous study showed that none of the three traits showed sexual dimorphism, and therefore, sexes were pooled (Chavez et al 2011).

Cline Analysis

To estimate the relationship between spatial position and clinal variation of genetic and phenotypic data, we fitted maximum likelihood clines to geographic variation of spectral reflectance of the ventral region, four skull characters, and microsatellite genotype probabilities using CFIT-7 (Gay et al. 2008). CFIT uses a simulated annealing function that includes Metropolis algorithms to fit three-part clines that include a central sigmoid

part and two exponential tails (Szymura and Barton 1986). We treated ventral color and cranial morphology as quantitative characters for this anlaysis and compared three different candidate models to find the best-fitting curve: unimodal, bimodal, and trimodal. Unimodal distributions are characteristic of situations where intermediate phenotypes predominate or of relatively weak disruptive selection (Jiggins and Mallet 2000). Bimodal distributions are characteristic of very high selection against intermediate phenotypes. Trimodal distributions can be interpreted as having a pattern somewhere between a unimodal and a bimodal distributions (Gay et al. 2008).

Next, we examined whether all characters shared the same cline center (coincidence) and same cline width (slope: concordance) using four models of constraint: (1) the same cline center, (2) same cline slope, (3) same cline center and slope, or (4) center and slope were left unconstrained. For this analysis we performed two tests to see whether ventral fur color was similar or not with all cranial characters by testing two sets of models including fur color and cranial characters together and another with only cranial characters together. Finally, we tested another two set of models to see whether forest canopy openness fit clinal patterns of ventral color and all cranial colors. All model testing was analyzed with Akaike Information Criterion (AIC) to rank candidate models. Evidence ratios were also provided for each AIC model comparison to show the relative likelihood of the best model being correct when compared against other models. Different starting positions and an optimal number of chains were used for each analysis to ensure that the algorithms used in CFIT were adequately exploring parameter space. Data for each character were transformed to a scale of 0–1, with values near 0

representing coastal *T. douglasii* populations and values near 1 representing interior *T. douglasii* populations.

Results

Population Structure and Assignment

The STRUCTURE analysis using allele profiles from 18 microsatellites found that K = 2 was the most likely number of clusters of nuclear variation in the dataset (mean ln Prob(Data) = -4996.3; Fig. 2). The two clusters were mostly geographically distinct as cluster 1 contained all individuals from the western and eastern side of the Cascade Mountains and cluster 2 encompassed all individuals found in the Blue Mountains of central Oregon.

Historical Population Demography

Our LAMARC results show evidence for a slight decline in historical population size in *Tamiasciurus douglasii* in Oregon. The maximum likelihood estimate (MLE) of *g* was small and negative (MLE = -0.053) and was shown with 99% certainty to be nonzero (range: -0.0903 to -0.0214). All independent runs of LAMARC provided similar results suggesting that the settings for the analyses were appropriate.

Gene Flow

Results from MIGRATE-N 3.2.6 supported the model of panmixia between coastal and interior populations over all other models of gene flow (Table 2).

Clinal Patterns of Phenotypic Variation and Canopy Openness

To assess clinal variation of phenotypic traits in the face of high levels of gene flow, we restricted the cline analysis in CFIT to samples from cluster 1 (Cascade Mountains group) from the STRUCTURE analyses (Fig. 3).

The major overall pattern that emerged from the percent tree canopy data along the ecological gradient was that forest canopy was less open in the coastal forest on the western portion of the study transect than in the dry interior forest on the eastern portion of the transect (Fig. 3A). However, the cline center of canopy openness (115 km from Loc 1) occurred within the wet coastal forests rather than in the subalpine transitional forest (mountain hemlock). The estimate of the cline center for fur color (95 km from Loc 1) was also located within the wet coastal forest rather than in the transitional forest zone (Fig. 3B). Cline centers for all cranial traits (<1.3 km from Loc 1) were also located in the wet coastal forests and unexpectedly near the western extent of the study transect (Figs. 3C-3F). Our model selection results showed that weak selection against intermediate phenotypes of the angular moment arm (AMA) trait resulted in a unimodel model pattern of clinal variation (Table 3). In contrast, strong selection against intermediates for all other cranial triats resulted in bimodal patterns of clinal variation.

To see whether we should examine ventral color and cranial morphology together or separately with tree canopy openness, we evaluated how well clines for fur color and all cranial traits fit with each other using AIC. We found that cline centers and slopes between fur color and cranial morphology were unconstrained (neither coincident or concordant) (Table 4). However, all cranial traits shared similar clines and slopes (Table 4). Based on these results, we separated fur color and cranial traits in our examination of

their cline similarities with forest canopy openness. We found that clinal variation of canopy openness shared a similar cline center with ventral color, but did not share similar cline centers or slopes with all cranial traits Table 5).

Discussion

The combined analyses of phenotypic clines and population genetic structure in Douglas squirrels show the existence of relatively sharp clinal variation in ventral fur color, but only gradual clines of cranial morphology, within a single panmictic population across an ecological gradient through the Cascade Mountains in western Oregon. These findings suggest that divergent selection on fur color, but not cranial morphology associated with bite force, in Douglas squirrels may be overriding the homogenizing effects of gene flow. Douglas squirrels possess a darker ventral color in the coastal forests than in the interior forests (Steele 1999). Furthermore, the coincidence of cline centers between variation in tree canopy openness and ventral fur color further supports the notion that fur color is related to forest structure and possibly predator avoidance. Wet coastal forests on the west side of the Cascade Mountains receive greater precipitation than interior forests and thus are much denser in canopy structure and understory (Franklin and Dyrness 1973). Unlike typical ground-dwelling rodents, tree squirrels often feed and rest in a sitting posture in the forest canopy, which exposes their ventral region to detection by predators. For example, the northern goshawk (*Accipiter gentilis*) is a major predator of *Tamiasciurus* and hunts its prey within complex canopy structures (Kenward 1982; Beier and Drennan 1997). In light of these predatory pressures, natural selection apparently favors darker ventral coloration of Douglas squirrels in coastal forests so they are better

matched against the low-light background environment, whereas, the brighter forest environment of interior forests would favor lighter ventral coloration (Smith 1981).

Gradual clines in cranial morphology did not provide overwhelming evidence that coastal and interior squirrel populations have diverged in skull characteristics associated with bite force. In fact, similar clinal patterns between bite-force related cranial traits and a non-bite force cranial trait suggests that selective pressures for greater bite force were not strong, especially in the face of strong gene flow between coastal and interior populations. This finding was a surprise given strong differences in hardness of cones in several important conifer species between coastal and interior conifer species. A critical part of the Douglas squirrel's feeding activity is dismantling cones by biting off cone scales to extract the seeds (Smith 1968). Conifer seeds are the most important food item for Douglas squirrels, and during winter the cones cached in the ground are essentially their only food item (Smith 1968). Two important conifer species within the Douglas squirrel's range on the eastern side of the Cascade Mountains include lodgepole pine (*Pinus contorta*) and ponderosa pine (*Pinus ponderosa*). Both of these species produce very hard cones, and lodgepole pine also produces serotinous cones that can remain closed for several years, thus providing a well-preserved food resource. In contrast, on the western side of the Cascade Mountains, all the major conifer species used by Douglas squirrels produce relatively soft cones, which include a coastal variety of Douglas fir (*Pseudotsuga menziesii var. menziesii*), Sitka spruce (*Picea sitchensis*), and Pacific silver fir (*Abies amabilis*). One factor that may dampen the selective pressure on interior populations for stronger bite force is that the Rocky Mountain Douglas fir (*P. m. glauca*) is also present and provides a a valuable "soft" cone resource. Gene flow may very well

be swamping out divergence in cranial morphology between coastal and interior populations. However, cranial dimensions in the genetically distinct and isolated population of Douglas squirrels found in the dry interior forests of the southern Blue Mountains in central Oregon are also similar to coastal populations (unpublished data), thus further supporting the idea that even without gene flow, divergent selection on skull morphology due to different cone hardness is not very strong.

Another factor to consider for the lack of major divergence in cranial lever arm ratios between coastal and interior populations is the strong conservatism in the cranial morphology of tree squirrels since their origin in the late Oligocene (Emry and Thorington 1984). Tree squirrels belonging the tribe Tamiasciurini and its sister taxon, Sciurini, are considered "living fossils" due to their relatively primitive masticatory anatomy (Emry and Thorington 1984). In fact, studies have shown that rather than the modification of individual cranial bones, the cranium is well integrated in tree squirrels and most cranial traits of linear dimension scale isometrically across different body sizes (Roth 1996; Swiderski and Zelditch 2010) rather than allometrically (Huxley 1932; Sweet 1980). Douglas squirrels in central Oregon are known to be larger in body size than coastal squirrels (Verts and Carraway 1998). We examined the ratio of cranial lever arms to skull length to minimize effects of different body size on clinal patterns of cranial morphology. The lack of major clinal transitions in moment arm ratios across the forest gradient within Douglas squirrels reinforces the theory that strong cranial integration may be limiting the modification of individual cranial traits away from what is predicted by isometric scaling.

The conservatism of cranial morphology in tree squirrels may be a result of their arboreal lifestyle. Tree squirrels are capable of rapid arboreal locomotion, which necessitates quick processing of complex spatial data and coordination. Many arboreal mammals have relatively larger brain sizes to accommodate this high level of information processing (Lemen 1980; Eisenberg and Wilson 1981). The cranial features that encompass the brain and eyes also provide attachment surfaces for muscles related to bite force. Therefore, it has been suggested that strong conservatism of cranial morphology may be due to counteracting selective pressures for both greater brain capacity and bite force (Roth 1996; Swiderski and Zelditch 2010).

Population genetic theory (Excoffier et al. 2009), as well as limited empirical experiments (Hallatschek et al. 2007), show that clinal patterns of allelic variation can also be caused by increases in rare allelic variants to high frequencies at the geographic range margins of a rapidly expanding population (Hallatschek et al. 2007; Excoffier et al. 2009). This phenomenon, called "surfing," can produce clinal patterns of allelic variation that can be mistakenly interpreted as having been caused by disruptive selection. Klopfstein et al (2006) found that "surfing" will occur more often in smaller populations with limited dispersal abilities that are undergoing rapid range expansion. These factors do not appear to fit the situation we have observed in Douglas squirrels, because the location of our study is near the center of the entire species range and our estimates of historical population growth show a slight decline in effective population size.

Our finding of only one population-of-origin for *T. douglasii* through the ecological gradient across the Cascade Mountains supports the scenario that clinal patterns arose from primary intergradation rather than secondary contact. This is further

supported by a previous range-wide phylogenetic analysis of Douglas squirrels using both mitochondrial and nuclear data that did not reveal significant genetic structuring through most of the species range, much less in Oregon (Arbogast et al 2001; Chavez et al In review). Furthermore, these phylogenetic analyses also reveal the relatively recent origins of *Tamiasciurus douglasii* (<400 ka), which highlights the relatively rapid evolution of phenotypic divergence in Douglas squirrels.

Studies of phenotypic divergence in the face of gene flow are important for learning about adaptation, because the selective agents responsible for these phenotypic differences are presumed to be still active and can therefore actually be identified. This is not always the case when adaptive divergence took place in ancestral populations and the selective agents are difficult to discern. Furthermore, identifying the adaptive significance of traits can be difficult when populations are also genetically structured because of the conundrum of whether divergent adaptation led to the isolation or the other way around. Cline research also provides biologists a natural experiment to examine how genes underlying ecologically important traits are structured in a natural context (Mullen and Hoekstra 2008). The present study represents an initial examination of patterns of local adaptation in Douglas squirrel populations across an ecological gradient. To examine the basis of local adaptation more thoroughly, it is also important to investigate the processes that produce divergent selective pressures and the degree to which phenotypic plasticity is affecting the morphology of the traits through common garden or reciprocal transplant experiments.

Literature Cited

Arbogast, B. S., R. A. Browne, and P. D. Weigl. 2001. Evolutionary genetics and Pleistocene biogeography of North American tree squirrels (*Tamiasciurus*). J. Mammal. 82:302–319.

Barton, N. H. 2000. Genetic hitchhiking. Phil. Trans. R. Soc. Lond., B, Biol. Sci. 355:1553–1562.

Beerli, P. 2006. Comparison of Bayesian and maximum-likelihood inference of population genetic parameters. Bioinformatics 22:341–345.

Beerli, P., and J. Felsenstein. 2001. Maximum likelihood estimation of a migration matrix and effective population sizes in n subpopulations by using a coalescent approach. Proc. Nat. Acad. Sci. USA 98:4563–4568.

Beerli, P., and M. Palczewski. 2010. Unified framework to evaluate panmixia and migration direction among multiple sampling locations. Genetics 185:313–326.

Beier, P., and J. E. Drennan. 1997. Forest structure and prey abundance in foraging areas of northern goshawks. Ecol. Appl. 7:564–571.

Benkman, C. W. 1995. The impact of tree squirrels (*Tamiasciurus*) on limber pine

seed dispersal adaptations. Evolution 49:585–592.

Chavez, A. S., C. J. Saltzberg, and G. J. Kenagy. 2011. Genetic and phenotypic variation across a hybrid zone between ecologically divergent tree squirrels (*Tamiasciurus*). Mol. Ecol. 20:3350–3366.

Chavez, A. S., S. P. Maher, B. S. Arbogast, and G. J. Kenagy. In review. Diversification and gene flow in nascent lineages of island and mainland North American pine squirrels (*Tamiasciurus* spp.).

Eisenberg, J. F., and D. E. Wilson. 1981. Relative brain size and feeding strategies in didelphid marsupials. Am. Nat. 118:110–126.

Emry, R. J., and R. W. Thorington. 1984. The tree squirrel *Sciurus* as a living fossil. In: Living fossils (eds. N. Eldredge and S. Stanley), pp. 23-31. Springer-Verlag, New York.

Endler, J. A. 1977. Geographic variation, speciation, and clines. Vol. 10. Princeton University Press.

Elliott, P. F. 1974. Evolutionary responses of plants to seed-eaters: pine squirrel predation on lodgepole pine. Evolution 28:221–231.

Excoffier, L., M. Foll, and R. J. Petit. 2009. Genetic consequences of range expansions. Annu. Rev. Ecol. Evol. Syst. 40:481–501.

Felsenstein, J. 1981. Skepticism towards Santa Rosalia, or why are there so few kinds of animals? Evolution 35:124–138.

Fisher, R. A. 1937. The wave of advance of advantageous genes. Ann. Eugen. 7:355-369.

Franklin, J. F., and C. T. Dyrness. 1973 Natural Vegetation of Oregon and Washington, Oregon State University Press, Corvallis, Oregon.

Gallant, S. L., R. F. Preziosi, and D. J. Fairbairn. 1993. Clinal variation in eastern populations of the waterstrider *Aquarius remigis*: gradual intergradation or discontinuity? Evolution 47:957–964.

Gay, L., P. A. Crochet, D. A. Bell, and T. Lenormand. 2008. Comparing clines on molecular and phenotypic traits in hybrid zones: a window on tension zone models. Evolution 62:2789–2806.

Gunn M. R., D. A. Dawson, A. Leviston, K. Hartnup, C. S. Davis, C. Strobeck, J. Slate, and D. W. Coltman. 2005. Isolation of 18 polymorphic microsatellite loci from the North American red squirrel, *Tamiasciurus hudsonicus* (Sciuridae, Rodentia), and their cross-utility in other species. Mol. Ecol. Notes 5:650–653.

Haldane, J. B. S. 1948. The theory of a cline. J. Genet. 48:277–284.

Hallatschek, O., and D. R. Nelson. 2008. Gene surfing in expanding populations. Theor. Popul. Biol. 73:158–170.

Homer, C. H., J. A. Fry, and C. A. Barnes. 2012. The National Land Cover Database, U.S. Geological Survey Fact Sheet 2012-3020, 4 p.

Huxley, J. S. 1932. Problems of relative growth. Baltimore, MD: Johns Hopkins University Press.

Huxley, J. S. 1938. Clines: an auxiliary method in taxonomy. Nature 142:219–220.

Jiggins, C. D., and J. Mallet. 2000. Bimodal hybrid zones and speciation. Trends Ecol. Evol.15:250–255.

Kawecki, T. J., and D. Ebert. 2004. Conceptual issues in local adaptation. Ecol. Lett. 7:1225–1241.

Kenward, R. E. 1982. Goshawk hunting behaviour, and range size as a function of food and habitat availability. J. Anim. Ecol. 51:69–80.

Kiilsgaard, C., and C. Barrett. 1999. Oregon current wildlife-habitat types. http://www.nwhi.org.

Klopfstein, S., M. Currat, and L. Excoffier. 2006. The fate of mutations surfing on the wave of a range expansion. Mol. Biol. Evol. 23:482–490.

Kuhner, M. K. 2006. LAMARC 2.0: maximum likelihood and Bayesian estimation of population parameters. Bioinformatics 22:768–770.

Lemen, C. A. 1980. Relationship between relative brain size and climbing ability in *Peromyscus*. J. Mammal. 61:360–364.

Lenormand, T. 2012. From local adaptation to speciation: specialization and reinforcement. Int. J. Ecol. 2012:1–11.

Lindsay, S. L. 1986. Geographic size variation in *Tamiasciurus douglasii*: significance in relation to conifer cone morphology. J. Mammal. 67:317–325.

Maynard Smith, J., and J. Haigh. 1974. The hitch-hiking effect of a favorable gene. Genet. Res. 23:23–35.

Mullen, L. M., and H. E. Hoekstra. 2008. Natural selection along an environmental gradient: a classic cline in mouse pigmentation. Evolution 62:1555–1570.

Nosil, P., D. J. Funk, and D. Ortiz-Barrientos. 2009. Divergent selection and heterogeneous genomic divergence. Mol. Ecol. 18:375–402.

Pritchard, J. K., M. Stephens, and P. Donnelly. 2000. Inference of population structure using multilocus genotype data. Genetics 155:945-959.

Reist, J. D. 1986. An empirical evaluation of coefficients used in residual and allometric adjustments of size covariation. Can. J. Zool. 64:1363–1368.

Roth, V. L. 1996. Cranial integration in the Sciuridae. Am. Zool. 36:14–23.

Slatkin, M. 1973. Gene flow and selection in a cline. Genetics 75:733–756.

Slatkin, M. 1985. Gene flow in natural populations. Annu. Rev. Ecol. Syst. 16:393–430.

Smith C. C. 1968. The adaptive nature of social organization in the genus of three squirrels *Tamiasciurus*. Ecol. Monogr. 38:31–64.

Smith C. C. 1970. The coevolution of pine squirrels (*Tamiasciurus*) and conifers. Ecol. Monogr. 40:349–371.

Smith C. C. 1981. The indivisible niche of *Tamiasciurus*: an example of nonpartitioning

of resources. Ecol. Monogr. 51:343–364.

Steele M. A. 1999. *Tamiasciurus douglasii*. Mammal. Species 630:1–8.

Sweet, S. S. 1980. Allometric inference in morphology. Am. Zool. 20:643–652.

Swiderski, D. L., and M. L. Zelditch. 2010. Morphological diversity despite isometric scaling of lever arms. Evol. Biol. 37:1-18.

Szymura, J., and N. Barton. 1986. Genetic analysis of a hybrid zone between the fire-bellied toads, *Bombina bombina* and *Bombina variegata*, near Cracow in southern Poland. Evolution 40:1141–1159.

Thorpe, R. S. 1984. Primary and secondary transition zones in speciation and population differentiation: a phylogenetic analysis of range expansion. Evolution 38:233–243.

Van Oosterhout, C., W. F. Hutchinson, D. P. M. Wills, and P. Shipley. 2004. MICRO-CHECKER: software for identifying and correcting genotyping errors in microsatellite data. Mol. Ecol. Notes 4:535–538.

Verts, B. J., and L. N. Carraway. 1998. Land Mammals of Oregon. University of California Press.

Vignieri, S. N., J. G. Larson, H. E. Hoekstra. 2010. The selective advantage of crypsis in mice. Evolution 64:2153–2158.

Wheatley, M. 2007. Relating red squirrel body size to different conifer cone morphologies within the same geographic location. J. Mammal. 88:220–225.

Table 1. Specimens of *Tamiasciurus douglasii* collected from Oregon and analyzed in this study with locality numbers (Fig 1), county, locality description, latitude and longitude, and museum number.

Loc. #	County	Locality	Lat (dec)	Long (dec)	UWBM Museum Number									
1	Lane	Dunes City	43.8802	-124.1516	82028									
	Douglas	Dunes City	43.8994	-123.8637	82029	82030	82031							
	Lane	Dunes City	43.9223	-123.9449	82032	82033								
	Douglas	Dunes City	43.8936	-123.8711	82034	82035	82036	82037						
2	Lane	Siuslaw Falls County Park	43.8606	-123.3609	82038	82039	82040	82041	82042	82043	82044	82045	82046	
	Lane	Siuslaw Falls County Park	43.8236	-123.3242	82047									
3	Lane	Oakridge	43.7251	-122.6956	82048	82049								
	Lane	Oakridge	43.6966	-122.6654	82050	82051								
	Lane	Oakridge	43.7258	-122.7016	82052									
	Lane	Oakridge	43.6970	-122.7194	82053									
	Lane	Oakridge	43.6677	-122.6103	82054	82055	82056	82057						
4	Deschutes	Waldo Lake	43.7465	-121.9464	82071	82072	82073	82074	82075	82076	82077	82078	82080	82081
5	Deschutes	Wickiup Reservoir	43.7431	-121.6903	82061	82062	82063	82064	82065	82066	82067	82068	82069	82070
6	Deschutes	Newberry Crater	43.7070	-121.3268	81487	81488	81489	81490	81491	81492	81493	82058	82059	82060
7	Crook	Prineville	44.5070	-120.6604	82079	82082	82083	82084	82085	82086				
	Crook	Prineville	44.5350	-120.5411	82087	82088	82089							
	Crook	Prineville	44.4971	-120.3940	82090									

8	Crook	Ochoco Mts.	44.3951	-120.0300	81494	81495								
	Wheeler	Mitchell	44.4525	-119.9423	82091	82092	82093	82094	82095	82096	82097	82098		
9	Grant	John Day	44.2571	-119.0087	82099	82100	82101	82102	82103	82104	82105	82106	82107	82108
	Grant	Aldrich Mts.	44.2876	-118.9788	81496									
	Grant	Aldrich Mts.	44.1973	-118.8636	81508									

Table 2. Comparison of migration models using Bayes Factors in MIGRATE-N. The best model is in bold.

Migration Direction	Bezier approximation	ln Bayes Factor	Model Probability
Panmictic (1 Migr Rate)	**-371235.24**	**0**	**1**
FullModel (2 Migr Rates)	-374351.37	-3116.13	0
East to West Migration	-377473.04	-6237.8	0
West to East Migration	-512957.06	-141721.82	0

Table 3. Comparison of cline models using the Akaike Information Criteria (AIC) for clinal variation in whiteness of ventral fur color and cranial morphology. The best model for each cline is in bold.

Phenotypic Trait	Model	Parameters	Likelihood	AIC_c	Δ_{AIC}	AIC weights
Ventral Fur Color	**Unimodal**	**7**	**24.35**	**-32.55**	**0.00**	**0.86**
	Trimodal	14	30.21	-23.08	9.47	0.01
	Bimodal	8	23.78	-28.73	3.82	0.13
Angular Moment Arm	**Unimodal**	**7**	**5.94**	**5.85**	**0.00**	**0.71**
	Trimodal	14	9.22	27.81	21.96	~0
	Bimodal	8	6.68	7.60	1.75	0.29
Coronoid Moment Arm	Unimodal	7	7.13	3.60	3.01	0.18
	Trimodal	14	17.63	11.84	11.25	~0
	Bimodal	**8**	**10.27**	**0.59**	**0.00**	**0.82**

Sagittal Crest	Unimodal	7	3.67	10.52	4.82	0.08
	Trimodal	14	12.92	21.24	15.54	~0
	Bimodal	**8**	**7.72**	**5.70**	**0.00**	**0.92**
Foramen Magnum	Unimodal	7	0.12	18.06	2.84	0.19
	Trimodal	14	4.93	40.24	25.02	0.00
	Bimodal	**8**	**3.27**	**15.22**	**0.00**	**0.81**

Table 4. Comparison of models for coincidence and concordance between fur color and cranial morphology using the AIC. The best models are in bold.

Trait Comparison	Constraint Models	Parameters	Likelihood	AIC_c	Δ_{AIC}	AIC weights
Ventral Fur Color &	Center Constraint	33	33.70	12.99	16.88	~0
All Cranial Traits	Slope Constraint	34	39.68	3.99	7.88	0.02
	Slope and Center Constraints	31	35.92	2.71	6.60	0.04
	Unconstrained	**38**	**49.76**	**-3.90**	**0.00**	**0.98**
Only Cranial Traits	**Center Constraint**	**28**	**22.71**	**25.21**	**0.00**	**0.98**
	Slope Constraint	28	14.27	42.08	16.87	~0
	Slope and Center Constraints	25	13.86	33.69	8.48	0.01
	Unconstrained	31	22.51	35.35	10.14	0.01

Table 5. Comparison of models for coincidence and concordance between clines of tree canopy openness, fur color and cranial morphology using the AIC. The best models are in bold.

Trait Comparison	Constraint Models	Parameter	Likelihood	AIC_c	Δ_{AIC}	AIC weights
Tree Canopy Openness	**Center Constraint**	**20**	**88.10**	**-127.72**	**0.00**	**1.00**
& Ventral Fur Color	Slope Constraint	20	79.63	-110.78	16.94	~0
	Slope and Center Constraints	19	77.59	-109.59	18.13	~0
	Unconstrained	21	79.63	-107.83	19.89	~0
Tree Canopy Openness	Center Constraint	41	68.36	-31.44	33.00	~0
& All Cranial Traits	Slope Constraint	41	80.00	-56.31	8.14	0.02
	Slope and Center Constraints	37	73.65	-54.80	9.65	0.01
	Unconstrained	**45**	**91.60**	**-64.45**	**0.00**	**0.98**

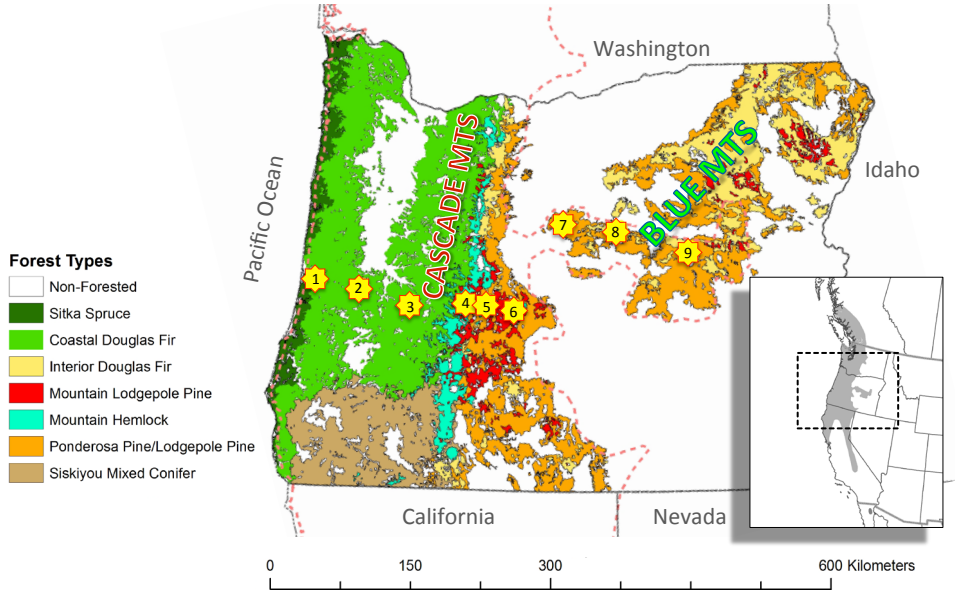

Figure 1. Map of Oregon with major forest zones and *T. douglasii* sampling localities (yellow stars). Light red-dashed line represents approximate species boundary of *T. douglasii*. The study transect consists of 9 localities across a forest gradient representing wet coastal forests (light and dark green colors), subalpine transitional forest (blue color), and dry interior forests (light and dark orange colors). Nonforested areas in Oregon are are white. The Cascade Mountains and Blue Mountains are labeled on the map. Inset shows entire range of *T. douglasii* from British Columbia to California, as well as the relict population in Baja California. Dashed box shows location of this study.

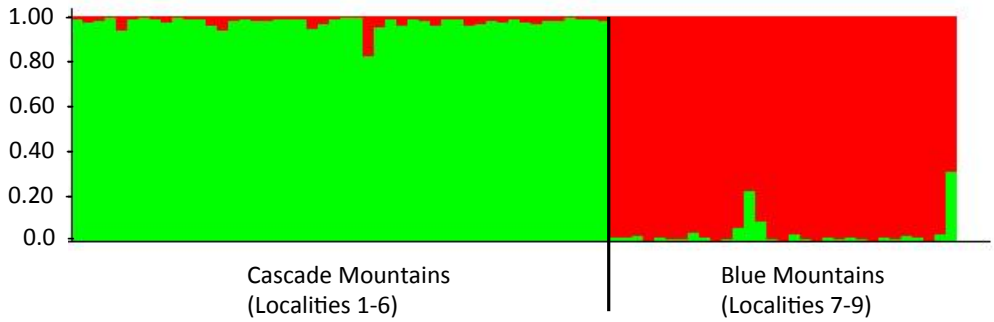

Figure 2. Bar plot from STRUCTURE using 18 microsatellite loci shows two genetic clusters of Douglas squirrels that are geographically discreet along the study transect. Each vertical line represents an individual broken into the proportion of its assignment to each genetic cluster. The x-axis is oriented from west-to-east and the vertical black line separates samples from the Cascade Mountains region (localities 1-6) from samples in the southern Blue Mountains (localities 7-9).

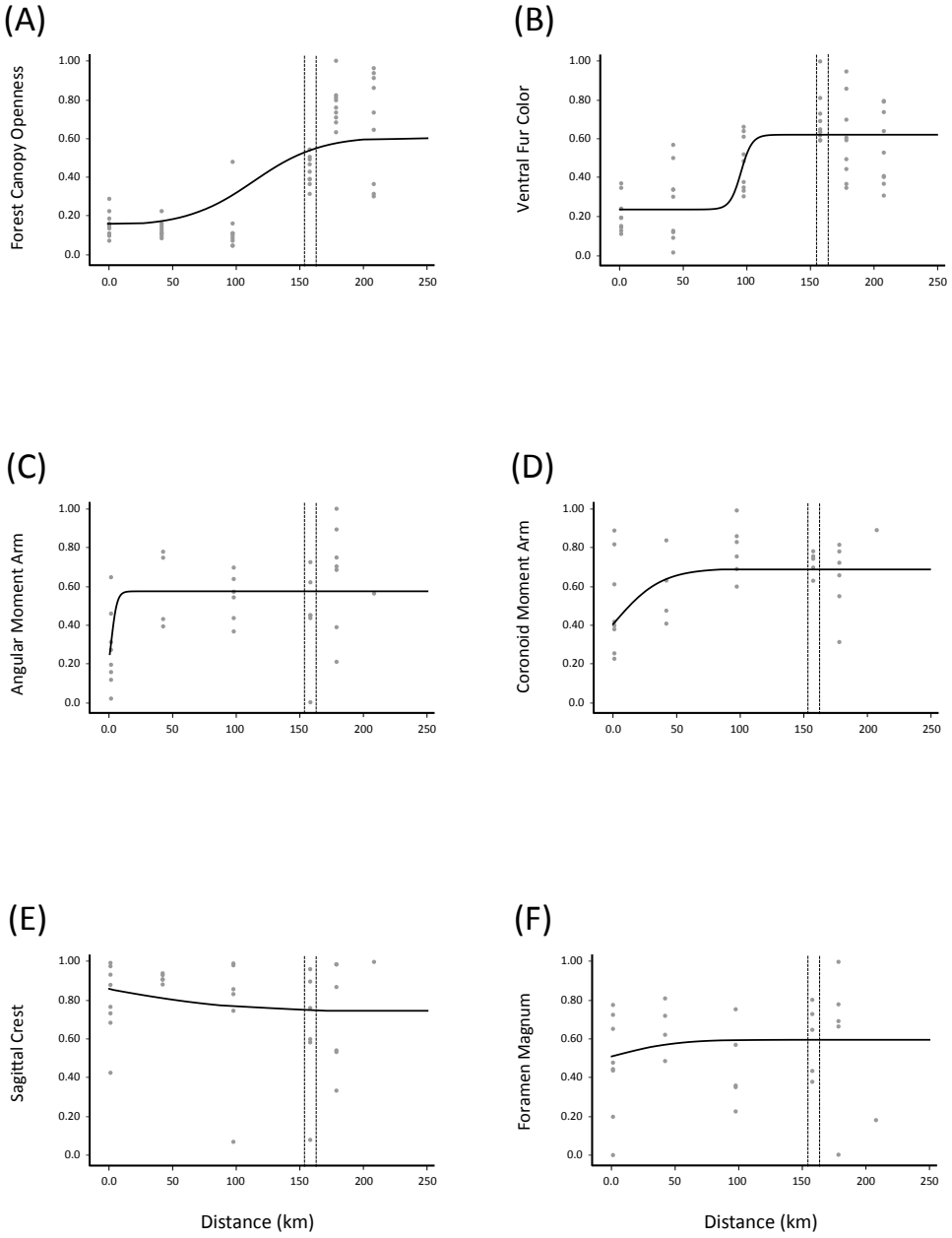

Figure 3. Clinal patterns of variation among individuals at 6 localities in the three forest zones across the west-to-east study transect. All six localities are within the Cascade Mountains population according to our STRUCTURE results. The ~200-km transect (x-axis) is described in **Material and Methods**. Dotted vertical lines represent limits between the three forest zones. The area west (left) of the dotted lines represents the wet

coastal forest zone (Sitka Spruce and Coastal Douglas Fir zones), between the lines is the transitional subalpine forest zone (Mountain Hemlock zone), and the area east (right) of the dotted lines represents the dry interior forest zone (Ponderosa Pine, Lodgepole Pine, and Interior Douglas Fir zones). (A) Percentage of tree canopy openness of 10 randomly sampled points at each sampling locality (B) Ventral color score using a CIE whiteness index from spectrometer measurements of 60 individuals (C) Ratio of angular moment arm (AMA) to skull length for 38 individuals (D) Ratio of coronoid moment arm (CMA) to skull length for 37 individuals (E) Inverse ratio of sagittal crest width to skull length for 37 individuals (F) Ratio of foramen magnum to skull length for 34 individuals. All scores were transformed to a scale of 1 – 0 to make plots comparable.

VITA

Andreas Shintaro Chavez, son of Hector Javier and Kazue Chavez, was born in Albuquerque, New Mexico on November 10, 1973. He received his secondary education at Davis Senior High School in Davis, California. He attended the University of California, Berkeley, where he received a Bachelor of Arts degree in Integrative Biology in 1996. He received a Master of Science degree in Widllife Ecology from Utah State University in 2001 under Dr. Eric Gese. Andreas completed his Doctor of Philosophy degree in Biology at the University of Washington in 2013 under Dr. George James Kenagy.